

Uncertainty Analyses of Molten Salt Property Measurements

Chemical and Fuel Cycle Technologies Division

About Argonne National Laboratory

Argonne is a U.S. Department of Energy laboratory managed by UChicago Argonne, LLC under contract DE-AC02-06CH11357. The Laboratory's main facility is outside Chicago, at 9700 South Cass Avenue, Argonne, Illinois 60439. For information about Argonne and its pioneering science and technology programs, see www.anl.gov.

DOCUMENT AVAILABILITY

Online Access: U.S. Department of Energy (DOE) reports produced after 1991 and a growing number of pre-1991 documents are available free at OSTI.GOV (http://www.osti.gov/), a service of the US Dept. of Energy's Office of Scientific and Technical Information.

Reports not in digital format may be purchased by the public from the National Technical Information Service (NTIS):

U.S. Department of Commerce National Technical Information Service 5301 Shawnee Rd Alexandria, VA 22312

www.ntis.gov

Phone: (800) 553-NTIS (6847) or (703) 605-6000

Fax: (703) 605-6900 Email: orders@ntis.gov

Reports not in digital format are available to DOE and DOE contractors from the Office of Scientific and Technical Information (OSTI):

U.S. Department of Energy Office of Scientific and Technical Information P.O. Box 62

Oak Ridge, TN 37831-0062

www.osti.gov

Phone: (865) 576-8401 Fax: (865) 576-5728 Email: reports@osti.gov

Disclaimer

This report was prepared as an account of work sponsored by an agency of the United States Government. Neither the United States Government nor any agency thereof, nor UChicago Argonne, LLC, nor any of their employees or officers, makes any warranty, express or implied, or assumes any legal liability or responsibility for the accuracy, completeness, or usefulness of any information, apparatus, product, or process disclosed, or represents that its use would not infringe privately owned rights. Reference herein to any specific commercial product, process, or service by trade name, trademark, manufacturer, or otherwise, does not necessarily constitute or imply its endorsement, recommendation, or favoring by the United States Government or any agency thereof. The views and opinions of document authors expressed herein do not necessarily state or reflect those of the United States Government or any agency thereof, Argonne National Laboratory, or UChicago Argonne, LLC.

Uncertainty Analyses of Molten Salt Property Measurements

prepared by L.D. Gardner and M.A. Rose Chemical and Fuel Cycle Technologies Division, Argonne National Laboratory

March 31, 2025

CONTENTS

1.	Introduction	1
2.	Approach	2
3.	Uncertainty Analyses	4
	3.1. Thermal Analysis	4
	3.1.1. Method	4
	3.1.2. Instrument Calibration	4
	3.1.3. Uncertainty Analysis	5
	3.1.4. Effect of Heating Rate on Thermal Transitions	10
	3.2. Density	13
	3.2.1. Method	13
	3.2.2. Uncertainty Analysis	13
	3.2.3. Effects of Bob Mass, Wire Diameter, and Surface Tension	17
	3.3. Thermal Diffusivity	23
	3.3.1. Method	23
	3.3.2. Uncertainty Analysis	24
	3.4. Viscosity	27
	3.4.1. Method	27
	3.4.2. Instrument Calibration	28
	3.4.3. Uncertainty Analysis	30
4.	Conclusion	33
	Acknowledgements	34
	References	35
	Appendix A	37
	Appendix B	40
	Appendix C	54
	Appendix D	65

LIST OF TABLES

Table 1.	Uncertainty budget for thermal analyses of FLiNaK	6
Table 2.	Measured transition temperatures of FLiNaK salt	9
Table 3.	Measured transition temperatures of FLiNaK-L salt	9
Table 4.	Measured transition temperatures of FLiNaK-H salt	9
Table 5.	Melting onsets of reference metals measured at different heating rates	12
Table 6.	Uncertainty budget for density measurements of FLiNaK	15
Table 7.	Densities and expanded uncertainties calculated for FLiNaK	16
Table 8.	Densities and expanded uncertainties calculated for FLiNaK-L	16
Table 9.	Densities and expanded uncertainties calculated for FLiNaK-H	16
Table 10.	Densities of demineralized water with and without the surface tension term	20
Table 11.	Densities of water containing 2 wt% liquid dish soap with and without the surface tension term	21
Table 12.	Densities of clean and soapy water without the surface tension term	22
Table 13.	Uncertainty budget for thermal diffusivity measurements of FLiNaK	25
Table 14.	Thermal diffusivities and expanded uncertainties calculated for FLiNaK, FLiNaK-L, and FLiNaK-H	.27
Table 15.	Calculated viscosities for silicone reference oil measurements	30
Table 16.	Uncertainty budget for viscosity measurements of FLiNaK 1	31
Table 17.	Bias-corrected viscosities and expanded uncertainties calculated for FLiNaK1, FLiNaK 2, FLiNaK-L, and FLiNaK-H	.32
Table A.1.	Average transition temperatures of FLiNaK, FLiNaK-L, and FLiNaK-H	38
Table A.2.	Linear fits used to calculate melting onsets corresponding to 0 °C min ⁻¹	38
Table A.3.	Parabolic fits used to correct temperature measurements	39
Table B.1.	Bob and wire masses, bob volumes, and wire diameters in the gas space	41
Table B.2.	Immersed masses of bob and wire set 1 used in FLiNaK density measurements	41
Table B.3.	Immersed masses of bob and wire set 2 used in FLiNaK density measurements	42
Table B.4.	Immersed masses of bob and wire set 1 used in FLiNaK-L measurements	42
Table B 5	Immersed masses of hob and wire set 2 used in FL iNaK-L measurements	43

Table B.6. Immersed masses of bob and wire set 1 used in FLiNaK-H measurements	.43
Table B.7. Immersed masses of bob and wire set 2 used in FLiNaK-H measurements	. 44
Table B.8. Immersed masses of bob and wire set 3 used in FLiNaK-H measurements	. 44
Table B.9. Immersed masses of bob and wire set 4 used in FLiNaK-H measurements	. 45
Table B.10. Standard uncertainties in masses of bob and wire sets immersed in salt	. 46
Table B.11. Standard uncertainties of a type K thermocouple	. 47
Table B.12. Standard uncertainties in density and thermal expansion of tungsten and nickel	. 47
Table B.13. Sensitivity coefficients used to calculate combined standard uncertainties in set 1 of FLiNaK density measurements	. 48
Table B.14. Sensitivity coefficients used to calculate combined standard uncertainties in set 2 of FLiNaK density measurements	. 48
Table B.15. Sensitivity coefficients for set 1 of FLiNaK-L density measurements	. 49
Table B.16. Sensitivity coefficients for set 2 of FLiNaK-L density measurements	. 49
Table B.17. Sensitivity coefficients for set 1 of FLiNaK-H density measurements	. 49
Table B.18. Sensitivity coefficients for set 2 of FLiNaK-H density measurements	. 50
Table B.19. Sensitivity coefficients for set 3 of FLiNaK-H density measurements	. 50
Table B.20. Sensitivity coefficients for set 4 of FLiNaK-H density measurements	. 50
Table B.21. Average masses of bobs used in density measurements of water	.51
Table B.22. Average masses of bobs used in density measurements of soapy water	.51
Table B.23. Average diameters of wires used in density measurements of water with and without the addition of dish soap	.51
Table B.24. Masses of bob and wire sets measured in the gas space and submerged in water	. 52
Table B.25. Masses of bob and wire sets measured in the gas space and submerged in soapy water at room temperature	. 52
Table B.26. Sensitivity coefficients used in uncertainty analyses of water measurements	. 53
Table B.27. Sensitivity coefficients used in uncertainty analyses of soapy water measurements	. 53
Table C.1. Salt layer thicknesses used in thermal diffusivity measurements of FLiNaK, FLiNaK-L, and FLiNaK-H with standard uncertainties	. 55
Table C.2. Half-rise times used to calculate thermal diffusivities of FLiNaK	. 56
Table C.3. Half-rise times used to calculate thermal diffusivities of FLiNaK-L	. 57

Table C.4. Half-rise times used to calculate thermal diffusivities of FLiNaK-H58
Table C.5. Standard uncertainties of a type S thermocouple
Table C.6. Linear fits of thermal diffusivity data used to calculate sensitivity coefficients59
Table C.7. Sensitivity coefficients used to calculate combined standard uncertainties in thermal diffusivities of FLiNaK
Table C.8. Sensitivity coefficients used to calculate combined standard uncertainties in thermal diffusivities of FLiNaK-L
Table C.9. Sensitivity coefficients used to calculate combined standard uncertainties in thermal diffusivities of FLiNaK-H
Table C.10. Standard uncertainties in salt thickness attributed to distortions in the salt layer 61
Table C.11. Measured thermal diffusivities of FLiNaK with expanded uncertainties
Table C.12. Measured thermal diffusivity of FLiNaK-L with expanded uncertainties
Table C.13. Measured thermal diffusivity of FLiNaK-H with expanded uncertainties
Table D.1. Torque measurements of FLiNaK 1 salt
Table D.2. Torque measurements of FLiNaK 2 salt
Table D.3. Torque measurements of FLiNaK-L salt
Table D.4. Torque measurements of FLiNaK-H salt
Table D.5. Standard uncertainties in torque measurements of FLiNaK 1 salt70
Table D.6. Standard uncertainties in torque measurements of FLiNaK 2 salt71
Table D.7. Standard uncertainties in torque measurements of FLiNaK-L salt72
Table D.8. Standard uncertainties in torque measurements of FLiNaK-H salt73
Table D.9. Crucible and spindle dimensions used in silicone oil measurements 1 and 274
Table D.10. Crucible and spindle dimensions used in silicone oil measurements 3 and 474
Table D.11. Crucible and spindle dimensions used for viscosity calculations of FLiNaK 1 75
Table D.12. Crucible and spindle dimensions used for viscosity calculations of FLiNaK 2 75
Table D.13. Crucible and spindle dimensions used for viscosity calculations of FLiNaK-L 75
Table D.14. Crucible and spindle dimensions used for viscosity calculations of FLiNaK-H76
Table D.15. Sensitivity coefficients used to calculate uncertainties in FLiNaK 1 viscosity measurements at 500 °C

ivity coefficients use ements at 550 °C		
ivity coefficients use ements at 600 °C		
ivity coefficients use ements at 650 °C		_
ivity coefficients use ements at 700 °C		-
ivity coefficients use ements at 800 °C		
ivity coefficients use ements at 900 °C		•
ivity coefficients use ements at 500 °C		
ivity coefficients use ements at 550 °C		
ivity coefficients use ements at 600 °C		
ivity coefficients use ements at 750 °C		•
ivity coefficients use ements at 700 °C		
ivity coefficients use ements at 800 °C		
ivity coefficients use ements at 900 °C		
ivity coefficients use ements at 500 °C		
ivity coefficients use ements at 550 °C		-
ivity coefficients use ements at 600 °C		
ivity coefficients use ements at 650 °C		
ivity coefficients use ements at 700 °C		

Table D.34. Sensitivity coefficients used to calculate uncertainties in FLiNaK-L viscosity measurements at 800 °C	. 86
Table D.35. Sensitivity coefficients used to calculate uncertainties in FLiNaK-L viscosity measurements at 900 °C	. 87
Table D.36. Sensitivity coefficients used to calculate uncertainties in FLiNaK-H viscosity measurements at 500 °C	. 87
Table D.37. Sensitivity coefficients used to calculate uncertainties in FLiNaK-H viscosity measurements at 550 °C	. 88
Table D.38. Sensitivity coefficients used to calculate uncertainties in FLiNaK-H viscosity measurements at 600 °C	. 88
Table D.39. Sensitivity coefficients used to calculate uncertainties in FLiNaK-H viscosity measurements at 650 °C	. 89
Table D.40. Sensitivity coefficients used to calculate uncertainties in FLiNaK-H viscosity measurements at 700 °C	. 89
Table D.41. Sensitivity coefficients used to calculate uncertainties in FLiNaK-H viscosity measurements at 800 °C	. 90
Table D.42. Sensitivity coefficients used to calculate uncertainties in FLiNaK-H viscosity measurements at 900 °C	. 90
Table D.43. Fitted equations for viscosities of FLiNaK 1, FLiNaK 2, FLiNaK-L, and FLiNaK-H	.91
Table D.44. Calculated viscosities of FLiNaK 1 with expanded uncertainties	.91
Table D.45. Calculated viscosities of FLiNaK 2 with expanded uncertainties	.91
Table D.46. Calculated viscosities of FLiNaK-L with expanded uncertainties	. 92
Table D.47. Calculated viscosities of FLiNaK-H with expanded uncertainties	. 92

LIST OF FIGURES

Figure 1.	DSC temperature calibration results	5
Figure 2.	DSC responses of (a) FLiNaK, FLiNaK-L, and FLiNaK-H salt	8
Figure 3.	Thermal analyses of an aluminum reference sample	11
Figure 4.	Melting onsets of reference metals at different heating rates	11
Figure 5.	Parabolic fits of melting onsets and associated residuals	12
Figure 6.	Densities of FLiNaK, FLiNaK-L, and FLiNaK-H salts	17
Figure 7.	Density of water measured at different depths	19
Figure 8.	Average thermal diffusivities and expanded uncertainties for FLiNaK, FLiNaK-L, and FLiNaK-H.	26
Figure 9.	Measured torque and calculated viscosity of silicone reference oil	29
Figure 10.	Viscosities of FLiNaK 1, FLiNaK 2, FLiNaK-L, and FLiNaK-H	32
Figure D.1	1. Torque measurements of silicone oil performed in different sized crucibles	94

1. Introduction

Thermophysical and thermochemical property values of molten salts and associated uncertainties are used by reactor developers to evaluate reactor performance and model accident scenarios. These activities support fuel qualification objectives by demonstrating that fundamental safety functions (e.g., limit the release of radioactive materials, remove heat from the reactor, and control reactivity) can be performed effectively in a variety of conditions over the operating life of the reactor [1]. Fuel qualification activities are still in the development phase due to a lack of reliable property data for salt mixtures being considered for use in molten salt reactors (MSR).

The measurement methods used to generate property values have not yet been standardized for application to molten salts. Modifications of existing standards are required to address unique aspects of measurements with molten salts including high operating temperatures, air and moisture sensitivities, corrosivity and material compatibility issues, preferential volatilization of some constituents from salt mixtures, and changes in solubility and stability due to composition changes. The measures required to control or otherwise take these factors into account may limit the precision of property measurements. Changes in the composition of multi-component fuel salts over time due to fission reactions, periodic refueling activities, chemical adjustments for redox control, and the ingression of contaminants are expected to affect the properties of the salt. The effects of composition on the measured values must be distinguished from instrumental and environmental effects to accurately represent the salt properties.

Uncertainty analyses that identify factors affecting the precision and accuracy of measurements are essential in the development of standard methods of property measurements to provide confidence in the measured values. Argonne has been engaged in several activities supporting the development of property measurement methods for several years and steps for controlling quality-affecting variables used in several derived properties of molten salts have been developed to ensure that high-quality data are generated [2]. A set of standard operating procedures for the measurement of different properties of molten salts were developed and implemented to evaluate the effects of fission product dopants on the thermal properties of eutectic LiF-NaF-KF (FLiNaK) [3]. Measurements of two salt mixtures doped with different amounts of surrogate fission products for comparison to properties of FLiNaK without dopants [4, 5] were performed. Properties of FLiNaK are commonly used to represent those of fluoride-based MSR salts, and measuring properties of the same salt spiked with fission product dopants provides a comparison point for determining if effects of composition can be distinguished from instrumental uncertainties. The objective of the work summarized herein is to quantify the uncertainties due to different sources of measurement error and propagate those quantities to determine the overall uncertainties in derived property values. Recommendations suitable for inclusion in future measurement standards for molten salt properties related to minimizing measurement uncertainties are provided. Standardization will distinguish effects of composition and environmental factors from measurement operations, adding confidence to measured property values that are used to design, license and operate MSRs.

2. Approach

All physical measurements have inherent errors or effects that can cause a measured value to differ from the true value. Errors may be introduced from various elements including measurement equipment and operating parameter values (e.g., scan rates, sensitivities), environmental conditions (e.g., temperature and turbulence), and the statistical limitations of a finite data set. Given that the true values of most molten salt properties are not known, it is necessary to use all relevant information that is available to estimate the range of probable error for measurements. Uncertainty analysis is the process of identifying sources of error and estimating the possible range of error in the stated value of a measured variable [6].

The approach being used to analyze and quantify uncertainties in properties of molten salts described herein is based on principles outlined in the Guide to the Expression of Uncertainty in Measurement (GUM) [7]. In this approach, errors associated with the measurement of quality affecting variables are identified, categorized based on suitable methods of evaluation, and combined to provide an expanded uncertainty of measured values.

Sources of measurement error are commonly categorized as being random or systematic errors affecting the measurement precision and accuracy. Precision refers to the closeness of replicate measured values to each other and accuracy refers to closeness to the true value. Random errors are effects that cause an unpredictable and inconsistent variation in the measured value found during repeated measurements of a variable. The effect of random errors are typically evaluated by using statistical analyses of replicate measurements. The average contribution of random errors generally decreases and tends to zero as the number of observations increases. Systematic errors are remain constant in repeated measurements under fixed operating conditions due to a bias in the measurement device, procedure, or environment. Systematic errors are evaluated using non-statistical methods including measurements using certified materials. Systematic errors do not change with an increasing number of observations and tend to a non-zero value (i.e., bias).

The method of uncertainty quantification outlined in the GUM categorizes uncertainty components arising from random effects and from corrections for systematic effects in the same way by assigning suitable probability distributions to each source. Assigned probability distributions are used to convert uncertainties calculated at different confidence levels to equivalent standard uncertainties corresponding to one standard deviation. [7].

To demonstrate application of the approach, all measurement uncertainties of quality-affecting variables used to calculate property values of molten salts were identified and quantified from measurements made previously at Argonne. Those uncertainties were converted to equivalent standard uncertainties by assigning normal or rectangular distributions. Uncertainty from random sources of error were evaluated by using the standard deviation of repeated measurements and

assigned a normal distribution. The standard uncertainty $u(x_i)$ was calculated by using Equation 1, where s is the standard deviation of the data set and N is the number of measurements.

$$u(x_i) = \frac{s}{\sqrt{N}} \tag{1}$$

Sources of systematic error that were evaluated by using non-statistical methods (e.g., manufacturer specifications, calibration certificates, handbooks, expert knowledge, or other non-statistical sources to quantify uncertainty, instrument resolution, and certified uncertainties) were assigned a rectangular distribution in which measured values within a specified range are equally likely [7]. Standard uncertainties associated with these sources of error were calculated by using Equation 2. Sources of uncertainty tabulated for each property measurement method provide information on the category of uncertainty and the probability distribution used.

$$u(x_i) = \frac{U}{\sqrt{3}} \tag{2}$$

The total standard uncertainty of a quality-affecting variable is calculated by using the root-sum-square (RSS) method (Equation 3) to combine all sources of uncertainty calculated with different probably distributions.

$$u_{x_i} = \sqrt{\sum_{i=1}^{j} (u(x_i))^2}$$
 (3)

The combined standard uncertainty u_c is calculated by propagating the standard uncertainties in quality affecting variables using Equation 4 where y is the function used to calculate a given salt property and x_i represents one of the j quality-affecting variables that are included. The sensitivity coefficients were calculated as partial derivatives of the equation used to calculate properties of molten salts.

$$u_c = \sqrt{\sum_{i=1}^{j} \left(\frac{\partial y}{\partial x_i} \cdot u(x_i)\right)^2}$$
 (4)

The expanded uncertainty is determined by multiplying the combined standard uncertainty u_c by a coverage factor k. The value of k is based on the confidence interval being applied (where k=1.96 corresponds to 95% confidence).

In each of the sections in Chapter 3, sources of uncertainty are identified, categorized and quantified for the molten salt property measurement methods used at Argonne. This quantification of uncertainty

for measurement methods can be used to distinguish effects of composition and environmental factors, develop the technical justification for aspects of future standard methods and provide a more complete understanding of the quality of existing property data. Previously reported measurements of FLiNaK salt with and without impurities (FLiNaK, FLiNaK-L and FLiNaK-H) [5, 8] are used to assess expanded uncertainties in measured properties. Opportunities for improvement in measurement procedures or control of a variable during measurement are indicated and recommendations are made to improve data quality in future measurements.

3. Uncertainty Analyses

3.1 Thermal Analysis

3.1.1 Method

Thermal transition temperatures of molten salts are measured at Argonne by performing differential scanning calorimetry (DSC) using a model STA 449C Jupiter® (NETZSCH Instruments North America, LLC, Burlington, MA) simultaneous thermal analyzer (STA) housed within an inert atmosphere glovebox. The STA is located on a marble slab within the glovebox to reduce vibrational interference. An additional ultra-high purity argon purge is used to maintain atmospheric conditions within the heated zone during measurements. Salt samples are hermetically sealed in gold crucibles (TA Instruments, New Castle, DE) for thermal analyses.

3.1.2 Instrument Calibration

The DSC temperature response is calibrated by measuring the onset melting temperatures of five pure metal reference materials (Sn, Zn, Al, Ag, and Au). A known amount of each material is placed in a separate alumina DSC crucible. The melting behavior is measured by performing two consecutive 5 °C min⁻¹ heating cycles. A calibration curve is generated within the operating software by regression of the differences between the average of onset temperatures in the duplicate measurements of each reference material and the known melting temperature using a quadratic equation. The calibration curve is used within the NETZSCH Proteus® software to automatically adjust temperatures measured in subsequent analyses. The calibration is updated frequently using new measurements of the reference metals.

A control chart of temperature calibrations performed over time has been maintained to track repeatability and detect long-term drift of the DSC performance and degradation of the reference materials. Twenty calibration curves generated over a six-year period are plotted in Figure 1a as ΔT = nominal - measured with quadratic regression curves that replicate calibration curves generated within the instrument software. The variance in ΔT for each reference material that is shown in Figure 1a indicates measurement reproducibility and bias over this period. Results of measurements on September 8, 2021 (blue circles) and March 23, 2022 (red circles) are highlighted to represent the range of deviations in melting temperatures of individual standards that were measured. The double-

headed arrows show the residuals for several data points in regressions of two calibration curves. The measured melting temperature of the aluminum reference was usually higher than the nominal value of 660.3 °C (ΔT < 0) and resulted in positive parabolic fits for all but three calibrations.

The residuals for each reference material in the series of calibrations are plotted in Figure 1b. Lines are drawn connecting values for individual reference metals to guide the eye and indicate variations over time. All but three of the 100 calculated differences of $\Delta T = \Delta T$ nominal - ΔT fit (corresponding to 97% of the measurements) are less than 2 °C and do not show a significant trend over time. Both the precision and accuracy of calibration curves calculated using the individual calibration curves are within 2 °C over this time span and across this temperature range: the accuracy based on representing the combined results for five reference metals used to generate the curve and the precision based on the consistency of 100 calibrations. No trends are evident in the individual measurements or regression curves, and the uncertainty in the temperatures that are determined is random.

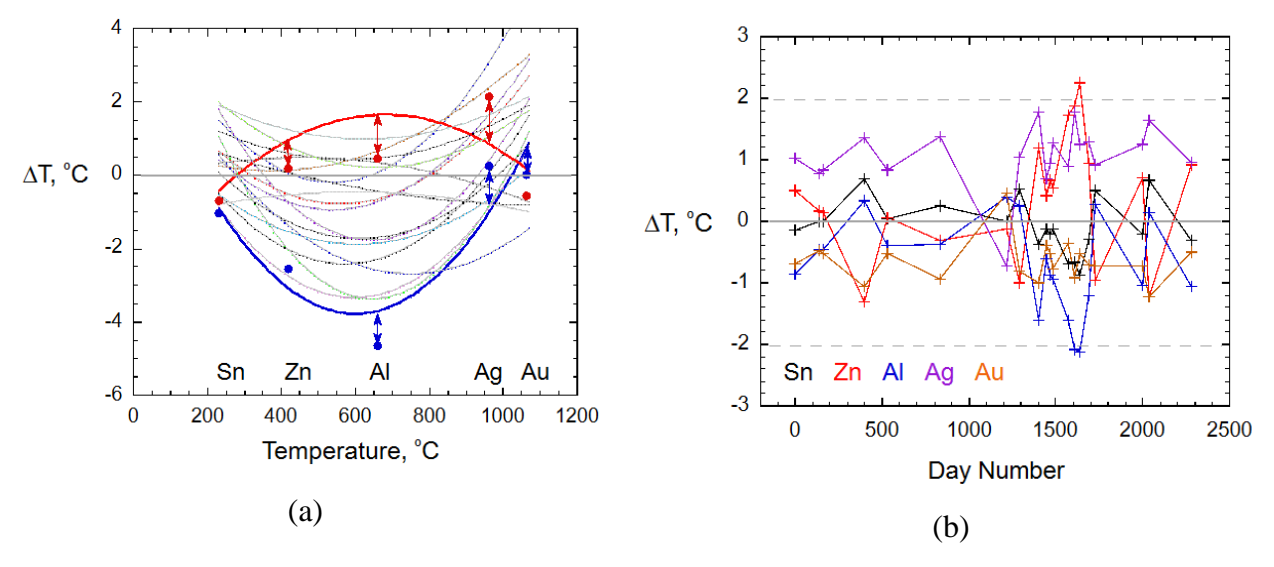


Figure 1. Calibration results showing (a) differences between measured and nominal melting temperatures of five reference materials with regression curves and (b) residuals for each reference material in calibrations spanning 2278 days.

3.1.3 Uncertainty Analysis

An uncertainty budget based on temperature calibration data and measurements of FLiNaK [8] is shown in Table 1. Adjustment of the measured DSC temperatures using the calibration curve is considered to be accurate to within 2 °C across this temperature range based on results for each reference metal. The precision of the calibration curve is also 2 °C over this temperature range. The expanded uncertainty of 2.04 °C is calculated by using the RSS method to combine these contributions to uncertainty.

Table 1. Uncertainty budget for thermal analyses of FLiNaK

Variable,	Source of Uncertainty	Expanded	Units	Uncertainty	Probability	Sensitivity
x_i		Uncertainty		Type	Distribution	Coefficient $\partial T/\partial x_i$
		$u(x_i)$				
T	Expanded uncertainty in	2.00	°C	Random	Normal	1.00
	temperature due to calibration					
	Random uncertainty due to six	0.40	°C	Random	Normal	1.00
	measurements of salt					
U(T)	Total Expanded Uncertainty	2.04	°C			

Thermal analyses of FLiNaK, FLiNaK-L, and FLiNaK-H salts were performed previously [5,8] by loading hermetically sealed gold crucibles containing salt samples onto the instrument sample carrier. The DSC was programmed to perform three heating cycles at the same heating rates used in the temperature calibration procedure. Prepared samples of each salt were heated and cooled over the ranges of 390–575 °C to ensure complete melting then solidification occurred during each heating cycle. Three samples of each salt mixture were analyzed and NETZSCH Proteus® software was used to calculate all transition temperatures.

Figure 2a shows the heat flow measurements during two sequential runs at 5 °C min⁻¹ (Ramp 1 and Ramp 2) made previously with each of the three samples of FLiNaK, FLiNaK-L, and FLiNaK-H salts. The vertical lines mark the averages of transition temperatures determined for three samples of each mixture. Lower onset of melting and liquidus point temperatures were measured for both FLiNaK-L and FLiNaK-H compared to those of FLiNaK, for which the onset of melting and liquidus point temperatures were 454.9 °C and 475.9 °C, respectively. Plots of heat flow measurements of FLiNaK-L and FLiNaK-H are shown on expanded scales in Figures 2b and 2c, respectively. A small peak is detected with an onset at 445 °C in analyses with both FLiNaK-L and FLiNaK-H salts. An additional pre-peak with an onset near 419 °C is observed in measurements with FLiNaK-H. Calculated averages and expanded uncertainties of transition temperatures for each salt mixture are reported in Tables 2, 3, and 4. Differences in melting onsets and liquidus endpoints for all salt mixtures are greater than the measurement uncertainty with the exceptions of two pairs of average temperatures: first, the melting onset of FLiNaK and the Transition 2 onset of FLiNaK-L and second, the Transition 1 onset of FLiNaK-L and the Transition 2 onset of FLiNaK-H.

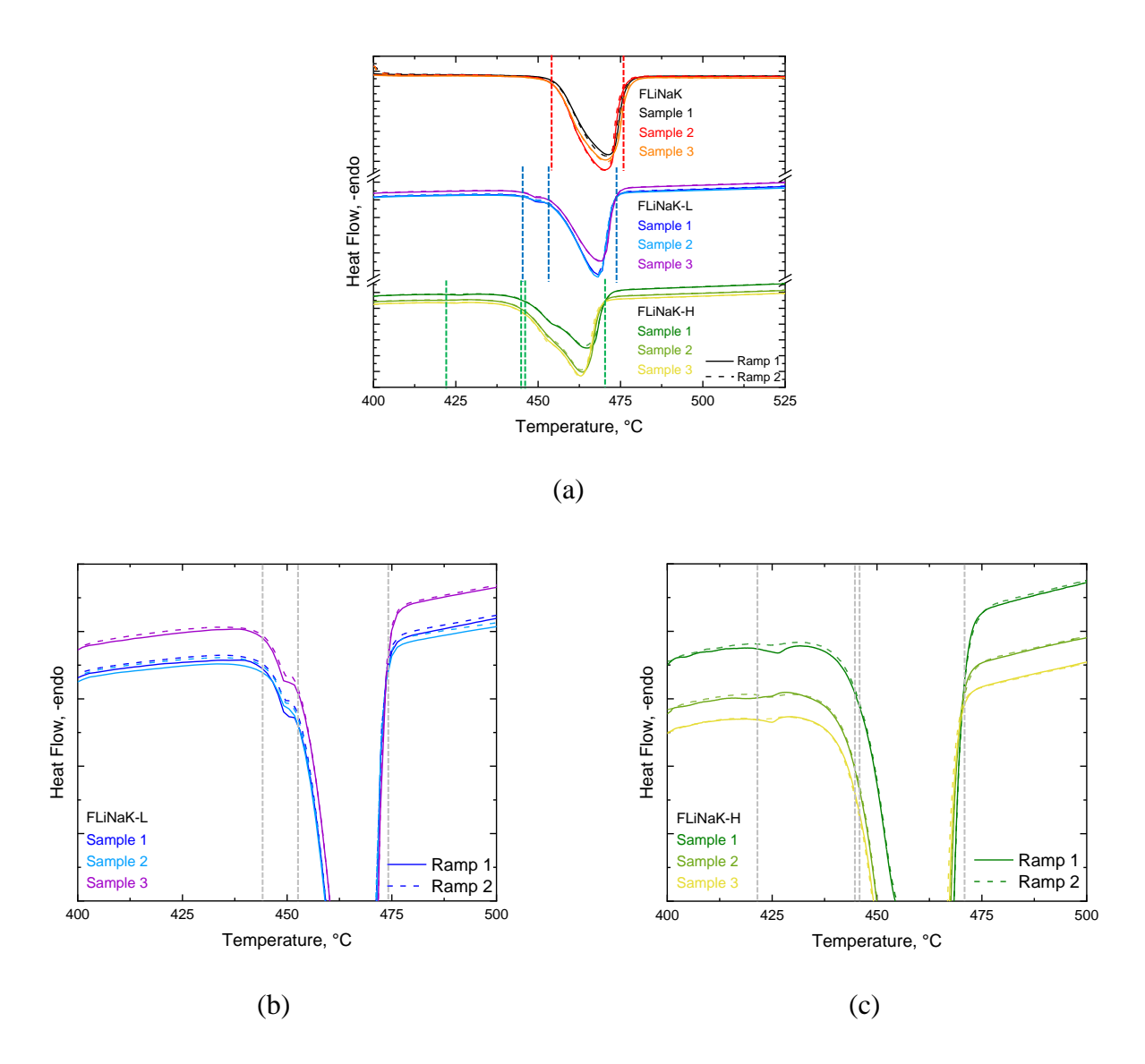


Figure 2. DSC responses of (a) FLiNaK, FLiNaK-L, and FLiNaK-H salt and expanded plots of (b) FLiNaK-L and (c) FLiNaK-H responses showing onset of melting [5].

Table 2. Measured transition temperatures of FLiNaK salt, in °C [8]

Sample	Mass ma	Dun	Onset	Liquidus
No.	Mass, mg	Run	Temperature, °C	Endpoint, °C
1	1 21.55	454.4	475.1	
1	21.33	2	454.3	474.6
2	21.51	1	455.1	477.1
2	21.31	2	455.0	475.8
3	21.22	1	455.4	476.4
3	21.23	455.4	476.5	
		Average	454.9	475.9
Expanded Uncertainty			2.0	2.1

Table 3. Measured transition temperatures of FLiNaK-L salt, in °C [5]

Sample No.	Mass, mg	Ramp	Transition 1 Onset	Transition 2 Onset	Liquidus Endpoint
1	22.20	1	445.3	454.4	•
1	22.28	2	445.4	454.3	
2	22.14	1	445.6	454.5	472.2
2	22.14	2	445.3	454.5	472.3
3	22.16	1	445.0	453.6	473.1
3	22.10	2	445.1	453.6	472.9
Average		445.3	454.2	472.5	
Expanded Uncertainty			2.0	2.0	2.0

Table 4. Measured transition temperatures of FLiNaK-H salt, in °C [8]

Sample No.	le No. Mass, mg	Domn	Transition 1	Transition 2	Transition 3	Liquidus
Sample No.	wass, mg	Ramp	Onset	Onset	Onset	Endpoint
1	22.19	1	420.1	444.5	446.7	470.2
1	22.19	2	420.2	444.0	446.0 470.6	470.6
2	22.21	1	416.8	444.7	446.4	468.7
2	22.21	2	420.0	445.3	446.7	468.8
3	21.06	1	421.0	444.8	445.8	468.3
3	21.86	2	418.3	445.1	446.4	467.7
	Average		419.4	444.9	446.3	469.1
Expanded Uncertainty		2.4	2.0	2.0	2.2	

3.1.4 Effect of Heating Rate on Thermal Transitions

Limitations in heat transfer efficiency during DSC measurements result in a small temperature difference between the sample and the temperature sensor that contributes to uncertainty in the temperature measurement. This temperature gradient increases with increased heating rate and can affect calibrations and associated corrections. The effect of this thermal lag on measured transition temperature was measured by performing thermal analyses at several heating rates. Measurements of five reference metals (Sn, Zn, Al, Ag, and Au) were performed at four different heat rates (1, 3, 5, and 10 °C min⁻¹). Thermograms of the aluminum reference metal measured at different heating rates are shown in Figure 3. Peak broadening and positive shifts in melting onsets and liquidus endpoints to higher temperatures in measurements performed at higher heating rates are attributed to increased lag of the thermocouple response due to thermal resistance.

Melting onsets were calculated by using Proteus® DSC software and reported as differences in temperature plotted as $\Delta T = \text{nominal} - \text{measured}$ for all reference metals and heating rates are shown in Figure 4. Linear fits were applied to determine y-intercepts representing melting points of individual reference materials corresponding to heating rates of 0 °C min⁻¹ such that effects of thermal lag are eliminated [9]. Melting onsets of reference metals calculated from measurements at different heating rates are reported in Table 5. Decreases in calculated melting onsets in measurements performed at lower heating rates are attributed to decreases in thermal lag.

Parabolic fits to melting onset data collected at different heating rates are used in the DSC software to correct measured temperatures for day-to-day variations in instrument performance and environmental conditions. The effect of the heating rate on the calibration curve (rather than on individual reference materials) was used to determine the effect of the lag on measured salt values. A comparison of parabolic fits of data collected at different heating rates is shown in Figure 5a. Residuals of the curve fits at temperatures corresponding to the reference materials are plotted in Figure 5b and residual sum of squares values (RSS) for the data sets are given in the legend. The RSS values show the accuracy of the fits over the temperature range do not improve at heating rates below 5 °C min⁻¹. Although temperature calibrations using measurements at low heating rates are expected to decrease effects of thermal lag, the differences between heating rates below 5 °C min⁻¹ are within the overall measurement uncertainty. Extended thermal cycles using slow heating rates increase effects of environmental and instrumental instabilities during measurements. Performing temperature calibrations and salt measurements at a heating rate of 5 °C min⁻¹ provides an appropriate compromise to decrease thermal lag and maintain system stability.

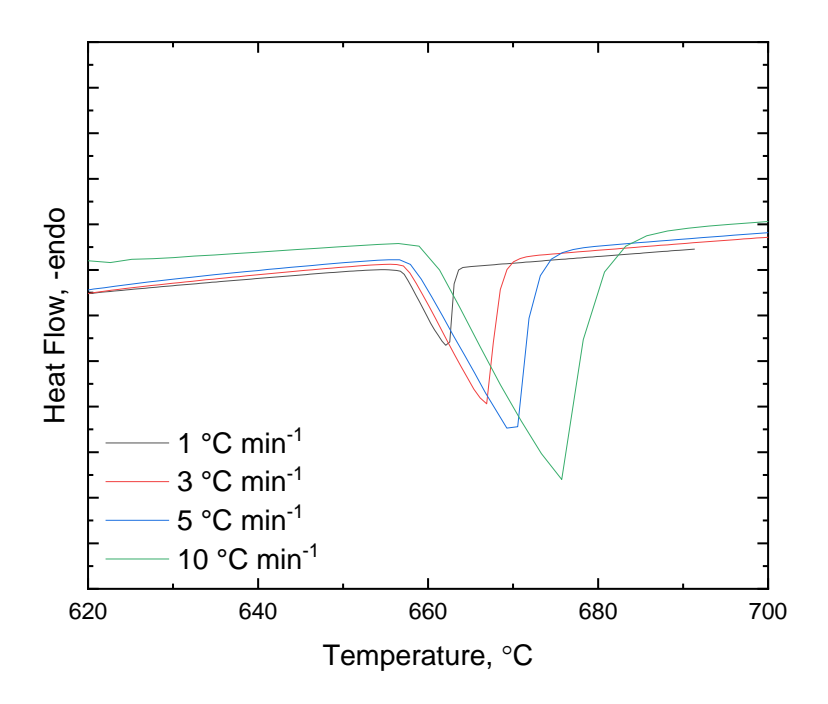


Figure 3. Thermal analyses of an aluminum reference sample performed at four different heating rates.

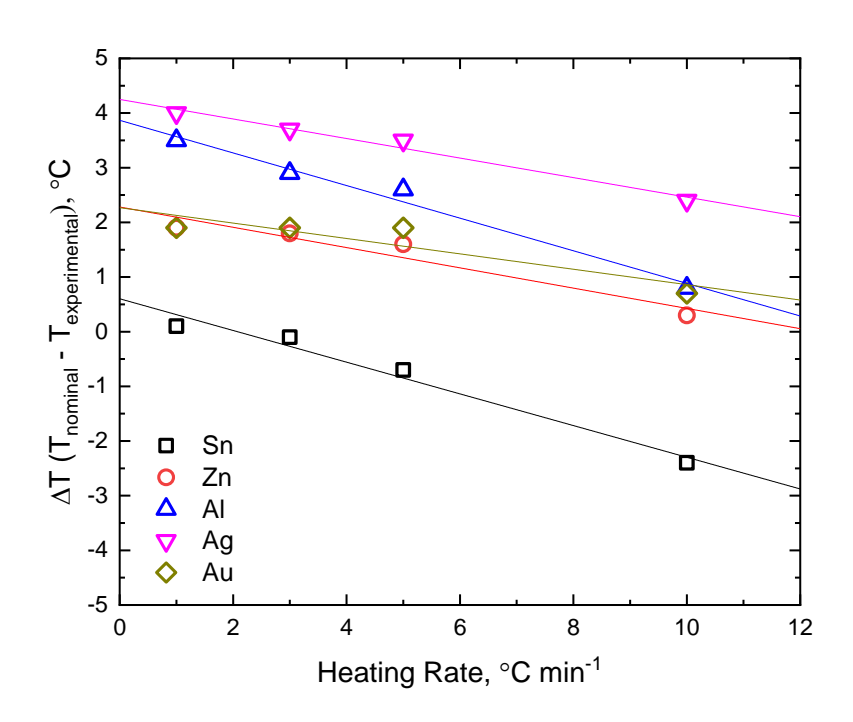


Figure 4. Melting onsets of reference metals measured at different heating rates.

Table 5. Melting onsets of reference metals measured at different heating rates

Heating Rate,			Melting Onset	, °C	
°C min ⁻¹	Sn	Zn	Al	Ag	Au
10	234.3	419.3	659.5	959.4	1063.5
5	232.6	418	657.7	958.3	1062.3
3	232	417.8	657.4	958.1	1062.3
1	231.8	417.7	656.8	957.8	1062.3
0^*	231.3	417.3	656.4	957.6	1061.9
Reference Value	231.9	419.6	660.3	961.8	1064.2

^{*}Linear extrapolations were used to calculate melting onset temperatures corresponding to 0 °C min⁻¹

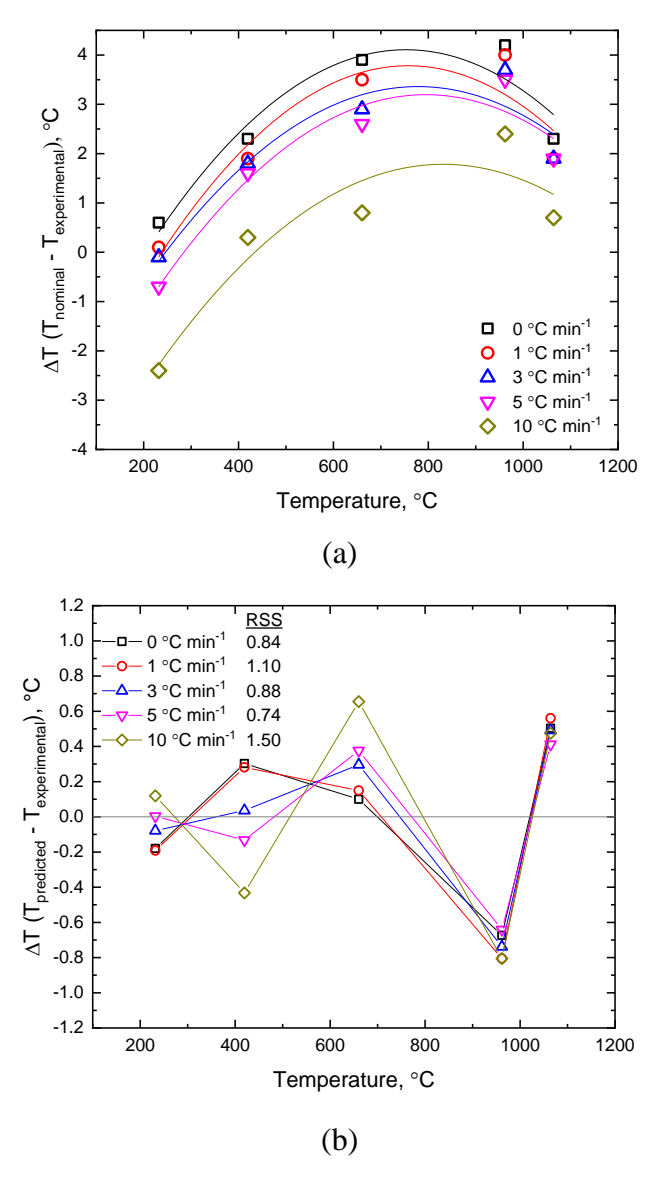


Figure 5. (a) Parabolic fits of melting onset temperatures from measurements of five reference metals at different heating rates and (b) associated residuals at each temperature and heating rate

The uncertainty in DSC measurements of molten salt is affected by the measures required to control salt purity during preparation and measurements. Contamination of salt by moisture or oxygen is mitigated by preparing salts and performing measurements in an inert atmosphere glovebox. Preferential volatilization of some salt components during heating alters the salt composition, requiring the use of sealed cells. Use of a control chart of calibrations performed over time facilitates the tracking of measurement repeatability, drift in DSC responses, and degradation of reference materials. Calibrations and salt measurements should be performed using the same heating rate. The availability of a well-characterized reference salt would facilitate uncertainty assessment activities. A new test method for DSC measurements of molten salts addressing these factors is needed to standardize procedures and analyses performed by end users.

3.2 Density

3.2.1 Method

The densities of molten salts are being measured at Argonne by using the Archimedes method. This method is based on the fact that an upward buoyant force acting on an object submerged in a fluid is equal to the weight of the fluid it displaces, which decreases the measured weight of the object due to gravity. In this hydrostatic method, the mass of a solid bob of known volume is measured in a gas space and again when fully immersed in the molten salt and compared. The difference in measured weights corresponds to the mass of fluid that is displaced. The density of the molten salt is calculated from the volume of the bob that displaced an equal volume of salt by using Equation 5, where m_a is the measured mass of the bob in a gas space, m_s is the measured mass of the bob immersed in molten salt, V is the volume of the bob at room temperature, ρ_{bob} is the density of the bob material (a nickel bob was used for measurements of FLiNaK-L and FLiNaK-H) at room temperature (nickel: 8.91 g cm⁻³, tungsten: 19.25 g cm⁻³) [10–11], α_{bob} is the thermal expansion of the bob material (nickel: 1.3×10^{-5} K⁻¹, tungsten: 4.4×10^{-6} K⁻¹) [12–13], and ΔT is the difference between the temperature of the bob and room temperature. The volume of the bob was calculated by weighing the bob at room temperature and dividing by the known density of the bob material.

$$\rho(T) = \frac{m_a - m_s}{V(1 + \alpha_{bob}\Delta T)^3} = \frac{(m_a - m_s)\rho_{bob}}{m_a(1 + \alpha_{bob}\Delta T)^3}$$
(5)

Density measurements of FLiNaK-L and FLiNaK-H were performed by using two different bob and wire pairs for each salt. Heavier bobs (40 g) were paired with the thinner wire (0.1 mm) and lighter bobs (24 g) were paired with the thicker wire (0.2 mm).

3.2.2 Uncertainty Analysis

Uncertainty budgets for density measurements of FLiNaK, FLiNaK-L, and FLiNaK-H at each measurement temperature were used to quantify expanded uncertainties. The uncertainty budget for density measurements of FLiNaK performed at 500 °C is shown in Table 6. The uncertainty in

measured mass is affected by the resolution of the balance and the standard deviation of 10 mass measurements of the suspended bob in the gas space or immersed in salt at different temperatures. The uncertainty in the temperature is due to the resolution of the furnace temperature controller, the calibration of the furnace set points, the uncertainty of the type K thermocouple, and the stability of the equilibrated temperature. Sensitivity coefficients for all quality-affecting variables were calculated by taking partial derivatives of Equation 5. The combined standard uncertainty u_c for the density of FLiNaK at 500 °C was calculated by using Equation 6. The expanded uncertainty was calculated by multiplying the combined standard uncertainty by a coverage factor of 1.96, corresponding to 95% confidence. The expanded uncertainty of 8.10E-3 g cm⁻³ corresponds to a relative uncertainty of 0.4%. The largest contributions to the expanded uncertainty are from the uncertainties in the density of the bob material and measured temperature.

Expanded uncertainties in density measurements of FLiNaK, FLiNaK-L, and FLiNaK-H at each measurement temperature are reported in Tables 7–9. The relative uncertainties at all measurement temperatures for all salts are less than 1.5%. The densities and expanded uncertainties for replicate measurements of different salt mixtures are shown in Figure 6. The densities of FLiNaK-L and FLiNaK-H are higher than those for FLiNaK without fission product dopants and the differences exceed the uncertainties in the measurements. However, differences in the densities in measurements FLiNaK-L 2, FLiNaK-H 2, and FLiNaK-H 4 made using thin wires are less than the measurement uncertainties. The presence of fission products impacts the density of FLiNaK, but effects of low and high concentrations are indistinguishable. Measured values used to calculate expanded uncertainties for all salt mixtures at all measurement temperatures are provided in Appendix B.

Other factors that could affect the density measurement include interfacial effects between the molten salt and wire such as wetting. These data, and data collected for other salts with other paired sets of bobs and wires, indicated the need to further investigate the effects of bob mass, wire diameter, and interfacial properties on measured density to accurately differentiate effects of fission products and impurity contents.

Density measurements of FLiNaK-H were repeated due to the relatively large difference between measurements made using the first two bob and wire sets [5]. The repeated measurements (FLiNaK-H 3 and FLiNaK-H 4) closely matched the initial measurements (FLiNaK-H 1 and FLiNaK-H 2). The greater differences in measurements of FLiNaK-L and FLiNaK-H made with different bob and wire sets compared to measurements with FLiNaK indicated there were effects of bob mass and wire diameter. Calculations to take surface tension effects into account using a proposed term based on measurements of multiple bob and wire pairs showed they were either negative or within the measurement uncertainty [5]. The effect of bob weight and wire diameter on measured densities and surface tension values are further discussed in section 3.2.3.

Table 6. Uncertainty budget for density measurements of FLiNaK performed at 500 °C

Source of Uncertainty	Standard	Units	Uncertainty	Probability	Sensitivity
	Uncertainty		Type	Distribution	Coefficient $\partial \rho / \partial x_i$
	$u(x_i)$				
Balance resolution	5.77E-4	g	Random	Rectangular	4.64E-1
Standard deviation of 10 mass	2.98E-4	g	Random	Normal	4.64E-1
measurements of the bob and					
wire in salt					
Controller resolution	5.77E-2	°C	Random	Rectangular	1.47E-4
Furnace calibration	5.77E-1	°C	Systematic	Rectangular	1.47E-4
Thermocouple uncertainty	3.75	°C	Systematic	Rectangular	1.47E-4
Temperature stability	2.50E-1	°C	Random	Normal	1.47E-4
Uncertainty in density of the bob	1.73E-2	g cm ⁻³	Systematic	Rectangular	2.36E-1
material					
Uncertainty in thermal expansion	5.77E-8	°C ⁻¹	Systematic	Rectangular	5.44E3
of the bob material					
Combined Standard Uncertainty	4.13E-3	g cm ⁻³			
Coverage Factor	1.96				
Expanded Uncertainty	8.10E-3	g cm ⁻³			
	Balance resolution Standard deviation of 10 mass measurements of the bob and wire in salt Controller resolution Furnace calibration Thermocouple uncertainty Temperature stability Uncertainty in density of the bob material Uncertainty in thermal expansion of the bob material Combined Standard Uncertainty Coverage Factor	Uncertainty $u(x_i)$ Balance resolution5.77E-4Standard deviation of 10 mass measurements of the bob and wire in salt2.98E-4Controller resolution5.77E-2Furnace calibration5.77E-1Thermocouple uncertainty3.75Temperature stability2.50E-1Uncertainty in density of the bob material1.73E-2Uncertainty in thermal expansion of the bob material5.77E-8Combined Standard Uncertainty Coverage Factor4.13E-31.96	Uncertainty $u(x_i)$ Balance resolution5.77E-4gStandard deviation of 10 mass measurements of the bob and wire in salt2.98E-4gController resolution Furnace calibration5.77E-2°CFurnace calibration5.77E-1°CThermocouple uncertainty3.75°CTemperature stability2.50E-1°CUncertainty in density of the bob material1.73E-2g cm-3Uncertainty in thermal expansion of the bob material5.77E-8°C-1Combined Standard Uncertainty Coverage Factor4.13E-3g cm-31.96	$\begin{array}{c ccccccccccccccccccccccccccccccccccc$	Uncertainty $u(x_i)$ TypeDistributionBalance resolution $5.77E-4$ gRandomRectangularStandard deviation of 10 mass measurements of the bob and wire in salt $2.98E-4$ gRandomNormalController resolution Furnace calibration $5.77E-2$ °CRandomRectangularThermocouple uncertainty Temperature stability 3.75 °CSystematic CRectangularUncertainty in density of the bob material $1.73E-2$ g cm $^{-3}$ Systematic Corbined Standard UncertaintyRectangularCombined Standard Uncertainty Coverage Factor $4.13E-3$ 1.96g cm $^{-3}$ SystematicRectangular

^{*}The standard deviation of 10 mass measurements of the bob and wire in the gas space was zero and therefore was not included in the uncertainty budget.

$$u_{c} = \sqrt{\left(\frac{\partial \rho}{\partial m_{a}} \cdot u(m_{a})\right)^{2} + \left(\frac{\partial \rho}{\partial m_{s}} \cdot u(m_{s})\right)^{2} + \left(\frac{\partial \rho}{\partial \rho_{bob}} \cdot u(\rho_{W})\right)^{2} + \left(\frac{\partial \rho}{\partial \alpha_{bob}} \cdot u(\alpha_{bob})\right)^{2} + \left(\frac{\partial \rho}{\partial \Delta T} \cdot u(\Delta T)\right)^{2}}$$
(6)

Table 7. Densities and expanded uncertainties calculated for FLiNaK

Temperature,	Density, g cm ⁻³			
$^{\circ}\mathrm{C}$	FLiNaK 1	FLiNaK 2		
500	2.130 ± 0.008	2.122 ± 0.008		
550	2.106 ± 0.008	2.093 ± 0.008		
600	2.076 ± 0.008	2.063 ± 0.008		
650	2.046 ± 0.008	2.035 ± 0.007		
700	2.015 ± 0.008	2.006 ± 0.007		

Table 8. Densities and expanded uncertainties calculated for FLiNaK-L

Temperature,	Density, g cm ⁻³			
°C	FLiNaK-L 1	FLiNaK-L 2		
500	2.250 ± 0.024	2.197 ± 0.025		
550	2.206 ± 0.024	2.176 ± 0.024		
600	2.154 ± 0.023	2.151 ± 0.024		
650	2.113 ± 0.022	2.134 ± 0.024		
700	2.085 ± 0.022	2.116 ± 0.024		
800	1.972 ± 0.021	2.084 ± 0.023		
900	1.910 ± 0.020	2.043 ± 0.023		

Table 9. Densities and expanded uncertainties calculated for FLiNaK-H

Temperature,	Density, g cm ⁻³				
°C	FLiNaK-H 1	FLiNaK-H 2	FLiNaK-H 3	FLiNaK-H 4	
500	2.366 ± 0.025	2.252 ± 0.025	2.410 ± 0.025	2.265 ± 0.024	
550	2.357 ± 0.025	2.212 ± 0.025	2.397 ± 0.024	2.242 ± 0.024	
600	2.338 ± 0.025	2.177 ± 0.024	2.400 ± 0.024	2.218 ± 0.024	
650	2.327 ± 0.024	2.150 ± 0.024	2.335 ± 0.024	2.195 ± 0.024	
700	2.317 ± 0.024	2.123 ± 0.024	2.312 ± 0.024	2.159 ± 0.023	
800	2.262 ± 0.024	2.071 ± 0.023	2.260 ± 0.023	2.098 ± 0.023	
900	2.221 ± 0.023	2.028 ± 0.023	2.236 ± 0.023	2.071 ± 0.023	

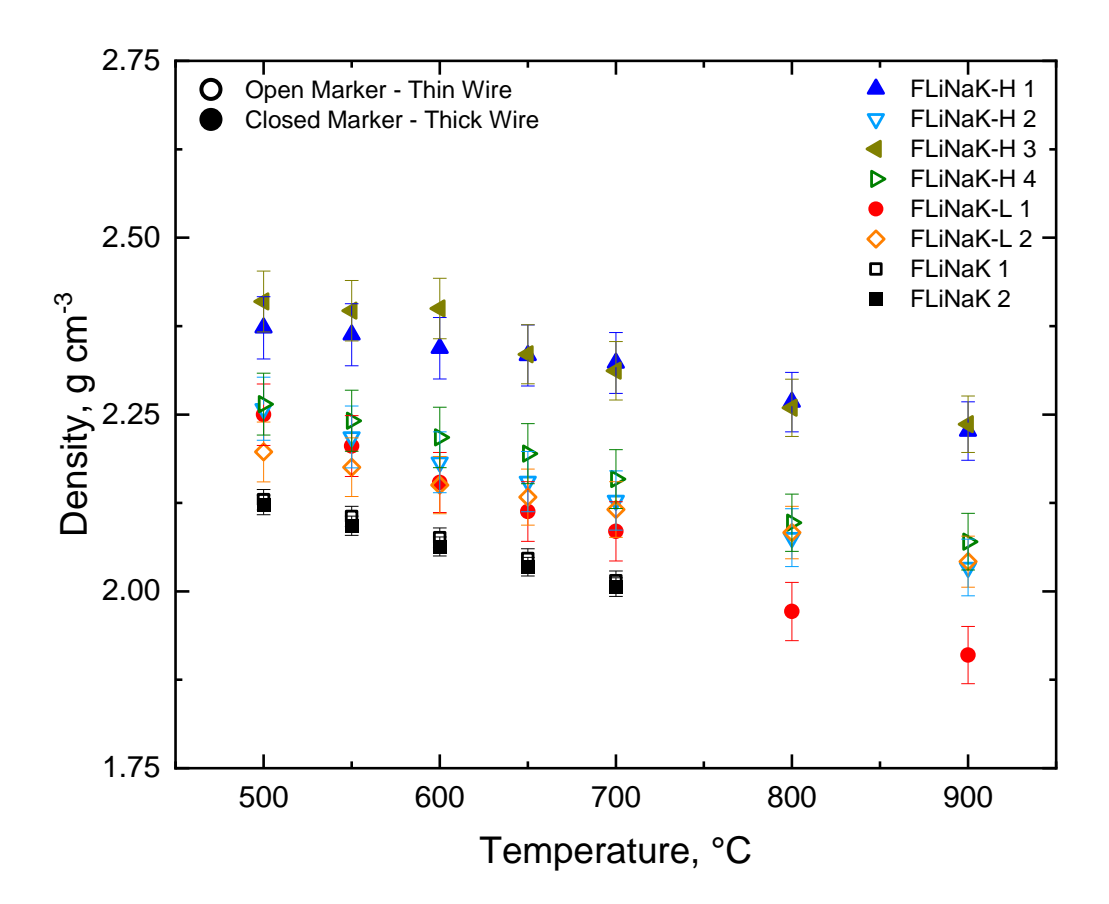


Figure 6. Densities of FLiNaK, FLiNaK-L, and FLiNaK-H salts measured at different temperatures with different bob and wire sets.

3.2.3 Effects of Bob Mass, Wire Diameter, and Surface Tension

An equation to take surface tension into account in Archimedes density measurements of molten salts was first used by Cheng et al. [14]. Surface tension values for molten salts have been calculated previously by using Equation 7, where D is the diameter of the wire, σ is the surface tension, and g is acceleration due to gravity. Because the density of molten salt is independent of the bob and wire used to measure it, measurements made with different bobs and wires have been used to determine the contribution of the surface tension term, as expressed in Equation 8. However, the use of this equation to determine surface tension effects on measurements of molten salts has generated inconsistent results [5].

$$\rho = \frac{\Delta m(T) + \frac{\pi D \sigma(T)}{g}}{V(1 + \alpha \Delta T)^3}$$
(7)

$$\frac{\Delta m_1(T) + \frac{\pi D_1 \sigma(T)}{g}}{V(1 + \alpha \Delta T)^3} = \frac{\Delta m_2(T) + \frac{\pi D_2 \sigma(T)}{g}}{V(1 + \alpha \Delta T)^3}$$
(8)

Density measurements of water were made following the same procedure used for molten salts to assess the effects of surface tension and wire diameter on measured density. The effectiveness of Equation 7 to quantify surface tension effects was assessed by performing density measurements of water with and without the addition of a liquid dish soap surfactant to intentionally change the surface tension. Measurements were made with the bob at different immersion depths.

Density measurements of water were performed at ambient temperature by using three tungsten bobs of different weights (40, 32, and 24 g) paired with wires of three different diameters (0.050, 0.025, and 0.0125 cm). Each bob and wire pair was suspended from the underside of a balance (Mettler-Toledo, Columbus, OH), weighed in air, and then weighed when immersed in water. The top of each immersed bob was maintained 1 cm below the surface of the water in all measurements. Ten mass measurements were performed over the course of a five-minute period in both air and water. The densities of water calculated by using Equation 5 without the surface tension term and by using Equation 7 including the surface tension term are shown in Table 10. All calculated values are within 0.006 g cm⁻³ of the reference value (0.998 g cm⁻³) [15] and within the uncertainty of the measurement (0.012 g cm⁻³ – uncertainty analyses of water measurements are reported in Appendix B). Differences in densities including the surface tension term are within the uncertainty of the measurement. The values of the surface tension derived from the measurements are included in Table 10.

Additional density measurements of water were performed to investigate the effect of bob depth and wire diameter on calculated density. Measurements were performed by using the smallest bob (24 g) and wires of 0.05 cm and 0.0125 cm diameters. Measurements were performed at different immersion depths by adjusting the distance between the top of the immersed bob and the surface of the water. The connection of the wire at the top of the bob was completely immersed in all measurements. Density measurements made with the bob using wires of two diameters are shown in Figure 7. The slopes of the fit lines indicate the effect of fluid displaced by the wire and the y-intercepts indicate the effect of fluid displaced by the bob alone. The effect of the thicker wire is more than 2000-times greater than the effect of the thinner wire. The densities measured using the 0.050-cm diameter wire increased by nearly 0.014 g cm⁻³ as the immersion depth increased to 4 cm, whereas densities measured using the 0.0125-cm diameter wire increased by less than 0.003 g cm⁻³. In the set of measurements with each diameter of wire, the effect of surface tension was the same for measurements at all depths (πd) , but the volume of fluid displaced by the length of immersed wire increased proportional to the immersion depth $(\pi d^2h/4)$. The use of a thin wire minimizes the interfacial perimeter between the wire and water at the surface and use of a large bob minimizes the proportion of fluid displaced by the immersed wire relative to that displaced by the immersed bob. The masses and other quantities used in density measurements of water and uncertainty analyses are tabulated in Appendix B).

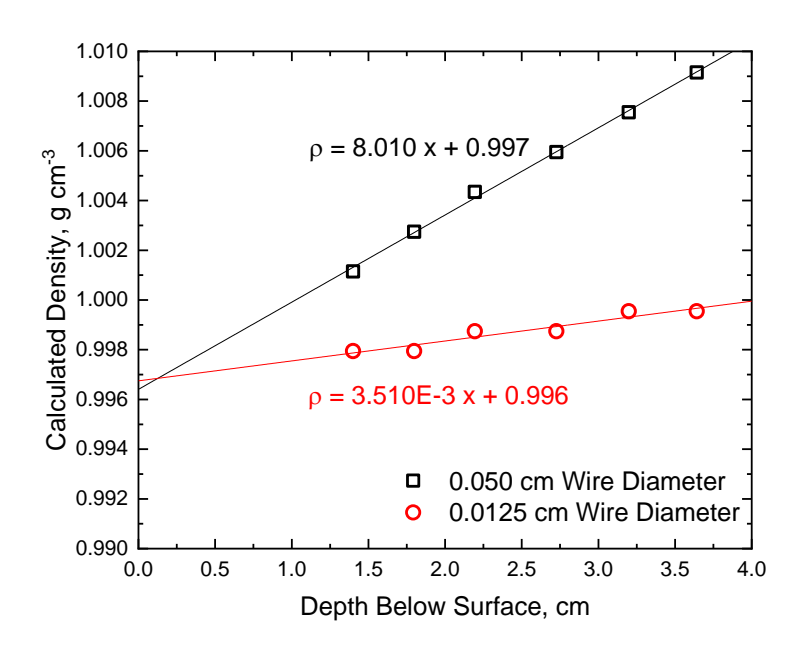


Figure 7. Density of water measured with two different bob and wire pairs at different immersion depths.

Table 10. Densities of demineralized water with and without the surface tension term

	Wires Paired by Diameter, cm	Densities without Surface Tension Term, Eq. 5 g cm ⁻³	Density with Surface Tension Term, Eq. 7 g cm ⁻³	Calculated Surface Tension, Eq. 7 mN m ⁻¹	
	Thick 0.0500	0.998	1.002	50	
	Medium 0.025	1.000			
Heavy Bob	Thick 0.0500	0.998	0.997	-17	
(40 g)	Thin 0.0125	0.997	0.997		
, 0,	Medium 0.0250	1.000	0.994	150	
	Thin 0.0125	0.997	0.774	-152	
	Thick 0.0500	0.997	0.997	0	
	Medium 0.0250	0.997	0.997	U	
Medium Bob	Thick 0.0500	0.997	1.001	33	
(32 g)	Thin 0.0125	1.000	1.001		
	Medium 0.0250	0.997	1.002	102	
	Thin 0.0125	1.000	1.002		
	Thick, 0.0500	0.996			
	Medium 0.0250	0.999	1.001	37	
Light Bob	Thick 0.0500	0.996	0.990	-50	
(24 g)	Thin 0.0125	0.992		30	
	Medium 0.0250	0.999	0.984	-228	
	Thin 0.0125	0.992	U.70 1	-220	

Densities of water containing 2 wt% liquid dish soap calculated using Eq. 5 are shown in Table 11. These values are within 0.003 g cm⁻³ of the reference value for water and consistent within the uncertainty of the measurement. Densities of water containing 2 wt% liquid dish soap calculated using Eq. 7 with the surface tension term are also shown in Table 11. Differences in densities calculated from measurements with different wire pairs are within the measurement uncertainty. The differences in calculated surface tension due to the addition of dish soap were negligible. A comparison of densities of clean and soapy water calculated without the surface tension term is reported in Table 12. Density measurements made with different wires are not sufficiently sensitive to calculate surface tension values of fluids with properties similar to water.

Table 11. Densities of water containing 2 wt% liquid dish soap with and without the surface tension term

Bob	Wires Paired by Diameter, cm	Densities Without Surface Tension Term, Eq. 5 g cm ⁻³	Density With Surface Tension Term, Eq. 7 g cm ⁻³	Calculated Surface Tension, mN m ⁻¹	
	Thick 0.0500	0.998			
	Medium 0.0250	1.000	1.002	50	
Heavy	Thick 0.0500	0.998			
Bob (40 g)	Thin 0.0125	1.000	1.001	42	
(10 8)	Medium 0.0250	1.000			
	Thin 0.0125	1.000	- 1.001	25	
Medium Bob (32 g)	Thick 0.0500	0.995	1.001	62	
	Medium 0.0250	0.998	- 1.001		
	Thick 0.0500	0.995	1.001	50	
	Thin 0.0125	0.999	1.001	59	
	Medium 0.0250	0.998,	1.000	£ 1	
	Thin 0.0125	0.999	- 1.000	51	
	Thick 0.0500	0.998	0.002		
Light Bob (24 g)	Medium 0.0250	0.996	- 0.993	-37	
	Thick 0.0500	0.998	1.000		
	Thin 0.0125	1.000	1.000	17	
	Medium 0.0250	0.996	1.004	107	
	Thin 0.0125	1.000	1.004	127	

Table 12. Densities of clean and soapy water without the surface tension term, in g cm⁻³

	Wires Paired by Diameter, cm	Density			
	Brameter, em	Clean Water	Soapy Water		
	Thick 0.0500	0.998	0.998		
	Medium 0.0250	1.000	1.000		
Heavy	Thick 0.0500	0.998	0.998		
Bob (40 g)	Thin 0.0125	1.000	0.997		
ζ ζ,	Medium 0.0250	1.000	1.000		
	Thin 0.0125	1.000	0.997		
	Thick 0.0500	0.995	0.997		
	Medium 0.0250	0.998	0.997		
Medium	Thick 0.0500	0.995	0.997		
Bob (32 g)	Thin 0.0125	0.999	1.000		
	Medium 0.0250	0.998	0.997		
	Thin 0.01250	0.999	1.000		
	Thick 0.0500	0.998	0.996		
	Medium 0.0250	0.996	0.999		
Light Bob (24 g)	Thick 0.0500	0.998	0.996		
	Thin 0.0125	1.000	0.992		
· · · · ·	Medium 0.0250	0.996	0.999		
	Thin 0.0125	1.000	0.992		

Densities measured for FLiNaK over the temperature ranges of 550–650 °C using different wire/bob combinations were reported previously by Argonne [8]. The densities were calculated using Equation 7 with a surface tension term, which has since been determined to be inappropriate . Therefore, the density values reported in ANL/CFCT-21/20 should be revised.

Regarding differences in measurements of FLiNaK-H 1, 2, 3 and 4 seen in Figure 6, the immersion depth was not controlled and cannot be deconvolved from other sources of uncertainty. Moreover, the use of thicker wire increases the probability of wire bends and defects inducing contact with the feedthrough surfaces. Therefore, measurements with the thicker wire are considered to be less

accurate than measurements using thinner wire. Measurements of FLiNaK-H 1 and 3 were made using wires of 0.2 mm diameter and measurements of FLiNaK-H 2 and 4 used wires of 0.1 mm diameter. Therefore measurements FLiNaK-H 2 and 4 are considered to be more accurate. Comparing measurements FLiNaK-H 2 and 4 with measurements of FLiNaK-L indicates that any difference in density due to increasing dopant concentrations at these levels is indistinguishable from the measurement uncertainty.

A variety of factors affecting the quality of data generated during Archimedes density measurements of molten salts have been evaluated throughout the process of method development and uncertainty analysis and several best practices are highlighted. Temperature set points of furnaces should be checked prior to measurements of molten salts to provide confidence that salts are maintained at prescribed temperatures and density measurements are not affected by temperature gradients. This avoids the use of an immersed thermocouple, which would introduce a significant heat sink. The use of a furnace and heat shield equipment to maintain a uniform salt temperature prevents visual inspection of the crucible and bob during the measurement. Alignment of the furnace and suspended bob, therefore, must be performed prior to heating the salt. That the balance remained level must be inspected each time the balance platform is raised and lowered to confirm proper operation after lifting. The use of a thin wire (i.e., < 5% of the mass of the bob) decreases the effect of immersing the wire, minimizes surface tension effects, and decreases the likelihood of warping or contact between the wire and the crucible wall or furnace surfaces. The diameter and strength of the wire must be sufficient to support the weight of the suspended bob at high temperatures. The effect of immersion depth on calculated density should be investigated and quantified as part of the bob and wire selection process.

3.3 Thermal Diffusivity

3.3.1 Method

Thermal diffusivity of molten salts is measured at Argonne by using the laser flash method [5]. Samples are prepared by loading known amounts of salt into two-piece graphite cells that are fabricated at Argonne. Graphite cells are dimensioned by using a digital micrometer. Thermal diffusivity measurements are performed by using a laser flash analyzer (LFA) model Discovery Light Flash 1200 (TA Instruments, New Castle, DE) that is evacuated and backfilled with ultra-high purity argon. The procedure for performing thermal diffusivity measurements of liquids provided in ASTM E2585 [16] was followed. The sample is heated to a target temperature and allowed to stabilize, after which a heat pulse is applied to the underside of the cell by a neodymium glass laser. The transient heat is conducted through the salt and the temperature change at the top of the cell is measured by using an indium antimonide infrared detector cooled with liquid nitrogen. The temperature rise over time is recorded by using FlashLineTM software. The Clark and Taylor model [17] is used by the software to derive thermal diffusivity from the measured temperature rise profile, specifically, based on the time to reach one-half the maximum temperature (the half-rise time). Three laser pulses are applied to each prepared sample once equilibrated at a target temperature.

The response of the LFA is periodically checked by measuring the thermal diffusivity of a molybdenum standard reference material coated with graphite spray to increase absorption and emission. Thermal diffusivities measured at different temperatures are compared to accepted values that were certified by the vendor to confirm the instrument response is within acceptable bounds. Out-of-bounds measurements indicate a need for instrument maintenance including checking the conditions of the optical windows and vacuum system.

3.3.2 Uncertainty Analysis

Uncertainty budgets for thermal diffusivity measurements of FLiNaK, FLiNaK-L, and FLiNaK-H at each measurement temperature were used to quantify expanded uncertainties. The uncertainty budget for thermal diffusivity measurements of FLiNaK performed at 500 °C is shown as an example in Table 13. The uncertainty in the measurement time is affected by the resolution of the LFA timer. The measured temperature is influenced by the resolution of the controller used to heat the sample and the uncertainty of the type S thermocouple probe in the heated zone. The uncertainty in the thickness of the prepared salt sample is affected by the resolution of the micrometer and the standard deviation of four measurements of the crucible thickness. Although the cell is designed to maintain a uniform thickness of salt, the melting and freezing of salt during preparation and analysis can result in distortions in the cell that increase the variance in the measurements. The variance in thermal diffusivities measured with different samples of each salt is attributed to small differences in thickness of the salt layers. The uncertainty due to thickness is calculated as the standard deviation of all thermal diffusivity measurements performed with different samples at each temperature.

Sensitivity coefficients for the half-rise time and salt thickness were calculated by taking partial derivatives and applying Equation 4. The sensitivity coefficient for temperature $\partial D/\partial T$ was calculated as the slope of a linear equation fitted to measured data for FLiNaK at all temperatures. The slopes of fitted equations used as sensitivity coefficients in uncertainty analyses of each salt are reported in Appendix C. The expanded uncertainty of 1.05E-4 cm² s⁻¹ for FLiNaK at 500 °C corresponds to a relative uncertainty of 8.3%. The largest contributions to the expanded uncertainty are from distortions in the salt layer and uncertainties in the environmental temperature.

Average thermal diffusivities and expanded uncertainties for FLiNaK, FLiNaK-L, and FLiNaK-H between 500 and 900 °C are shown in Figure 8. The measured values, averages, and expanded uncertainties are also reported in Table 14. Similar temperature dependencies in measurements of the three salt mixtures are observed. The maximum relative uncertainties in measurements of FLiNaK, FLiNaK-L, and FLiNaK-H at all temperatures are 8.3%, 8.8%, and 11.6%, respectively. The presence of fission products measurably impacts the thermal diffusivity of FLiNaK at temperatures below 700 °C.

Table 13. Uncertainty budget for thermal diffusivity measurements of FLiNaK performed at 500 $^{\circ}\mathrm{C}$

Variable,	Source of Uncertainty	Standard	Units	Uncertainty	Probability	Sensitivity
\mathcal{X}_{i}		uncertainty u(x _i)		Type	Distribution	Coefficient
						$\partial D/\partial x_{\rm i}$
<i>t</i> _{1/2}	LFA timer resolution	5.77E-06	S	Random	Rectangular	1.08E-04
L	Micrometer resolution	5.77E-07	m	Random	Rectangular	7.75E-03
	1s value for 4 measurements of	4.00E-06	m	Random	Normal	7.75E-03
	crucible thickness					
	Uncertainty due to distortions in	5.25E-05	$cm^2 s^{-1}$	Random	Normal	1.00
	salt thickness					
T	Controller resolution	5.77E-02	°C	Random	Rectangular	2.16E-06
	Type S Thermocouple uncertainty	8.66E-01	°C	Systematic	Rectangular	2.16E-06
$u_{\rm c}$	Combined Standard Uncertainty	5.26E-5	cm ² s ⁻¹			
k	Coverage Factor	1.96				
U(D)	Expanded Uncertainty	1.03E-4	$cm^2 s^{-1}$			

$$u_{c} = \sqrt{\left(\frac{\partial D}{\partial t_{1/2}} \cdot u(t_{1/2})\right)^{2} + \left(\frac{\partial D}{\partial L} \cdot u(L)\right)^{2} + \left(\frac{\partial D}{\partial T} \cdot u(T)\right)^{2}}$$
(9)

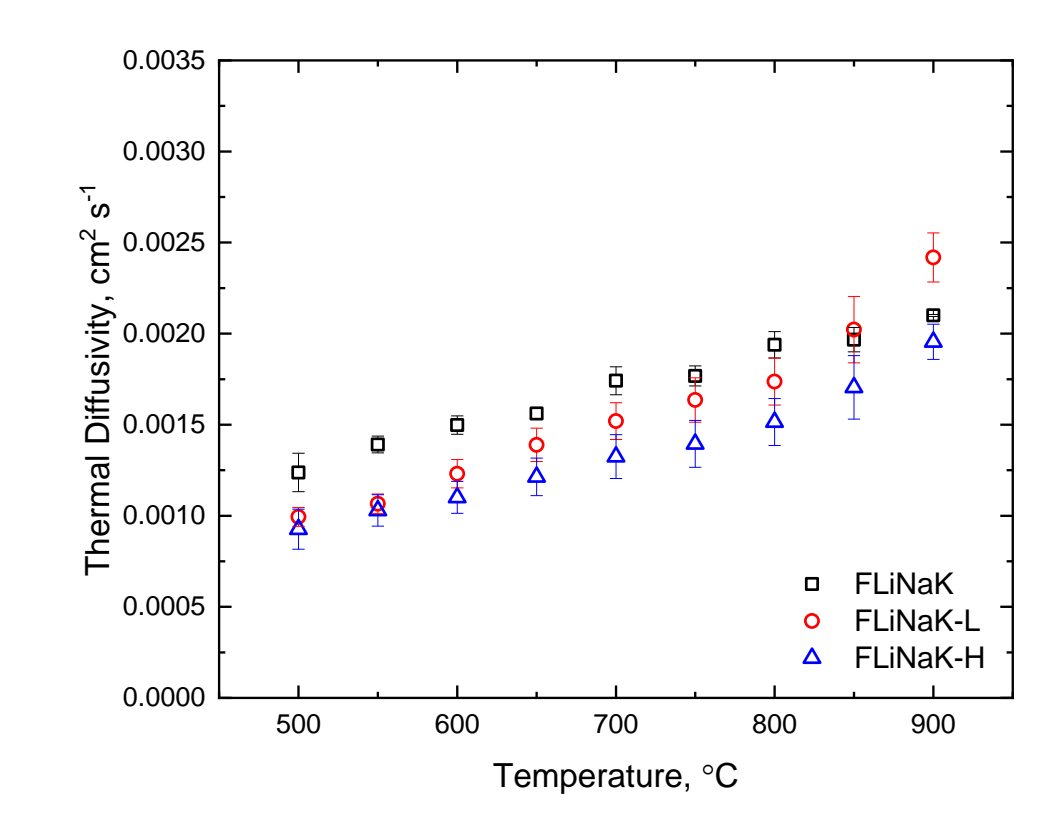


Figure 8. Average thermal diffusivities and expanded uncertainties for FLiNaK, FLiNaK-L, and FLiNaK-H.

Factors affecting thermal diffusivity measurements have been identified during method development and corresponding measures to control or take these effects into account are recommended. Periodic instrument response checks with a certified reference material provide confidence that errors associated with various instrument effects are controlled. Improvements in cell design that decrease the impact of salt volatilization, minimize interactions between the salt and crucible, and improve thermal contact would lead to better control of salt-induced distortions.

Table 14. Thermal diffusivities and expanded uncertainties calculated for FLiNaK, FLiNaK-L, and FLiNaK-H

Temperature, °C	Thermal Diffusivity, cm ² s ⁻¹						
Temperature, C -	FLiNaK	FLiNaK-L	FLiNaK-H				
500	1.24E-3 ± 1E-4	$1.0E-3 \pm 5E-5$	9.3E-4 ± 1E-4				
550	$1.39E-3 \pm 5E-5$	$1.1E-3 \pm 5E-5$	$1.0E-3 \pm 8E-5$				
600	$1.50E-3 \pm 5E-5$	$1.2E-3 \pm 8E-5$	$1.1E-3 \pm 9E-5$				
650	$1.56E-3 \pm 3E-5$	$1.4E-3 \pm 9E-5$	$1.2E-3 \pm 1E-4$				
700	$1.74E-3 \pm 8E-5$	$1.5E-3 \pm 1E-4$	$1.3E-3 \pm 1E-4$				
750	$1.77E-3 \pm 5E-5$	$1.6E-3 \pm 1E-5$	$1.4E-3 \pm 1E-4$				
800	$1.94E-3 \pm 7E-5$	$1.7E-3 \pm 1E-4$	$1.5E-3 \pm 1E-4$				
850	$1.97E-3 \pm 7E-5$	$2.0E-3 \pm 2E-4$	$1.7E-3 \pm 2E-4$				
900	$2.10E-3 \pm 6E-6$	$2.4E-3 \pm 1E-4$	$2.0E-3 \pm 9E-5$				

3.4 Viscosity

3.4.1 Method

Viscosities of molten salts are measured at Argonne by using the rotating cylinder method (ANL-CFCT/24-23). In this method, a nickel spindle is immersed within the molten salt maintained at a prescribed temperature and rotated at a known velocity to measure the resistance of a thin layer of salt to flow in the annular region between the spindle and the inner wall of a cylindrical nickel crucible. The torque required to maintain a given spindle velocity is measured by the viscometer. The viscosity μ is calculated by using Equation 10, where M is the measured torque, R_c is the inner radius of the crucible, R_b is the radius of the spindle, L is the spindle length, and ω is the imposed rotational velocity.

$$\mu = \frac{M(R_c^2 - R_b^2)}{4\pi R_c^2 R_b^2 L\omega} \tag{10}$$

Viscosity measurements are performed by using a DV2T-LV viscometer (AMETEK Brookfield, Middleborough, MA) mounted on a height-adjustable stand and a Kerr ElectroMelt furnace housed within an ultra-high purity argon atmosphere radiological glovebox. A known amount of salt is loaded into a cylindrical nickel crucible that was previously dimensioned and placed in the furnace. The horizontal levels of both the furnace and the viscometer are checked by using bubble levels. The spindle is then suspended from the viscometer and axially aligned with the crucible [5].

Use of Equation 10 requires that laminar flow exist in the annular region between the spindle and crucible. Measurements are performed at seven different rotational velocities at each temperature of interest in the range of 500–900 °C to determine if laminar flow occurred during the measurement.

Laminar flow is indicated by a linear increase in shear stress and the measured torque with increasing rotational velocity. Velocities that are too high will generate turbulence and velocities that are too low will result in end effects that disrupt laminar flow in the annulus and produce non-linear increases in shear stress with increasing rotational velocity. The order of the rotational velocities at which measurements are performed in each set is random to avoid any systematic effects that might not be detected by making regular incremental increases or decreases in velocity. Measurements performed at several velocities are repeated to confirm stability (e.g., salt composition) [5].

3.4.2 Instrument Calibration

The response of the viscometer was calibrated prior to performing measurements with FLiNaK 1 FLiNaK 2, FLiNaK-L, and FLiNaK-H by performing viscosity measurements with a silicone reference oil (Cannon Instrument Co., State College, PA). Measurements of the silicone oil were used quantify the effects of instrumental sensitivity and possible bias on the calculated viscosity. The viscosity of the reference fluid (4.8 cP) at room temperature is within the range of values measured for FLiNaK at temperatures relevant to MSR operation. Known amounts of silicone oil were loaded into the crucible and a series of measurements performed at rotational velocities in the range of 50–80 rpm. Measurements were repeated at 50, 60, and 70 rpm to check for consistency in measured torques. Viscosities were calculated by using torque values measured at different velocities and averages were then calculated for each data series [5].

Measured torques and calculated viscosities of silicone reference oil are shown in Figure 9. Repeated measurements at 50, 60, and 70 rpm within each data set are plotted with larger markers for visibility. Letter designations used in the legend entries refer to which of three viscometers (labeled A, B, and C) was used to perform each series of measurements. The numbers in the legend indicate the set of oil measurements that were performed prior to measurements with FLiNaK (1 and 2), FLiNaK-L (3) and FLiNaK-H (4). Torque values increase linearly with increasing rotational velocity, as seen in Figure 9a, and indicate laminar flow conditions were maintained at all velocities. The dashed line in Figure 9b represents the reference viscosity value of 4.8 cP for the silicone oil. The differences in measured viscosities of oil and the reference value are attributed to differences in the accumulated wear of the instrument bearings and gyration of the coupling rod. These instrumental effects are unavoidable when measuring salt viscosities at high temperatures due to the required length and strength of the rod. High temperature measurements require the use of long coupling rods to avoid heating the viscometer head and measurements of salt require spindles with high mass to achieve suitable torque values [5]. Wear on the bearings limits the service life of the viscometer head.

A correction was applied to viscosity values of molten salts to take bias in torque measurements into account. The correction term was calculated as the difference in the average viscosity of oil measured with each viscometer and the reference viscosity value. Viscosities of silicone reference oil and calculated correction terms for each data set are reported in Table 15. The uncertainty associated with the measurements are calculated as the 2s value of oil viscosities measured.

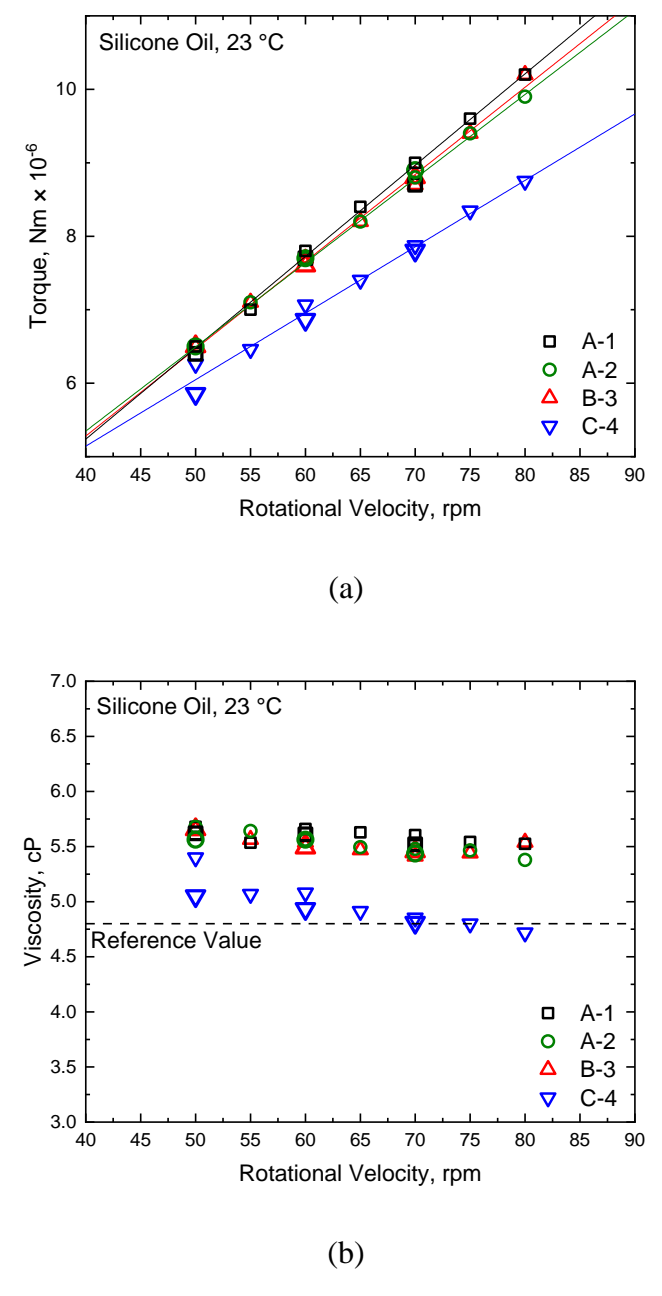


Figure 9. Measured torque (a) and calculated viscosity (b) of silicone reference oil used to calibrate the response of viscometers used in salt measurements [5].

Table 15. Calculated viscosities for silicone reference oil measurements [5]

		Viscos	sity, cP	
Rotational Velocity, rpm	A-1	A-2	B-3	C-4
60	5.7	5.6	5.5	5.1
55	5.5	5.6	5.6	5.1
80	5.5	5.4	5.5	4.7
70	5.6	5.5	5.4	4.9
50	5.7	5.7	5.7	5.4
75	5.5	5.5	5.4	4.8
65	5.6	5.5	5.5	4.9
70	5.7	5.4	5.5	4.8
60	5.5	5.6	5.5	4.9
50	5.5	5.6	5.7	5.1
Uncertainty	0.2	0.2	0.2	0.4
Average	5.6	5.5	5.5	5.0
Average – 4.8 cP Reference (Bias Correction)	0	0.8	0.7	0.2

3.4.3 Uncertainty Analysis

Uncertainty budgets for viscosity measurements of FLiNaK 1, FLiNaK 2, FLiNaK-L, and FLiNaK-H with and without fission products at each measurement temperature were used to quantify expanded uncertainties. The uncertainty budget for viscosity measurements of FLiNaK 1 performed at 500 °C and 60 rpm, is shown as an example, in Table 16. Uncertainty in the torque is affected by the resolution of the viscometer and variance associated with eight measurements. Uncertainties in dimensions of the crucible and spindle are due to the resolution of the measurement instrument (e.g., calipers, bore gauge) and quantified using the standard deviation of multiple measurements. The uncertainty in the temperature is due to the resolution of the furnace, the furnace calibration, and the uncertainty of the thermocouple. The sensitivity coefficients for the rotational velocity, torque, and dimensions of the spindle and crucible were calculated by taking partial derivatives of Equation 10. The sensitivity coefficient for temperature, $\partial \mu / \partial T$, was calculated by differentiating the temperaturedependent exponential fits of average measured viscosity values, examples of these fits can be seen in Figure 10. The temperature-dependent functions of viscosity generated for each salt and the calculated sensitivity coefficients used in uncertainty analyses are reported in Appendix D. The uncertainty in the viscometer calibration, μ_{cal} , was calculated based on analyses of calibrations performed with silicone reference oil. The combined standard uncertainty was calculated by using Equation 11. The expanded uncertainty of 3.79E-1 cP was determined by multiplying the combined standard uncertainty by a coverage factor of 1.96, corresponding to 95% confidence.

Table 16. Uncertainty budget for viscosity measurements of FLiNaK 1 performed at 500 °C and 60 rpm

Variable x_i	Source of Uncertainty	Standard	Units	Probability	Sensitivity
		Uncertainty $u(x_i)$		Distribution	Coefficient $\partial \mu / \partial x_i$
ω	Velocity resolution	6.05E-3	s ⁻¹	Rectangular	1.51E-3
M	Viscometer resolution	3.89E-8	Nm	Rectangular	6.92E2
	Standard deviation of 8 measurements of torque	2.38E-8	Nm	Normal	6.92E2
	at each velocity				
R_b	Caliper resolution	5.77E-6	m	Rectangular	3.95
	Standard deviation of 6 measurements of	1.22E-5	m	Normal	3.95
	spindle radius				
$R_{\rm c}$	Bore gauge resolution	5.77E-6	m	Rectangular	2.56
	Standard deviation of 6 measurements of	2.04E-5	m	Normal	2.56
	crucible radius				
L	Caliper resolution	5.77E-6	m	Rectangular	1.90E-1
	Standard deviation of 4 measurements of	1.50E-5	m	Normal	1.90E-1
	spindle length				
Τ	Temperature controller resolution	5.77E-2	°C	Rectangular	6.63E-2
	Furnace temperature calibration	5.77E-1	$^{\circ}\mathrm{C}$	Rectangular	6.63E-2
	Thermocouple uncertainty	2.17	$^{\circ}\mathrm{C}$	Rectangular	6.63E-2
u_{cal}	Viscometer calibration	1.15E-4	Pa-s	Rectangular	1.00
Ис	Combined Standard Uncertainty	1.93E-1	cР		
ζ	Coverage factor	1.96			
$U(\mu)$	Expanded Uncertainty	3.79E-1	cР		

$$u_{c} = \sqrt{\left(\frac{\partial \mu}{\partial \omega} \cdot u(\omega)\right)^{2} + \left(\frac{\partial \mu}{\partial M} \cdot u(M)\right)^{2} + \left(\frac{\partial \mu}{\partial R_{b}} \cdot u(R_{b})\right)^{2} + \left(\frac{\partial \mu}{\partial R_{c}} \cdot u(R_{c})\right)^{2} + \left(\frac{\partial \mu}{\partial L} \cdot u(L)\right)^{2} + \left(\frac{\partial \mu}{\partial T} \cdot u(T)\right)^{2} + \left(\frac{\partial \mu}{\partial \mu_{cal}} \cdot u(\mu_{cal})\right)^{2}}$$

$$(11)$$

Expanded uncertainties in viscosity measurements of FLiNaK 1, FLiNaK 2, FLiNaK-L, and FLiNaK-H are reported in Table 17. The uncertainty reported at each temperature represents the maximum uncertainty of those calculated for measurements of a salt at the 10 different rotational velocities. The standard uncertainties of the temperature and of the viscometer calibration have the greatest impact on the combined standard uncertainty. The viscosities of FLiNaK-L and FLiNaK-H are greater than those for FLiNaK without fission product dopants at each temperature. Measured values used to calculate expanded uncertainties in viscosity values for all salt mixtures are provided in Appendix D.

Table 17. Bias-corrected viscosities and expanded uncertainties calculated for FLiNaK1, FLiNaK 2, FLiNaK-L, and FLiNaK-H

Temperature,	Viscosity, cP					
$^{\circ}\mathrm{C}$	FLiNaK 1	FLiNaK 2	FLiNaK-L	FLiNaK-H		
500	9.2 ± 0.4	9.1 ± 0.4	10.2 ± 0.4	10.8 ± 0.6		
550	6.4 ± 0.3	6.5 ± 0.3	7.0 ± 0.3	7.2 ± 0.5		
600	4.6 ± 0.3	4.5 ± 0.3	5.4 ± 0.3	5.5 ± 0.5		
650	3.6 ± 0.3	3.5 ± 0.3	4.1 ± 0.3	4.4 ± 0.5		
700	2.8 ± 0.3	2.7 ± 0.3	3.7 ± 0.3	3.7 ± 0.5		
800	2.0 ± 0.3	1.9 ± 0.2	2.8 ± 0.3	2.6 ± 0.5		
900	1.5 ± 0.3	1.6 ± 0.2	2.4 ± 0.2	1.9 ± 0.5		

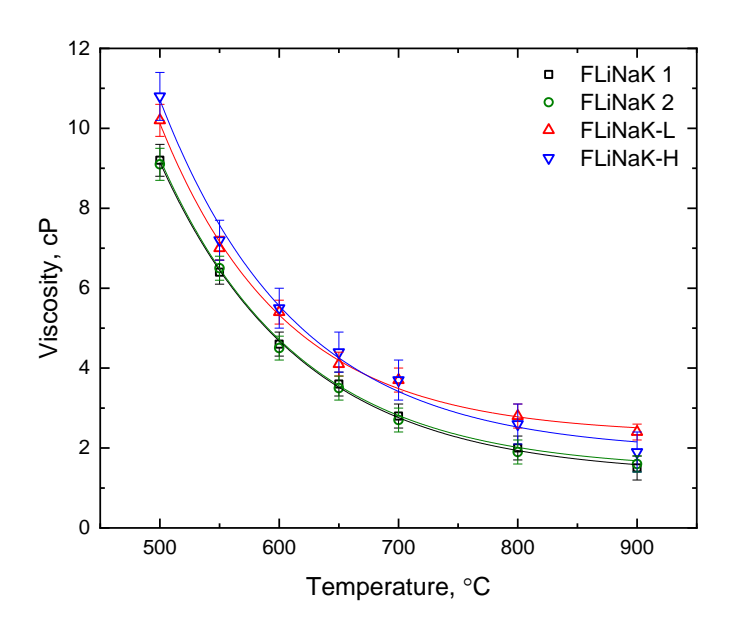


Figure 10. Bias-corrected viscosities of FLiNaK 1, FLiNaK 2, FLiNaK-L, and FLiNaK-H at different temperatures with expanded uncertainties.

Control of factors influencing quality-affecting variables in viscosity measurements of molten salt is required for the generation of reliable property data. The use of high rotational velocities can induce turbulence in the fluid, which manifests as a non-linear increase in shear stress with increasing rotational velocity [18]. Equation 10 is not applicable to responses measured in turbulent flow. Laminar flow at a wide range of rotational velocities is maintained by using a cell having a narrow gap between the spindle and the crucible walls. Increased spindle immersion depth increases the drag on the rotating shaft, which spuriously increases measured torque. This effect is mitigated by maintaining the top of the immersed spindle near the surface of the salt. The salt temperature must be controlled to within a prescribed threshold. However, the presence of a thermocouple probe in the salt disrupts the steady flow during spindle rotation. The temperature can be controlled by performing furnace set point calibrations at temperatures of interest prior to viscosity measurements. A long drive shaft is needed to avoid heating the viscometer head, which increases gyration. Effects of gyration and bearing wear on measured values can be determined by performing measurements with a reference fluid using same apparatus used for molten salts to determine a bias correction factor. The bias factor determined from measurements with silicone oil can be applied to measurements made in a molten salt with the same viscometer, drive shaft, and spindle size.

4. Conclusion

Uncertainty analyses of molten salt property measurements made previously at Argonne were performed to demonstrate application of quantification methods to measured data to add confidence that sources of measurement error have been identified and taken into account for reported property values. Sources of error in property measurements of molten FLiNaK, FLiNaK-L, and FLiNaK-H salts were identified and expanded uncertainties quantified using replicate measurements, calibrations, and known equipment accuracies and sensitivity limits. Prominent factors affecting some measurements were investigated separately to assess contributions to uncertainty, including the effect of heating rate on thermal lag in DSC responses, the effects of bob mass and wire thickness on density measurements, and viscometer wear and shaft gyration on viscosity measurements. Recommendations suitable for use in the development of standard test methods for property measurements of molten salts are made to minimize and quantify experimental uncertainties and to distinguish effects of salt composition (e.g., contaminants) and environmental factors (e.g., temperature) on the property values that are determined.

Acknowledgements

This work was conducted under the auspices of the DOE Advanced Reactor Technologies Molten Salt Reactors campaign and is issued to meet program milestone M3AT-25AN0705011.

This work was conducted at Argonne National Laboratory and supported by the U.S. Department of Energy, Office of Nuclear Energy, under Contract DE-AC02-06CH11357.

References

- [1] D. Holcomb, W. Poore, and G. Flanagan, Fuel Qualification for Molten Salt Reactors, NUREG/CR-7299, ORNL/TM-2022/2754, US Nuclear Regulatory Commission (2022).
- [2] W.L. Ebert and M.A. Rose, Data Quality of Salt Property Measurements, ANL/CFCT-21/18, Argonne National Laboratory (2021).
- [3] M.A. Rose, E. Wu, and M.A. Williamson, Thermophysical Property Measurements: Improved Density, Viscosity and Thermal Diffusivity Methods, ANL/CFCT-20/38, Argonne National Laboratory (2020).
- [4] M.A. Rose, L.D. Gardner, and T.T. Lichtenstein, Property Measurements of NaCl-UCl₃ and LiF-NaF-KF Molten Salts Doped with Surrogate Fission Products, ANL/CFCT-23/23, Argonne National Laboratory (2023).
- [5] L.D. Gardner, K.A. Chamberlain, and M.A. Rose, Property Measurements of LiF-NaF-KF Molten Salts Doped with Surrogate Fission Products, ANL/CFCT-24/23, Argonne National Laboratory (2024).
- [6] R.S. Figliola and D.E. Beasley, Theory and Design for Mechanical Measurements, 2nd Ed., John Wiley and Sons (1995).
- [7] Evaluation of measurement data Guide to the expression of uncertainty in measurement, JCGM 100:2008, Bureau International des Poids et Mesures (2008).
- [8] M.A. Rose, J.A. Krueger, T.T. Lichtenstein, E. Wu, and L.D. Gardner, Precision of Property Measurements with Reference Molten Salts, ANL/CFCT-21/20, Argonne National Laboratory (2021).
- [9] G.W.H. Höhne, W.F. Hemminger, H.-J. Flammersheim (2003). <u>Differential Scanning Calorimetry</u>, 2nd ed., Springer, New York, NY.
- [10] L. Jordan and W.H. Swanger, Properties of Pure Nickel, *J. Res. Natl. Bur. Stand.*, **5**, 6 (1930), https://dx.doi.org/10.6028/jres.005.075.
- [11] P. Tolias and EUROfusion MST1 Team, Analytical expressions for thermophysical properties of solid and liquid tungsten relevant for fusion applications, *Nucl. Mater. En.*, **13**, 42-57 (2017), http://dx.doi.org/10.1016/j.nme.2017.08.002.
- [12] T.G. Kollie, Measurement of the thermal-expansion coefficient of nickel from 300 to 1000 K and determination of the power-law constants near the Curie temperatures, *Phys. Rev. B*, **16**, 11 (1977), https://doi.org/10.1103/PhysRevB.16.4872.
- [13] R.H. Knibbs, The measurement of thermal expansion coefficient of tungsten at elevated temperatures, *J. Phys. E: Sci. Inst.*, **2**, 6 (1969), https://doi.org/10.1007/BF01184332.
- [14] J.-H. Cheng, P. Zhang, X.-H. An, K. Wang, Y. Zuo, H.-W. Yan, and Z. Li, A Device for Measuring the Density and Liquidus Temperature of Molten Fluorides for Heat Transfer and Storage, *Chin. Phys. Lett.*, 30, 126501 (2013), http://dx.doi.org/10.1088/0256-307X/30/12/126501.
- [15] M. Tanaka, G. Girard, R. Davis, A. Peuto, and N. Bignell, Recommended table for the density of water between 0 C and 40 C based on recent experimental reports, *Metrologia*, **38**, 4 (2001), DOI: 10.1088/0026-1394/38/4/3.
- [16] American Society for Testing and Materials, E2585-09(2015) Standard Practice for Thermal Diffusivity by the Flash Method (2015) E 2585-09, https://doi.org/10.1520/E2585-09R15.

- [17] L.M. Clark and R.E. Taylor, Radiation loss in the flash method for thermal diffusivity, J. Appl. Phys., 46, 714–719 (1975), https://doi.org/10.1063/1.321635.
- [18] P.R.N. Childs, Rotating Flow, Elsevier Science, (2011), https://doi.org/10.1016/C2009-0-30534-6.

Appendix A: Thermal Transition Calculations

The average transition temperatures and standard deviations of FLiNaK, FLiNaK-L, and FLiNaK-H are reported in Table A.1. Standard uncertainties in temperature due to the scatter in six DSC measurements were calculated by dividing the standard deviations by $\sqrt{6}$. Linear fits of $\Delta T = T_{\text{nominal}} - T_{\text{measured}}$ for melting onsets calculated by using measurements of reference metals at different heating rates are reported in Table A.2. The y-intercepts correspond to melting onsets at a heating rate β of 0 °C min⁻¹ for which thermal lag is minimized. Table A.3 shows parabolic fits of melting onset data measured at different heating rates.

Table A.1. Average transition temperatures of FLiNaK, FLiNaK-L, and FLiNaK-H and standard uncertainties due to multiple DSC measurements

Salt Mixture	Transition	Average Temperature, °C	1 s, °C	Standard Uncertainty
FLiNaK	Melting Onset	454.9	0.5	0.2
	Liquidus Endpoint	475.9	0.9	0.4
FLiNaK-L	Transition 1 Onset	445.3	0.2	0.1
	Transition 2 Onset	Transition 2 Onset 454.2		0.2
	Liquidus Endpoint	472.5	0.4	0.2
FLiNaK-H	Transition 1 Onset	419.4	1.6	0.7
	Transition 2 Onset	444.7	0.5	0.2
	Transition 3 Onset	446.3	0.4	0.2
	Liquidus Endpoint	469.1	1.1	0.4

Table A.2. Linear fits used to calculate melting onsets corresponding to 0 °C min⁻¹

Reference Metal	Equation
Sn	$T(^{\circ}C) = -2.90\beta(^{\circ}C \ min^{-1}) + 0.60$
Zn	$T(^{\circ}C) = -0.19\beta(^{\circ}C \ min^{-1}) + 2.28$
Al	$T(^{\circ}C) = -0.30\beta(^{\circ}C \ min^{-1}) + 3.87$
Ag	$T(^{\circ}C) = -0.18\beta(^{\circ}C \ min^{-1}) + 4.25$
Au	$T(^{\circ}C) = -0.14\beta(^{\circ}C \ min^{-1}) + 2.27$

Table A.3. Parabolic fits used to correct temperature measurements based on measurements at different heating rates

Heating Rate, °C min ⁻¹	Equation
0	$T(^{\circ}C) = -3.61 + 2.05 \times 10^{-2}T - 1.36 \times 10^{-5}T^{2}$
1	$T(^{\circ}C) = -4.27 + 2.13 \times 10^{-2}T - 1.40 \times 10^{-5}T^{2}$
3	$T(^{\circ}C) = -3.82 + 1.85 \times 10^{-2}T - 1.19 \times 10^{-5}T^{2}$
5	$T(^{\circ}C) = -4.57 + 1.95 \times 10^{-2}T - 1.23 \times 10^{-5}T^{2}$
10	$T(^{\circ}C) = -6.03 + 1.88 \times 10^{-2} - 1.13 \times 10^{-5}T^{2}$

Appendix B: Density Calculations

The bob and wire measurements used in density calculations are reported in Table B.1. The wire and bob diameters were measured by using digital calipers and bob and wire masses were measured by using a balance. The volumes of the bobs were determined by dividing the mass of the bob measured on the balance at room temperature by the density of the bob material (nickel: 8.91 g cm⁻³, tungsten: 19.25 g cm⁻³) [9–10]. The masses of each bob and wire set measured while immersed in FLiNaK, FLiNaK-L and FLiNaK-H at different temperatures are reported in Tables B.2–B.3, B.4–B5, and B.6–B.9, respectively. Values for Δm were calculated by subtracting the mass of the submerged bob and wire measured at each temperature from the bob and wire masses measured in the gas space at room temperature.

Table B.1. Bob and wire masses, bob volumes, and wire diameters in the gas space at room temperature [5,8]

Salt Mixture-	Bob and Wire	Bob and Wire	Bob Volume,	Wire Diameter,
Measurement	Material	Mass, g	cm^3	mm
Number				
FLiNaK 1	Nickel	18.851	2.089	0.25
FLiNaK 2	Nickel	19.700	2.088	0.5
FLiNaK-L - 1	Tungsten	25.859	1.255	0.2
FLiNaK-L - 2	Tungsten	40.276	2.061	0.1
FLiNaK-H - 1	Tungsten	26.128	1.256	0.2
FLiNaK-H - 2	Tungsten	40.253	2.059	0.1
FLiNaK-H - 3	Tungsten	25.937	1.196	0.2
FLiNaK-H - 4	Tungsten	40.118	2.007	0.1

Table B.2. Measured immersed masses of bob and wire set 1 used in FLiNaK density measurements [8]

Measurement		Те	emperature, °	°C	
Number	500	550	600	650	700
1	14.318	14.360	14.416	14.470	14.529
2	14.318	14.358	14.415	14.470	14.530
3	14.318	14.360	14.416	14.471	14.530
4	14.318	14.360	14.416	14.470	14.529
5	14.318	14.360	14.415	14.470	14.529
6	14.318	14.360	14.416	14.470	14.529
7	14.320	14.360	14.415	14.470	14.529
8	14.318	14.361	14.416	14.470	14.527
9	14.318	14.360	14.416	14.470	14.529
10	14.316	14.360	14.417	14.469	14.529
Average	14.318	14.3599	14.4158	14.47	14.529
1s	0.0009	0.0007	0.0006	0.0005	0.0008

Table B.3. Measured immersed masses of bob and wire set 2 used in FLiNaK density measurements [8]

Measurement	Temperature, °C							
Number	500	550	600	650	700			
1	15.186	15.240	15.294	15.347	15.399			
2	15.185	15.240	15.294	15.347	15.399			
3	15.186	15.239	15.293	15.347	15.401			
4	15.185	15.240	15.293	15.346	15.401			
5	15.186	15.239	15.294	15.347	15.400			
6	15.185	15.241	15.295	15.345	15.401			
7	15.188	15.240	15.294	15.347	15.400			
8	15.186	15.242	15.295	15.348	15.399			
9	15.185	15.241	15.295	15.345	15.401			
10	15.188	15.240	15.294	15.347	15.400			
Average	15.186	15.240	15.294	15.347	15.400			
1s	0.0012	0.0009	0.0007	0.0010	0.0009			

Table B.4. Measured immersed masses of bob and wire set 1 used in FLiNaK-L density measurements [5]

Measurement			Te	mperature,	°C		
Number	500	550	600	650	700	800	900
1	23.020	23.068	23.134	23.183	23.226	23.359	23.020
2	23.017	23.069	23.133	23.180	23.214	23.358	23.017
3	23.011	23.068	23.137	23.190	23.219	23.359	23.011
4	23.016	23.070	23.136	23.185	23.213	23.354	23.016
5	23.012	23.067	23.133	23.183	23.212	23.360	23.012
6	23.020	23.065	23.134	23.184	23.219	23.356	23.020
7	23.024	23.083	23.133	23.184	23.220	23.358	23.024
8	23.005	23.071	23.136	23.182	23.230	23.360	23.005
9	23.013	23.077	23.129	23.181	23.209	23.358	23.013
10	23.028	23.069	23.134	23.190	23.216	23.358	23.028
Average	23.017	23.071	23.134	23.184	23.218	23.358	23.017
1s	0.0067	0.0054	0.0022	0.0034	0.0065	0.0018	0.0032

Table B.5. Measured immersed masses of bob and wire set 2 used in FLiNaK-L density measurements [5]

Measurement			Te	mperature,	°C		
Number	500	550	600	650	700	800	900
1	35.720	35.762	35.811	35.834	35.881	35.938	35.720
2	35.720	35.768	35.809	35.840	35.877	35.940	35.720
3	35.717	35.761	35.811	35.843	35.878	35.941	35.717
4	35.722	35.761	35.811	35.844	35.874	35.936	35.722
5	35.719	35.760	35.802	35.844	35.873	35.937	35.719
6	35.723	35.760	35.815	35.850	35.873	35.935	35.723
7	35.717	35.752	35.803	35.845	35.876	35.938	35.717
8	35.719	35.759	35.812	35.843	35.875	35.937	35.719
9	35.715	35.760	35.814	35.843	35.881	35.937	35.715
10	35.719	35.767	35.816	35.841	35.873	35.940	35.719
Average	35.719	35.761	35.810	35.843	35.876	35.938	35.719
1s	0.0024	0.0044	0.0047	0.0041	0.0031	0.0019	0.0024

Table B.6. Measured immersed masses of bob and wire set 1 used in FLiNaK-H density measurements [5]

Measurement		Temperature, °C							
Number	500	550	600	650	700	800	900		
1	23.130	23.140	23.164	23.175	23.186	23.248	23.300		
2	23.130	23.141	23.162	23.175	23.185	23.251	23.298		
3	23.130	23.142	23.161	23.174	23.184	23.250	23.299		
4	23.130	23.141	23.161	23.172	23.186	23.250	23.298		
5	23.129	23.140	23.162	23.171	23.186	23.250	23.299		
6	23.129	23.139	23.162	23.172	23.184	23.250	23.300		
7	23.130	23.139	23.161	23.171	23.184	23.250	23.299		
8	23.130	23.140	23.163	23.173	23.184	23.254	23.299		
9	23.130	23.140	23.163	23.173	23.184	23.253	23.299		
10	23.130	23.140	23.163	23.176	23.183	23.253	23.300		
Average	23.130	23.140	23.162	23.173	23.185	23.251	23.299		
1s	0.0004	0.0009	0.0010	0.0018	0.0011	0.0019	0.0007		

Table B.7. Measured immersed masses of bob and wire set 2 used in FLiNaK-H density measurements [5]

Measurement		Temperature, °C							
Number	500	550	600	650	700	800	900		
1	35.574	35.653	35.720	35.782	35.832	35.933	36.014		
2	35.573	35.653	35.729	35.780	35.832	35.933	36.016		
3	35.574	35.653	35.727	35.777	35.830	35.933	36.019		
4	35.573	35.652	35.727	35.778	35.831	35.934	36.018		
5	35.575	35.653	35.727	35.779	35.831	35.934	36.014		
6	35.575	35.653	35.727	35.777	35.832	35.934	36.016		
7	35.576	35.654	35.727	35.778	35.832	35.935	36.016		
8	35.573	35.656	35.722	35.778	35.830	35.937	36.017		
9	35.575	35.657	35.721	35.779	35.830	35.936	36.017		
10	35.575	35.656	35.724	35.778	35.831	35.936	36.018		
Average	35.574	35.654	35.725	35.779	35.831	35.935	36.017		
1s	0.0011	0.0017	0.0031	0.0015	0.0009	0.0014	0.0016		

Table B.8. Measured immersed masses of bob and wire set 3 used in FLiNaK-H density measurements [5]

Measurement		Temperature, °C							
Number	500	550	600	650	700	800	900		
1	23.042	23.050	23.046	23.121	23.147	23.210	23.231		
2	23.039	23.052	23.047	23.124	23.147	23.210	23.232		
3	23.036	23.051	23.046	23.123	23.144	23.211	23.234		
4	23.035	23.053	23.046	23.122	23.145	23.209	23.233		
5	23.035	23.051	23.044	23.120	23.150	23.205	23.231		
6	23.035	23.050	23.042	23.124	23.149	23.204	23.231		
7	23.038	23.048	23.047	23.120	23.148	23.205	23.233		
8	23.037	23.050	23.044	23.118	23.146	23.206	23.231		
9	23.035	23.050	23.044	23.121	23.147	23.205	23.230		
10	23.038	23.051	23.044	23.119	23.151	23.205	23.230		
Average	23.037	23.051	23.045	23.121	23.147	23.207	23.232		
1s	0.0023	0.0013	0.0016	0.0020	0.0022	0.0027	0.0013		

Table B.9. Measured immersed masses of bob and wire set 4 used in FLiNaK-H density measurements [5]

Measurement		Temperature, °C							
Number	500	550	600	650	700	800	900		
1	35.545	35.589	35.631	35.675	35.748	35.864	35.912		
2	35.546	35.589	35.631	35.677	35.752	35.866	35.915		
3	35.544	35.590	35.636	35.678	35.748	35.862	35.915		
4	35.546	35.590	35.639	35.677	35.744	35.867	35.919		
5	35.542	35.589	35.637	35.676	35.748	35.863	35.917		
6	35.544	35.588	35.630	35.672	35.746	35.869	35.915		
7	35.544	35.589	35.632	35.680	35.745	35.869	35.913		
8	35.543	35.588	35.631	35.677	35.743	35.867	35.909		
9	35.544	35.589	35.634	35.681	35.747	35.869	35.914		
10	35.545	35.586	35.632	35.674	35.745	35.861	35.917		
Average	35.544	35.589	35.633	35.677	35.747	35.866	35.915		
1s	0.0013	0.0012	0.0031	0.0027	0.0026	0.0030	0.0028		

Standard uncertainties in the mass due to variance in repeated measurements of the suspended bob and wire sets immersed in salt at different temperatures are reported in Table B.10. Standard uncertainties were calculated by dividing the standard deviation of mass measurements by $\sqrt{10}$. The standard deviations of measured masses of the bob and wire sets suspended in the gas space are zero and therefore not reported. The standard uncertainty in mass due to the resolution of the balance (5.77E-4 g) was calculated by dividing the lowest digit of the balance (0.001 g) by $\sqrt{3}$, corresponding to a rectangular distribution.

Table B.10. Standard uncertainties in measured masses of bob and wire sets immersed in salt at different temperatures, in grams

Tommonotumo		Standard Uncertainty, g								
Temperature, - °C	FL	iNaK	FLi	NaK-L		FLiNaK-H				
	1	2	1	2	1	2	3	4		
500	0.0003	0.0004	0.0021	0.0008	0.0001	0.0003	0.0007	0.0004		
550	0.0002	0.0003	0.0017	0.0014	0.0003	0.0005	0.0004	0.0004		
600	0.0002	0.0002	0.0007	0.0015	0.0003	0.0010	0.0005	0.0010		
650	0.0001	0.0003	0.0011	0.0013	0.0006	0.0005	0.0006	0.0008		
700	0.0003	0.0003	0.0020	0.0010	0.0003	0.0003	0.0007	0.0008		
800	_		0.0006	0.0006	0.0006	0.0005	0.0008	0.0010		
900	_		0.0010	0.0008	0.0002	0.0005	0.0004	0.0009		

The standard uncertainties in the response of a type K thermocouple at different temperatures, reported in Table B.11, were calculated by using Equation B.1. Other standard uncertainties in temperature were calculated by dividing the resolution of the furnace controller (0.1 °C), the uncertainty in the furnace temperature calibration (1 °C), and the furnace stability (0.5 °C) by $\sqrt{3}$, corresponding to rectangular distributions.

$$u(T) = \frac{0.0075T(^{\circ}C)}{\sqrt{3}}$$
 (B.1)

Table B.11. Standard uncertainties of a type K thermocouple evaluated at different temperatures, in °C

Temperature, °C	Standard Uncertainty, °C
500	2.2
550	2.4
600	2.6
650	2.8
700	3.0
800	3.5
900	3.9

The standard uncertainties in density and thermal expansion of nickel and tungsten at room temperature, reported in Table B.12, were evaluated by dividing the reported uncertainties (Nickel: $\pm 3E-2$ g cm⁻³, $\pm 1E-7$ K⁻¹; Tungsten: $\pm 1.925E-1$ g cm⁻³, $\pm 4.40E-8$ K⁻¹) by $\sqrt{3}$ [9–12].

Table B.12. Standard uncertainties in density and thermal expansion of tungsten and nickel at room temperature

Dah Matawal	Standard	Uncertainties
Bob Material	Density, g cm ⁻³	Thermal Expansion, K ⁻¹
Nickel	1.73E-2	5.77E-8
Tungsten	1.11E-1	2.54E-8

The sensitivity coefficients used to calculate combined standard uncertainties in density were determined by taking partial derivatives of Equation 5. The sensitivity coefficients for different sets of density measurements performed with different bob and wire sets were calculated by using Equations B.2–B.6 and are reported in Tables B.13–B.20.

$$\frac{\partial \rho}{\partial m_a} = -\frac{m_s \rho_{bob}}{m_a (1 + \alpha \Delta T)^3}$$
 (B.2)

$$\frac{\partial \rho}{\partial m_s} = -\frac{\rho_{bob}}{m_s (1 + \alpha \Delta T)^3} \tag{B.3}$$

$$\frac{\partial \rho}{\partial \rho_{hah}} = \frac{m_a - m_s}{m_a (1 + \alpha \Delta T)^3} \tag{B.4}$$

$$\frac{\partial \rho}{\partial \alpha} = \frac{3\rho_{bob}\Delta T(m_s - m_a)}{m_a(1 + \alpha \Delta T)^4}$$
 (B.5)

$$\frac{\partial \rho}{\partial \Delta T} = \frac{3\rho_{bob}\alpha(m_s - m_a)}{m_a(1 + \alpha \Delta T)^4}$$
 (B.6)

Table B.13. Sensitivity coefficients used to calculate combined standard uncertainties in set 1 of FLiNaK density measurements

Temperature,	$\frac{\partial \rho}{\partial m_a}$	$\frac{\partial \rho}{\partial m_s}$	$\frac{\partial \rho}{\partial a}$	$\frac{\partial \rho}{\partial \alpha}$	$\frac{\partial \rho}{\partial \Delta T}$
$^{\circ}\mathrm{C}$	cm^{-3}	cm ⁻³	∂ρ_{bob} Unitless	σα g °C cm ⁻³	$0\Delta \mathbf{I}$ g cm ⁻³ °C ⁻¹
500	-3.52E-01	-4.64E-1	2.36E-1	5.44E3	1.47E-4
550	-3.53E-01	-4.63E-1	2.33E-1	6.03E3	1.48E-4
600	-3.53E-01	-4.62E-1	2.30E-1	6.64E3	1.49E-4
650	-3.54E-01	-4.61E-1	2.27E-1	7.25E3	1.50E-4
700	-3.55E-01	-4.60E-1	2.23E-1	7.88E3	1.51E-4

Table B.14. Sensitivity coefficients used to calculate combined standard uncertainties in set 2 of FLiNaK density measurements

Tomporoturo	$\partial \rho$	$\partial \rho$	$\partial \rho$	∂ho	∂ho
Temperature, °C	$\overline{\partial m_a}$	$\overline{\partial m_s}$	$\overline{\partial ho_{bob}}$	$\overline{\partial \alpha}$	$\overline{m{\partial}\Delta T}$
C	cm ⁻³	cm ⁻³	Unitless	g °C cm ⁻³	g cm ⁻³ °C ⁻¹
500	-3.42E-01	-4.44E-1	2.25E-1	5.58E3	1.51E-4
550	-3.43E-01	-4.43E-1	2.22E-1	6.19E0	1.52E4
600	-3.43E-01	-4.42E-1	2.19E-1	6.81E3	1.53E-4
650	-3.44E-01	-4.41E-1	2.16E-1	7.44E3	1.53E-4
700	-3.44E-01	-4.40E-1	2.13E-1	8.07E3	1.54E-4

Table B.15. Sensitivity coefficients used to calculate combined standard uncertainties in set 1 of FLiNaK-L density measurements

Temperature, °C	$\frac{\partial \rho}{\partial m_a}$ cm ⁻³	$\frac{\partial \rho}{\partial m_s}$ cm ⁻³	$rac{\partial ho}{\partial ho_{bob}}$ Unitless	$\frac{\partial \rho}{\partial \alpha}$ g °C cm ⁻³	$\frac{\partial \rho}{\partial \Delta T}$ g cm ⁻³ °C ⁻¹
500	-4.21E-1	-4.75E-1	1.12E-1	1.53E4	1.40E-4
550	-4.21E-1	-4.75E-1	1.11E-1	1.69E4	1.40E-4
600	-4.22E-1	-4.74E-1	1.10E-1	1.85E4	1.40E-4
650	-4.22E-1	-4.74E-1	1.09E-1	2.02E4	1.41E-4
700	-4.22E-1	-4.74E-1	1.08E-1	2.18E4	1.41E-4
800	-4.22E-1	-4.73E-1	1.07E-1	2.50E4	1.41E-4
900	-4.22E-1	-4.72E-1	1.04E-1	2.83E4	1.41E-4

Table B.16. Sensitivity coefficients used to calculate combined standard uncertainties in set 2 of FLiNaK-L density measurements

Temperature,	∂ρ	∂ρ	дρ	дρ	∂ρ
°C	$\overline{\partial m_a}$	$\overline{\partial m_s}$	$\overline{\partial ho_{bob}}$	$\overline{\partial \alpha}$	$\overline{\partial \Delta T}$
	cm ⁻³	cm ⁻³	Unitless	g °C cm ⁻³	g cm ⁻³ °C ⁻¹
500	-6.58E-1	-7.40E-1	1.09E-1	1.54E4	1.41E-4
550	-6.60E-1	-7.39E-1	1.07E-1	1.70E4	1.41E-4
600	-6.61E-1	-7.39E-1	1.05E-1	1.87E4	1.41E-4
650	-6.62E-1	-7.38E-1	1.03E-1	2.04E4	1.42E-4
700	-6.62E-1	-7.38E-1	1.01E-1	2.21E4	1.42E-4
800	-6.66E-1	-7.37E-1	9.57E-2	2.55E4	1.43E-4
900	-6.67E-1	-7.36E-1	9.27E-2	2.89E4	1.44E-4

Table B.17. Sensitivity coefficients used to calculate combined standard uncertainties in set 1 of FLiNaK-H density measurements

Temperature,	<u></u> ∂ρ	<u></u> θρ	<u></u> θρ	∂ρ	∂ho
°C	∂m_a	∂m_s	∂ho_{bob}	$\overline{\partial \alpha}$	$\overline{\boldsymbol{\partial} \Delta \boldsymbol{T}}$
	cm ⁻³	cm ⁻³	Unitless	g °C cm ⁻³	g cm ⁻³ °C ⁻¹
500	-6.48E-1	-7.32E-1	1.14E-1	-7.75E3	-7.26E-5
550	-6.48E-1	-7.32E-1	1.14E-1	-8.54E3	-7.25E-5
600	-6.48E-1	-7.31E-1	1.13E-1	-9.32E3	-7.23E-5
650	-6.48E-1	-7.31E-1	1.12E-1	-1.01E4	-7.22E-5
700	-6.48E-1	-7.30E-1	1.12E-1	-1.09E4	-7.20E-5
800	-6.49E-1	-7.29E-1	1.09E-1	-1.24E4	-7.18E-5
900	-6.49E-1	-7.28E-1	1.07E-1	-1.40E4	-7.15E-5

Table B.18. Sensitivity coefficients used to calculate combined standard uncertainties in set 2 of FLiNaK-H density measurements

Temperature, °C	$\frac{\partial \rho}{\partial m_a}$ cm ⁻³	$\frac{\partial \rho}{\partial m_s}$ cm ⁻³	$rac{\partial ho}{\partial ho_{bob}}$ Unitless	$\frac{\partial \rho}{\partial \alpha}$ g °C cm ⁻³	$\frac{\partial \rho}{\partial \Delta T}$ g cm ⁻³ °C ⁻¹
500	-4.20E-1	-4.75E-1	1.15E-1	-7.66E3	-7.18E-5
550	-4.21E-1	-4.75E-1	1.13E-1	-8.44E3	-7.17E-5
600	-4.21E-1	-4.75E-1	1.12E-1	-9.22E3	-7.15E-5
650	-4.21E-1	-4.74E-1	1.10E-1	-1.00E4	-7.14E-5
700	-4.22E-1	-4.74E-1	1.09E-1	-1.08E4	-7.12E-5
800	-4.22E-1	-4.73E-1	1.06E-1	-1.23E4	-7.10E-5
900	-4.23E-1	-4.73E-1	1.04E-1	-1.38E4	-7.07E-5

Table B.19. Sensitivity coefficients used to calculate combined standard uncertainties in set 3 of FLiNaK-H density measurements

Tomporeture	$\partial \rho$	<u></u> θρ	∂ho	∂ho	дρ
Temperature, °C	$\overline{\partial m_a}$	$\overline{\partial m_s}$	$\overline{\partial ho_{bob}}$	$\overline{\partial \alpha}$	$\overline{\partial \Delta T}$
C	cm ⁻³	cm ⁻³	Unitless	g °C cm ⁻³	g cm ⁻³ °C ⁻¹
500	-4.22E-1	-4.77E-1	1.13E-1	1.53E4	1.40E-4
550	-4.23E-1	-4.76E-1	1.12E-1	1.69E4	1.40E-4
600	-4.23E-1	-4.76E-1	1.11E-1	1.85E4	1.40E-4
650	-4.23E-1	-4.76E-1	1.10E-1	2.01E4	1.41E-4
700	-4.24E-1	-4.76E-1	1.08E-1	2.18E4	1.41E-4
800	-4.25E-1	-4.75E-1	1.05E-1	2.51E4	1.42E-4
900	-4.25E-1	-4.74E-1	1.04E-1	2.84E4	1.42E-4

Table B.20. Sensitivity coefficients used to calculate combined standard uncertainties in set 4 of FLiNaK-H density measurements

Temperature,	∂ρ	∂ρ	дρ	дρ	∂ρ
°C	$\overline{\partial m_a}$	$\overline{\partial m_s}$	$\overline{\partial ho_{bob}}$	$\overline{\partial \alpha}$	$\overline{\partial \Delta T}$
	cm ⁻³	cm ⁻³	Unitless	g °C cm ⁻³	g cm ⁻³ °C ⁻¹
500	-6.55E-1	-7.38E-1	1.11E-1	2.44E4	1.41E-4
550	-6.55E-1	-7.37E-1	1.11E-1	2.69E4	1.41E-4
600	-6.54E-1	-7.37E-1	1.11E-1	2.95E4	1.40E-4
650	-6.56E-1	-7.36E-1	1.08E-1	3.21E4	1.41E-4
700	-6.56E-1	-7.36E-1	1.07E-1	3.46E4	1.41E-4
800	-6.57E-1	-7.35E-1	1.04E-1	3.98E4	1.42E-4
900	-6.57E-1	-7.34E-1	1.03E-1	4.48E4	1.42E-4

The bob and wire measurements used in density calculations of water with and without liquid dish soap are reported in Tables B.21–B.23. Tungsten bob masses were measured by using an analytical balance and wire diameters were measured by using digital calipers. The masses of different bob and wire sets are reported in Table B.24–B.25.

Table B.21. Average masses of bobs used in density measurements of water

Bob ID	Mass, g
Heavy	39.726
Medium	32.412
Light	24.116

Table B.22. Average masses of bobs used in density measurements of soapy water

Bob ID	Mass, g
Heavy	39.709
Medium	32.411
Light	24.114

Table B.23. Average diameters of wires used in density measurements of water with and without the addition of dish soap

Wire ID	Diameter
Thick	0.050
Medium	0.025
Thin	0.0125

Table B.24. Masses of bob and wire sets measured in the gas space and submerged in water at room temperature

		Mass of Bob	Mass of
Bob ID	Wire ID	and Wire in	Submerged
		Gas Space, g	Bob and Wire
	Thick	40.456	38.401
Heavy	Medium	39.915	37.856
	Thin	39.774	37.721
	Thick	33.211	31.536
Medium	Medium	32.595	30.920
	Thin	32.450	30.771
	Thick	24.866	23.621
Light	Medium	24.300	23.052
	Thin	24.163	22.924

Table B.25. Masses of bob and wire sets measured in the gas space and submerged in soapy water at room temperature

Bob ID	Wire ID	Mass of Bob and Wire in Gas Space, g	Mass of Submerged Bob and Wire
	Thick	40.638	38.585
Heavy	Medium	39.929	37.872
	Thin	39.762	37.704
	Thick	33.342	31.671
Medium	Medium	32.634	30.958
	Thin	32.467	30.789
	Thick	25.046	23.799
Light	Medium	24.336	23.092
	Thin	24.169	22.920

Sensitivity coefficients used in uncertainty analyses for density measurements of water with and without liquid dish soap are reported in Table B.26–B.27. Standard deviations of 10 mass measurements of each bob and wire set were zero. Therefore, the uncertainty in measured mass (5.77E-2 g) is due only to the resolution of the balance. The uncertainty in measured temperature due to the type K thermocouple is ± 2.2 °C.

Table B.26. Sensitivity coefficients used in uncertainty analyses for measurements of water density

		$\partial \rho$	$\partial \rho$	$\partial \rho$	∂ho	$\partial \rho$
Bob ID	Wire ID	$\overline{\partial m_a}$	$\overline{\partial m_{\scriptscriptstyle S}}$	$\overline{\partial ho_{bob}}$	$\overline{\partial \alpha}$	$\overline{\partial \Delta T}$
		cm ⁻³	cm ⁻³	Unitless	g °C cm ⁻³	g cm ⁻³ °C ⁻¹
	Thick	-4.53E-1	-4.77E-1	5.08E-2	1.45E-2	3.26E-8
Heavy	Medium	-4.59E-1	-4.84E-1	5.16E-2	1.54E-2	3.47E-8
	Thin	-4.60E-1	-4.85E-1	5.16E-2	1.57E-2	3.52E-8
	Thick	-5.52E-1	-5.81E-1	5.04E-2	6.55E-2	1.47E-7
Medium	Medium	-5.62E-1	-5.92E-1	5.14E-2	6.76E-2	1.52E-7
	Thin	-5.64E-1	-5.95E-1	5.17E-2	6.81E-2	1.53E-7
	Thick	-7.37E-1	-7.76E-1	5.01E-2	2.09E-1	4.70E-7
Light	Medium	-7.53E-1	-7.94E-1	5.14E-2	2.14E-1	4.81E-7
	Thin	-7.58E-1	-7.99E-1	5.13E-2	2.15E-1	4.84E-7

Table B.27. Sensitivity coefficients used in uncertainty analyses for measurements of soapy water density

		∂ho	∂ho	∂ho	∂ho	∂ho
Bob ID	Wire ID	$\overline{\partial m_a}$	$\overline{\partial m_{\scriptscriptstyle S}}$	$\overline{\partial ho_{bob}}$	$\overline{\partial \alpha}$	$\overline{\partial \Delta T}$
		cm ⁻³	cm ⁻³	Unitless	g °C cm ⁻³	g cm $^{-3}$ °C $^{-1}$
	Thick	-4.51E-1	-4.75E-1	5.05E-2	1.43E-2	3.21E-8
Heavy	Medium	-4.58E-1	-4.83E-1	5.15E-2	1.54E-2	3.48E-8
	Thin	-4.60E-1	-4.85E-1	5.18E-2	1.57E-2	3.54E-8
	Thick	-5.50E-1	-5.79E-1	5.01E-2	6.50E-2	1.46E-7
Medium	Medium	-5.61E-1	-5.91E-1	5.14E-2	6.75E-2	1.52E-7
	Thin	-5.64E-1	-5.94E-1	5.17E-2	6.81E-2	1.53E-7
	Thick	-7.32E-1	-7.71E-1	4.98E-2	2.07E-1	4.66E-7
Light	Medium	-7.53E-1	-7.93E-1	5.11E-2	2.14E-1	4.81E-7
	Thin	-7.57E-1	-7.99E-1	5.17E-2	2.15E-1	4.84E-7

Appendix C: Thermal Diffusivity Calculations

The thickness of the salt layer at room temperature was calculated by subtracting the measured thicknesses of the crucible and lid from the total thickness of the assembled cell. Cells were designed to be 2.0 mm thick. The standard uncertainty in the thickness of salt layers due to the resolution of the micrometer was calculated by dividing the resolution (1E-4 cm) by $\sqrt{3}$. The standard uncertainty due to the variance in multiple measurements of crucible thickness wer calculated by dividing the standard deviation of four measurements by $\sqrt{4}$. The calculated salt layer thicknesses for LFA samples of FLiNaK, FLiNaK-L, and FLiNaK-H are reported with associated total standard uncertainties in Table C.1.

Table C.1. Salt layer thicknesses used in thermal diffusivity measurements of FLiNaK, FLiNaK-L, and FLiNaK-H with associated standard uncertainties

Comple No		Salt Thickness, cm	
Sample No.	FLiNaK	FLiNaK-L	FLiNaK-H
1	9.19E-2±1.40E-3	9.59E-2±1.40E-3	9.17E-2±3.39E-3
2	9.44E-2±3.79E-4	8.24E-2±3.79E-4	9.10E-2±1.04E-3
3	9.64E-2±1.40E-4	9.30E-2±1.40E-4	8.39E-2±9.18E-4
4	_	9.28E-2±5.83E-4	$8.45E-2\pm4.04E-4$

The half-rise times used to calculate thermal diffusivities of FLiNaK, FLiNaK-L, and FLiNaK-H are reported in Tables C.2, C.3, and C.4, respectively. The uncertainty in half-rise time was calculated by dividing the resolution of the LFA timer (1E-5 s) by $\sqrt{3}$.

Table C.2. Half-rise times used to calculate thermal diffusivities of FLiNaK, in s.

	Sample 1								
•		Temperature (°C)							
Shot No.	500	550	600	650	700	750	800	850	900
1	3.328	3.115	2.834	2.816	2.496	2.400	2.207	_	_
2	3.160	3.050	2.834	2.780	2.496	2.440	2.230	_	_
3	3.254	3.050	2.909	2.780	2.496	2.400	2.230	_	_
				S	Sample 2				
•				Temp	perature (°C)			
Shot No.	500	550	600	650	700	750	800	850	900
1	3.303	3.029	2.816	2.712	2.349	2.440	2.153	_	_
2	3.353	3.050	2.852	2.745	2.362	2.414	2.143	_	_
3	3.278	3.050	2.798	2.728	2.362	2.400	2.164	_	_
				S	Sample 3				
•				Temp	perature (°C)			
Shot No.	499	549	599	648	698	748	797	847	897
1	4.393	3.379	3.138	2.928	2.745	2.745	2.440	2.312	2.092
2	3.993	3.379	3.138	2.928	2.745	2.584	2.440	2.196	2.092
3	4.393	3.379	3.138	2.928	2.745	2.584	2.440	2.196	2.092

Table C.3. Half-rise times used to calculate thermal diffusivities of FLiNaK-L, in s.

	Sample 1								
•	Temperature (°C)								
Shot No.	500	550	600	650	700	750	800	846	896
1	4.000	4.000	3.367	2.590	2.308	2.093	2.000	1.756	1.572
2	4.000	4.000	3.367	2.590	2.308	2.093	2.000	1.756	1.629
3	4.000	3.673	3.367	2.590	2.308	2.093	2.000	1.756	1.572
				S	Sample 2				
•				Temp	perature (°	°C)			
Shot No.	500	550	600	650	700	750	800	847	897
1	2.711	2.528	2.242	2.002	1.900	1.808	1.657	1.586	1.462
2	2.711	2.528	2.115	2.002	1.900	1.808	1.657	1.586	1.462
3	2.711	2.528	2.115	2.002	1.900	1.808	1.657	1.522	1.462
				S	Sample 3				
·				Temp	perature (°	°C)			
Shot No.	499	549	599	648	698	748	797	847	897
1	4.489	3.992	3.655	3.277	2.970	2.795	2.735	2.421	1.533
2	4.412	4.094	3.655	3.195	2.902	2.795	2.677	2.391	1.515
3	4.317	4.021	3.655	3.249	2.947	2.775	2.586	2.406	1.527
				S	Sample 3				
		Temperature (°C)							
Shot No.	500	551	600	650	700	749	798	847	897
1	3.783	3.439	2.910	2.702	2.702	2.364	2.225	1.645	1.455
2	3.783	3.439	2.910	2.910	2.522	2.364	2.225	1.645	1.455
3	3.783	3.439	2.910	2.910	2.522	2.364	2.225	1.645	1.455

Table C.4. Measured half-rise times used to calculate thermal diffusivities of FLiNaK-H, in s.

					Sample 1				
	Temperature (°C)								
Shot No.	500	551	600	650	699	748	798	848	897
1	4.615	4.196	3.846	3.846	3.552	3.298	3.078	2.886	1.776
2	4.615	4.196	3.846	3.846	3.552	3.298	3.078	2.886	1.776
3	4.615	4.196	4.196	3.846	3.552	3.298	3.078	2.886	1.776
				S	Sample 2				
					perature (°C)			
Shot No.	500	550	599	650	700	748	798	847	897
1	3.400	3.109	3.109	2.887	2.675	2.491	2.332	1.875	1.875
2	3.400	3.109	3.109	2.887	2.675	2.491	2.332	1.875	1.875
3	3.400	3.400	3.109	2.887	2.675	2.491	2.332	1.875	1.875
				S	Sample 3				
				Tem	perature (°C)			
Shot No.	500	551	599	648	699	749	798	848	898
1	2.711	2.485	2.294	2.130	1.864	1.754	1.657	1.491	1.420
2	2.711	2.485	2.294	2.130	1.864	1.754	1.657	1.491	1.420
3	2.485	2.485	2.294	1.988	1.864	1.754	1.657	1.491	1.420
				S	Sample 4				
	Temperature (°C)								
Shot No.	500	551	600	650	699	748	798	847	897
1	4.481	3.485	3.136	2.614	2.413	2.413	2.091	1.960	1.845
2	4.481	3.485	3.136	2.614	2.413	2.413	2.091	1.960	1.845
3	4.481	3.485	3.136	2.614	2.413	2.413	2.091	1.960	1.845

The standard uncertainties in the response of a type S thermocouple at different temperatures, reported in Table C.5, were calculated by using Equation C.1. The standard uncertainty in temperature due to the furnace controller was calculated by dividing the resolution of the controller (0.1 °C) by $\sqrt{3}$, corresponding to a rectangular distribution.

$$u(T) = \frac{0.0025T(^{\circ}C)}{\sqrt{3}}$$
 (C.1)

Table C.5. Standard uncertainties of a type S thermocouple evaluated at different temperatures, in °C

Temperature, °C	Standard Uncertainty, °C
500	0.7
550	0.8
600	0.9
650	0.9
700	1.0
750	1.1
800	1.2
850	1.2
900	1.3

Sensitivity coefficients were used to calculate combined standard uncertainties in thermal diffusivities of FLiNaK, FLiNaK-L, and FLiNaK-H. Sensitivity coefficients were calculated by taking partial derivatives of Equation C.2., where D is the thermal diffusivity, L is the thickness of the salt layer, and $t_{1/2}$ is the half-rise time. Sensitivity coefficients associated with uncertainties in temperature were calculated by differentiating linear fits of thermal diffusivities of FLiNaK, FLiNaK-L, and FLiNaK-H. Linear equations used to calculate these quantities are reported in Table C.6. Sensitivity coefficients used in uncertainty analyses of FLiNaK, FLiNaK-L, and FLiNaK-H are reported in Table C.7, C.8, and C.9, respectively.

$$D = \frac{1.38L^2}{\pi^2 t_{1/2}^2} \tag{C.2}$$

$$\frac{\partial D}{\partial L} = \frac{2.76L}{\pi^2 t_{1/2}^2} \tag{C.3}$$

$$\frac{\partial D}{\partial L} = -\frac{1.38L^2}{\pi^2 t_{1/2}^2} \tag{C.4}$$

Table C.6. Linear fits of thermal diffusivity data used to calculate sensitivity coefficients, in cm² s⁻¹

Salt ID	Linear Fit				
FLiNaK	$D = 2.16 \times 10^{-6} T(^{\circ}\text{C}) + 1.87 \times 10^{-4}$				
FLiNaK-L	$D = 3.30 \times 10^{-6} T(^{\circ}\text{C}) + 7.46 \times 10^{-4}$				
FLiNaK-H	$D = 2.41 \times 10^{-6} T(^{\circ}\text{C}) + 3.3 \times 10^{-4}$				

Table C.7. Sensitivity coefficients used to calculate combined standard uncertainties in thermal diffusivities of FLiNaK

Tamparatura	∂D	∂D	∂D
Temperature, °C	$\overline{\partial t_{1/2}}$	$\overline{\partial L}$	$\overline{\partial T}$
	$cm^2 s^{-2}$	cm s ⁻¹	${\rm cm}^2~{\rm s}^{\text{-1}}~{}^{\circ}{\rm C}^{\text{-1}}$
500	-1.08E-4	7.75E-3	2.16E-6
550	-1.40E-4	8.84E-3	2.16E-6
600	-1.62E-4	9.51E-3	2.16E-6
650	-1.76E-4	9.93E-3	2.16E-6
700	-2.18E-4	1.10E-2	2.16E-6
750	-2.26E-4	1.12E-2	2.16E-6
800	-2.71E-4	1.23E-2	2.16E-6
850	-2.80E-4	1.25E-2	2.16E-6
900	-3.20E-4	1.34E-2	2.16E-6

Table C.8. Sensitivity coefficients used to calculate combined standard uncertainties in thermal diffusivities of FLiNaK-L

Tommonotyma	∂D	∂D	∂D
Temperature, °C	$\overline{\partial t_{1/2}}$	$\overline{\partial L}$	$\overline{\partial T}$
	$cm^2 s^{-2}$	cm s ⁻¹	cm ² s ⁻¹ °C ⁻¹
500	-8.06E-5	6.71E-3	3.30E-6
550	-9.27E-5	7.20E-3	3.30E-6
600	-1.22E-4	8.27E-3	3.30E-6
650	-1.57E-4	9.37E-3	3.30E-6
700	-1.89E-4	1.03E-2	3.30E-6
750	-2.18E-4	1.10E-2	3.30E-6
800	-2.45E-4	1.17E-2	3.30E-6
850	-3.29E-4	1.36E-2	3.30E-6
900	-4.91E-4	1.66E-2	3.30E-6

Table C.9. Sensitivity coefficients used to calculate combined standard uncertainties in thermal diffusivities of FLiNaK-H

	2 -		
Temperature,	∂D	∂D	∂D
°C	$\partial t_{1/2}$	$\overline{\partial L}$	$\overline{\partial T}$
	$cm^2 s^{-2}$	cm s ⁻¹	$cm^2 s^{-1} {}^{\circ}C^{-1}$
500	-7.22E-5	6.36E-3	2.41E-6
550	-9.25E-5	7.19E-3	2.41E-6
600	-1.06E-4	7.69E-3	2.41E-6
650	-1.27E-4	8.41E-3	2.41E-6
700	-1.50E-4	9.16E-3	2.41E-6
750	-1.67E-4	9.66E-3	2.41E-6
800	-1.97E-4	1.05E-2	2.41E-6
850	-2.45E-4	1.17E-2	2.41E-6
900	-3.46E-4	1.39E-2	2.41E-6

The standard uncertainties attributed to distortions in the thickness of the salt layer, reported in Table C.10, were calculated by dividing the standard deviation of thermal diffusivities at each temperature by \sqrt{N} where N is the number of measurements at each temperature. The thermal diffusivities of FLiNaK, FLiNaK-L, and FLiNaK-H and expanded uncertainties are reported in Tables C.11, C.12, and C.13, respectively.

Table C.10. Standard uncertainties in salt thickness attributed to distortions in the salt layer at different temperatures, in cm² s⁻¹

Temperature,	Standard Uncertainty, cm ² s ⁻¹					
°C	FLiNaK	FLiNaK-L	FLiNaK-H			
500	5.25E-5	5.56E-5	5.49E-5			
550	2.31E-5	5.70E-5	4.31E-5			
600	2.50E-5	3.90E-5	4.37E-5			
650	1.64E-5	4.56E-5	5.16E-5			
700	3.83E-5	5.05E-5	6.01E-5			
750	2.73E-5	6.07E-5	6.43E-5			
800	3.60E-5	6.45E-5	6.44E-5			
850	3.33E-5	9.10E-5	8.71E-5			
900	_	6.72E-5	4.81E-5			

Table C.11. Measured thermal diffusivities of FLiNaK with expanded uncertainties, in cm 2 s $^{-1}$.

	Sample 1								
		Temperature (°C)							
Shot No.	500	550	600	650	700	750	800	850	900
1	0.0013	0.0014	0.0016	0.0016	0.0018	0.0018	0.0020	_	_
2	0.0014	0.0014	0.0016	0.0016	0.0018	0.0018	0.0020	_	_
3	0.0014	0.0014	0.0015	0.0016	0.0018	0.0018	0.0020	_	_
				5	Sample 2				
				Tem	perature (°C)			
Shot No.	500	550	600	650	700	750	800	850	900
1	0.0013	0.0015	0.0016	0.0016	0.0019	0.0018	0.0020	_	_
2	0.0013	0.0014	0.0015	0.0016	0.0019	0.0018	0.0020	_	_
3	0.0013	0.0014	0.0016	0.0016	0.0019	0.0018	0.0020	_	_
				5	Sample 3				
				Tem	perature (°C)			
Shot No.	499	549	599	648	698	748	797	847	897
1	0.0010	0.0013	0.0014	0.0015	0.0016	0.0016	0.0018	0.0019	0.0021
2	0.0011	0.0013	0.0014	0.0015	0.0016	0.0017	0.0018	0.0020	0.0021
3	0.0010	0.0013	0.0014	0.0015	0.0016	0.0017	0.0018	0.0020	0.0021
					FLiNaK				
				Tem	perature (°C)			
	500	550	600	649	699	749	799	847	897
Average	0.0012	0.0014	0.0015	0.0016	0.0017	0.0018	0.0019	0.0020	0.0021
U(D)	1E-4	5E-5	5E-5	3E-5	8E-5	5E-5	7E-5	7E-5	6E-6

Table C.12. Measured thermal diffusivity of FLiNaK-L with expanded uncertainties, in cm 2 s $^{-1}$.

				•		•			,
				5	Sample 1				
				Tem	perature (°C)			
Shot No.	499	549	598	648	697	747	796	846	896
1	0.0010	0.0010	0.0012	0.0016	0.0017	0.0019	0.0020	0.0023	0.0026
2	0.0010	0.0010	0.0012	0.0016	0.0017	0.0019	0.0020	0.0023	0.0025
3	0.0010	0.0011	0.0012	0.0016	0.0017	0.0019	0.0020	0.0023	0.0026
				5	Sample 2				
				Tem	perature (°C)			
Shot No.	499	549	599	649	699	748	797	847	897
1	0.0011	0.0012	0.0013	0.0015	0.0016	0.0016	0.0018	0.0019	0.0020
2	0.0011	0.0012	0.0014	0.0015	0.0016	0.0016	0.0018	0.0019	0.0020
3	0.0011	0.0012	0.0014	0.0015	0.0016	0.0016	0.0018	0.0020	0.0020
				5	Sample 3				
				Tem	perature (°C)			
Shot No.	499	549	599	649	699	748	797	847	897
1	0.0008	0.0010	0.0010	0.0012	0.0013	0.0014	0.0014	0.0016	0.0025
2	0.0009	0.0009	0.0010	0.0012	0.0013	0.0014	0.0014	0.0016	0.0025
3	0.0009	0.0009	0.0010	0.0012	0.0013	0.0014	0.0015	0.0016	0.0025
				5	Sample 4				
				Tem	perature (°C)			
Shot No.	500	551	600	650	700	749	798	848	897
1	0.0010	0.0011	0.0013	0.0014	0.0014	0.0016	0.0017	0.0023	0.0026
2	0.0010	0.0011	0.0013	0.0013	0.0015	0.0016	0.0017	0.0023	0.0026
3	0.0010	0.0011	0.0013	0.0013	0.0015	0.0016	0.0017	0.0023	0.0026
Average	0.0010	0.0011	0.0012	0.0014	0.0015	0.0016	0.0017	0.0020	0.0024
U(D)	5E-05	5E-05	8E-05	9E-05	1E-04	1E-04	1E-04	2E-04	1E-04

Table C.13. Measured thermal diffusivities of FLiNaK-H with expanded uncertainties, in cm $^2\ s^{-1}$

				C	Sample 1				
					oerature (°	°C)			
Shot No.	500	551	600	650	699	748	798	848	897
1	0.0008	0.0009	0.0010	0.0010	0.0010	0.0011	0.0012	0.0013	0.0021
2	0.0008	0.0009	0.0010	0.0010	0.0010	0.0011	0.0012	0.0013	0.0021
3	0.0008	0.0009	0.0009	0.0010	0.0010	0.0011	0.0012	0.0013	0.0021
				S	Sample 2				
				Temp	oerature (°	°C)			
Shot No.	500	550	599	650	699	748	798	847	897
1	0.0011	0.0012	0.0012	0.0013	0.0014	0.0015	0.0016	0.0019	0.0019
2	0.0011	0.0012	0.0012	0.0013	0.0014	0.0015	0.0016	0.0019	0.0019
3	0.0011	0.0011	0.0012	0.0013	0.0014	0.0015	0.0016	0.0019	0.0019
				S	Sample 3				
•				Temp	perature (°	°C)			
Shot No.	500	551	600	650	699	749	798	848	898
1	0.0011	0.0012	0.0013	0.0014	0.0016	0.0017	0.0018	0.0020	0.0021
2	0.0011	0.0012	0.0013	0.0014	0.0016	0.0017	0.0018	0.0020	0.0021
3	0.0012	0.0012	0.0013	0.0015	0.0016	0.0017	0.0018	0.0020	0.0021
				S	Sample 4				
•				Temp	oerature (°	°C)			
Shot No.	500	551	600	650	699	748	798	847	897
1	0.0007	0.0009	0.0010	0.0012	0.0013	0.0013	0.0015	0.0016	0.0017
2	0.0007	0.0009	0.0010	0.0012	0.0013	0.0013	0.0015	0.0016	0.0017
3	0.0007	0.0009	0.0009	0.0012	0.0013	0.0013	0.0015	0.0016	0.0017
Average	0.0009	0.0010	0.0011	0.0012	0.0013	0.0014	0.0015	0.0017	0.0020
U(D)	1E-04	8E-05	9E-05	1E-04	1E-04	1E-04	1E-04	2E-04	9E-05

Appendix D: Viscosity Calculations

Measurements of FLiNaK salts with and without fission product dopants were performed at 500, 550, 600, 650, 700, 800, and 900 °C. The torque values measured at each temperature for FLiNaK 1, FLiNaK 2, FLiNaK-L and FLiNaK-H are reported in Tables D.1–D.4, respectively. Standard uncertainties in torque measurements are reported in Tables D.5–D.8. Data were collected over a range of rotational velocities from 50 to 80 rpm. Results were provided by the instrument as percent maximum torque and torque values were calculated using a maximum torque value of 6.73×10^{-5} Nm (per Brookfield DV2T Operating Manual M13-167-B0614, p. 5). Torque measurements and geometric quantities were used to calculate the viscosity of each salt mixture by using Equation 10.

Table D.1. Torque measurements of FLiNaK 1 salt, in Nm \times 10⁻⁶ [5]

Rotational							Tempera	ature, °C						
Velocity ^a ,	50	00	55	50	60	00	65	50	70	00	80	00	90	00
rpm	% Max	Torque	% Max	Torque	% Max	Torque	% Max	Torque	% Max	Torque	% Max	Torque	% Max	Torque
60	20.4	13.7	14.4	9.7	11.1	7.5	8.9	6.0	7.4	5.0	5.8	3.9	4.9	3.3
55	18.8	12.7	13.4	9.0	10.1	6.8	8.2	5.5	6.9	4.6	5.2	3.5	4.3	2.9
80	27.2	18.3	19.1	12.9	14.3	9.6	11.3	7.6	9.5	6.4	7.6	5.1	6.5	4.4
70	23.5	15.8	16.8	11.3	12.8	8.6	10.2	6.9	8.6	5.8	6.7	4.5	5.4	3.6
50	17.0	11.4	12.4	8.3	9.5	6.4	7.6	5.1	6.3	4.2	4.7	3.2	4.0	2.7
75	25.2	17.0	17.8	12	13.6	9.2	10.9	7.3	9.1	6.1	6.8	4.6	5.7	3.8
65	21.9	14.7	15.6	10.5	11.8	7.9	9.5	6.4	8.1	5.5	6.1	4.1	5.1	3.4
70	23.4	15.7	16.7	11.2	12.7	8.5	10.3	6.9	8.7	5.9	6.6	4.4	5.3	3.6
60	20.1	13.5	14.5	9.8	11.0	7.4	8.7	5.9	7.3	4.9	5.5	3.7	4.7	3.2
50	17.0	11.4	12.4	8.3	9.4	6.3	7.5	5.0	6.3	4.2	4.8	3.2	3.9	2.6

^aListed in order of measurement.

Table D.2. Torque measurements of FLiNaK 2 salt, in Nm \times 10⁻⁶ [5]

Rotational							Tempera	ature, °C						
Velocity ^a ,	50	00	5:	50	60	00	6.	50	70	00	80	00	90	00
rpm	% Max	Torque	% Max	Torque	% Max	Torque	% Max	Torque	% Max	Torque	% Max	Torque	% Max	Torque
60	21.0	14.1	15.0	10.1	11.3	7.6	8.7	5.9	7.0	4.7	5.6	3.8	5.0	3.4
55	18.9	12.7	13.9	9.4	10.0	6.7	7.9	5.3	6.8	4.6	5.3	3.6	4.4	3.0
80	26.8	18.0	20.4	13.7	14.4	9.7	11.3	7.6	9.2	6.2	7.4	5.0	6.3	4.2
70	23.5	15.8	18.0	12.1	12.8	8.6	10.3	6.9	8.5	5.7	6.5	4.4	5.5	3.7
50	17.0	11.4	12.6	8.5	9.4	6.3	7.8	5.2	6.3	4.2	4.8	3.2	4.3	2.9
75	25.3	17.0	18.0	12.1	13.3	9.0	11.1	7.5	8.8	5.9	6.8	4.6	6.0	4.0
65	22.0	14.8	16.1	10.8	11.9	8.0	9.5	6.4	8.0	5.4	6.2	4.2	5.4	3.6
70	23.3	15.7	18.1	12.2	12.8	8.6	10.3	6.9	8.5	5.7	6.5	4.4	5.5	3.7
60	20.9	14.1	14.9	10.0	11.1	7.5	8.7	5.9	7.0	4.7	5.7	3.8	4.9	3.3
50	16.9	11.4	12.5	8.4	9.4	6.3	7.9	5.3	6.3	4.2	5.0	3.4	4.4	3.0

^aListed in order of measurement.

Table D.3. Torque measurements of FLiNaK-L salt, in Nm $\times\,10^{\text{-}6}$ [5]

Rotational							Tempera	ature, °C						
Velocity ^a ,	50	00	5:	50	60	00	6.	50	70	00	80	00	90	00
rpm	% Max	Torque	% Max	Torque	% Max	Torque	% Max	Torque	% Max	Torque	% Max	Torque	% Max	Torque
60	23.0	15.5	16.5	11.1	13.2	8.9	10.5	7.1	9.3	6.3	7.6	5.1	6.8	4.6
55	21.8	14.7	15.0	10.1	11.9	8.0	9.9	6.7	8.7	5.9	6.8	4.6	5.7	3.8
80	29.5	19.9	20.7	13.9	16.7	11.2	12.9	8.7	12.5	8.4	9.8	6.6	8.7	5.9
70	26.4	17.8	19.0	12.8	14.2	9.6	11.5	7.7	10.6	7.1	8.5	5.7	7.3	4.9
50	19.0	12.8	14.1	9.5	10.9	7.3	8.3	5.6	7.8	5.2	6.3	4.2	5.4	3.6
75	28.4	19.1	19.9	13.4	15.9	10.7	12.6	8.5	11.2	7.5	9.2	6.2	8.1	5.5
65	25.3	17.0	17.5	11.8	14.1	9.5	11.3	7.6	10.6	7.1	8.1	5.5	7.3	4.9
70	26.8	18.0	18.8	12.7	14.2	9.6	11.5	7.7	10.1	6.8	8.5	5.7	7.0	4.7
60	23.1	15.5	16.6	11.2	13.4	9.0	10.7	7.2	9.2	6.2	7.4	5.0	6.8	4.6
50	19.0	12.8	14.1	9.5	11.2	7.5	8.3	5.6	7.8	5.2	6.4	4.3	5.8	3.9

^aListed in order of measurement.

Table D.4. Torque measurements of FLiNaK-H salt, in Nm \times 10⁻⁶ [5]

Rotational							Tempera	ature, °C						
Velocity ^a ,	50	00	55	50	60	00	65	50	70	00	80	00	90	00
rpm	% Max	Torque	% Max	Torque	% Max	Torque	% Max	Torque	% Max	Torque	% Max	Torque	% Max	Torque
60	24.5	16.5	15.5	10.4	12.3	8.3	9.8	6.6	8.2	5.5	6.2	4.2	4.9	3.3
55	22.2	14.9	14.7	9.9	12.2	8.2	9.2	6.2	7.7	5.2	5.8	3.9	4.4	3.0
80	31.7	21.3	21.2	14.3	16.2	10.9	13.2	8.9	11.2	7.5	8.5	5.7	6.4	4.3
70	28.0	18.8	18.8	12.7	14.3	9.6	11.5	7.7	9.8	6.6	7.2	4.8	5.3	3.6
50	20.5	13.8	13.7	9.2	10.3	6.9	8.7	5.9	7.3	4.9	5.2	3.5	4.0	2.7
75	30.2	20.3	20.2	13.6	15.3	10.3	12.5	8.4	10.5	7.1	7.8	5.2	5.8	3.9
65	26.0	17.5	17.8	12.0	13.3	9.0	10.8	7.3	9.2	6.2	6.7	4.5	5.0	3.4
70	27.8	18.7	19.0	12.8	14.7	9.9	11.7	7.9	9.8	6.6	7.0	4.7	5.2	3.5
60	23.7	16.0	16.5	11.1	12.3	8.3	10.2	6.9	8.3	5.6	6.0	4.0	4.5	3.0
50	20.3	13.7	13.8	9.3	10.5	7.1	8.7	5.9	7.3	4.9	5.0	3.4	4.0	2.7
^a Listed in ord	ler of meas	surement.	•	•	•		•	•	•			•	•	

Table D.5. Standard uncertainties in torque measurements of FLiNaK 1 salt, in Nm \times 10⁻⁸

Rotational			Т	emperature, °	С		
Velocity ^a , rpm	500	550	600	650	700	800	900
60	4.56	4.56	4.56	3.89	4.56	3.89	3.89
55	4.56	4.56	4.56	4.56	4.56	6.14	6.14
80	4.56	4.56	4.56	3.89	3.89	3.89	3.89
70	4.56	3.89	4.56	4.56	4.56	4.56	4.56
50	6.14	4.56	4.56	4.56	6.14	6.14	4.56
75	4.56	4.56	4.56	4.56	4.56	4.56	4.56
65	3.89	4.56	4.56	4.56	4.56	6.14	4.56
70	4.56	4.56	4.56	3.89	4.56	6.14	4.56
60	3.89	4.56	4.56	3.89	3.89	3.89	4.56
50	4.56	4.56	3.89	6.14	6.14	4.56	6.14

^aListed in order of measurement.

Table D.6. Standard uncertainties in torque measurements of FLiNaK 2 salt, in Nm $\times\,10^{\text{-8}}$

Rotational _			Т	emperature, °	С		
Velocity ^a , rpm	500	550	600	650	700	800	900
60	4.56	4.56	6.14	4.56	4.56	4.56	4.56
55	4.56	4.56	6.14	6.14	6.14	4.56	4.56
80	4.56	3.89	4.56	4.56	3.89	3.89	3.89
70	4.56	4.56	4.56	4.56	4.56	4.56	3.89
50	8.13	4.56	4.56	3.89	8.13	4.56	4.56
75	4.56	6.14	4.56	4.56	4.56	4.56	3.89
65	4.56	4.56	4.56	4.56	4.56	6.14	4.56
70	6.14	4.56	4.56	3.89	4.56	6.14	3.89
60	4.56	4.56	4.56	3.89	4.56	4.56	4.56
50	4.56	4.56	4.56	4.56	4.56	4.56	4.56

^aListed in order of measurement.

Table D.7. Standard uncertainties in torque measurements of FLiNaK-L salt, in Nm \times 10⁻⁸

Rotational			Т	emperature, °	С		
Velocity ^a , rpm	500	550	600	650	700	800	900
60	6.14	4.56	8.13	6.14	4.56	8.13	4.56
55	4.56	6.14	8.13	6.14	4.56	6.14	6.14
80	4.56	4.56	4.56	6.14	4.56	6.14	6.14
70	6.14	3.89	4.56	4.56	6.14	6.14	8.13
50	4.56	3.89	8.13	4.56	6.14	8.13	4.56
75	4.56	4.56	4.56	4.56	4.56	8.13	4.56
65	4.56	6.14	8.13	4.56	4.56	6.14	4.56
70	6.14	4.56	6.14	3.89	6.14	6.14	4.56
60	6.14	6.14	4.56	3.89	6.14	4.56	4.56
50	4.56	4.56	4.56	4.56	6.14	4.56	4.56

^aListed in order of measurement.

Table D.8. Standard uncertainties in torque measurements of FLiNaK H salt, in Nm \times 10⁻⁸

Rotational			Т	emperature, °	С		
Velocity ^a , rpm	500	550	600	650	700	800	900
60	6.14	4.56	6.14	6.14	6.14	6.14	6.14
55	8.13	6.14	6.14	8.13	6.14	8.13	6.14
80	6.14	4.56	6.14	8.13	6.14	6.14	6.14
70	10.28	6.14	6.14	8.13	6.14	6.14	6.14
50	4.56	8.13	8.13	6.14	6.14	8.13	6.14
75	6.14	8.13	6.14	6.14	6.14	6.14	6.14
65	6.14	8.13	6.14	6.14	6.14	8.13	6.14
70	6.14	6.14	6.14	6.14	6.14	6.14	8.13
60	6.14	6.14	6.14	6.14	6.14	6.14	6.14
50	8.13	8.13	8.13	6.14	6.14	6.14	6.14

^aListed in order of measurement.

The diameters and lengths of the spindles and crucibles and associated uncertainties used in viscosity measurements of silicone reference oil and FLiNaK salts with are reported in Tables D.9–D.14. The diameters and lengths of the spindles were measured by using digital calipers and the inner diameters of the crucibles were measured by using a digital bore gauge. The radii of the spindle and crucible were calculated from the average diameters. Standard uncertainties of spindle and crucible dimensions were affected by the standard deviation of multiple measurements and the resolution of the calipers or bore gauge.

Table D.9. Crucible and spindle dimensions used in silicone oil measurements 1 and 2

Measurement Number	Spindle Diameter, mm	Spindle Length, mm	Crucible Inner Diameter, mm
1	19.01	49.99	22.07
2	19.00	49.98	22.06
3	19.00	49.98	22.06
4	19.00	49.98	22.06
5	19.01	_	22.05
6	19.00	_	22.05
Average	19.00	49.98	22.06
Standard Uncertainty	6.15E-3	6.29E-3	6.54E-3

Table D.10. Crucible and spindle dimensions used in silicone oil measurements 3 and 4

Measurement	Spindle Diameter,	Spindle Length, mm	Crucible Inner
Number	mm		Diameter, mm
1	19.02	49.98	22.07
2	19.01	50.01	22.09
3	19.01	49.98	22.03
4	19.02	49.99	22.03
5	19.01	_	22.06
6	19.01	_	22.09
Average	19.01	49.99	22.06
Standard Uncertainty	6.15E-3	9.13E-3	1.25E-3

Table D.11. Crucible and spindle dimensions used for viscosity calculations of FLiNaK 1

Measurement	Spindle Diameter,	Spindle Length, mm	Crucible Inner
Number	mm		Diameter, mm
1	18.97	49.99	22.03
2	18.96	49.99	22.04
3	18.96	49.99	22.04
4	18.96	49.98	22.04
5	18.97	_	22.04
6	18.96	_	22.04
Average	18.96	49.99	22.04
Standard Uncertainty	6.15E-3	6.29E-3	6.01E-3

Table D.12. Crucible and spindle dimensions used for viscosity calculations of FLiNaK 2

Measurement Number	Spindle Diameter, mm	Spindle Length, mm	Crucible Inner Diameter, mm
1	19.01	50.01	22.05
2	19.01	50.02	22.05
3	19.01	50.02	22.03
4	19.01	50.02	22.04
5	19.02	_	22.03
6	19.02	_	22.04
Average	19.01	50.02	22.04
Standard Uncertainty	6.15E-3	6.29E-3	6.83E-3

Table D.13. Crucible and spindle dimensions used for viscosity calculations of FLiNaK-L

Measurement	Spindle Diameter,	Spindle Length, mm	Crucible Inner	
Number	mm		Diameter, mm	
1	19.01	50.01	21.97	
2	19.01	50.00	21.99	
3	19.01	49.99	21.89	
4	19.01	50.01	21.93	
5	19.00	_	22.00	
6	19.01	-	22.04	
Average	19.01	50.00	21.97	
Standard Uncertainty	6.01E-3	7.50E-3	2.25E-3	

Table D.14. Crucible and spindle dimensions used for viscosity calculations of FLiNaK-H

Measurement	Spindle Diameter,	Spindle Length, mm	Crucible Inner
Number	mm		Diameter, mm
1	19.07	50.01	21.95
2	19.07	50.01	21.95
3	19.07	49.99	21.93
4	19.08	50.01	21.93
5	19.07	_	21.93
6	19.08	_	21.94
Average	19.07	50.01	21.94
Standard Uncertainty	6.15E-3	7.64E-3	7.03E-3

The standard uncertainties in temperature were calculated by dividing the resolution of the furnace temperature controller (0.1 °C) and the uncertainty in the temperature calibration (1.0 °C) by $\sqrt{3}$. The uncertainties of the type K thermocouple at different temperatures match those reported in Table B.11. The standard uncertainty in the rotational velocity due to the resolution of the viscometer (0.1 rpm) is calculated by dividing by $\sqrt{3}$.

Sensitivity coefficients for torque, crucible radius, spindle radius and length, and rotational velocity used in uncertainty analyses shown in Equations D.1–D.5 were calculated by taking partial derivatives of Equation 10. The sensitivity coefficient for temperature, $\partial \mu/\partial T$, was calculated by differentiating the temperature-dependent exponential fits of average viscosity values. Sensitivity coefficients used to calculated combined standard uncertainties for FLiNaK, FLiNaK-L, and FLiNaK-H are reported in Tables D.15–D.42. Exponential fits of viscosity data for FLiNaK 1, FLiNaK 2, FLiNaK-L, and FLiNaK-H are reported in Table D.43. Viscosities and expanded uncertainties at different temperatures for FLiNaK 1, FLiNaK 2, FLiNaK-L, and FLiNaK-H are shown in Tables D.44–D.47.

$$\frac{\partial \mu}{\partial M} = \frac{R_c^2 - R_b^2}{4\pi R_c^2 R_b^2 L\omega} \tag{D.1}$$

$$\frac{\partial \mu}{\partial R_c} = \frac{M}{4\pi R_c^3 L\omega} \tag{D.2}$$

$$\frac{\partial \mu}{\partial R_h} = -\frac{M}{4\pi R_h^3 L\omega} \tag{D.3}$$

$$\frac{\partial \mu}{\partial L} = -\frac{M(R_c^2 - R_b^2)}{4\pi R_c^2 R_b^2 L^2 \omega} \tag{D.4}$$

$$\frac{\partial \mu}{\partial L} = -\frac{M(R_c^2 - R_b^2)}{4\pi R_c^2 R_b^2 L\omega^2} \tag{D.5}$$

Table D.15. Sensitivity coefficients used to calculate combined standard uncertainties in FLiNaK 1 viscosity measurements at 500 $^{\circ}$ C

Temperature,	дμ	<u></u> θμ	дμ	<u> </u>	<u> </u>
°C	дМ	∂R_c	∂R_b	∂L	∂ω
C	$s m^{-3}$	Pa s m ⁻¹	Pa s m ⁻¹	Pa s m ⁻¹	Pa s ²
60	6.91E2	2.56	-3.95	-1.90E-1	-1.51E-3
55	7.99E2	2.61	-4.10	-2.02E-1	-1.76E-3
80	5.50E2	2.60	-4.08	-2.01E-1	-1.20E-3
70	6.28E2	2.57	-4.03	-1.99E-1	-1.36E-3
50	8.79E2	2.60	-4.08	-2.01E-1	-1.92E-3
75	5.86E2	2.57	-4.03	-1.99E-1	-1.27E-3
65	6.76E2	2.58	-4.05	-1.99E-1	-1.46E-3
70	6.28E2	2.56	-4.01	-1.98E-1	-1.35E-3
60	7.33E2	2.56	-4.02	-1.98E-1	-1.58E-3
50	8.79E2	2.60	-4.08	-2.01E-1	-1.92E-3

Table D.16. Sensitivity coefficients used to calculate combined standard uncertainties in FLiNaK 1 viscosity measurements at 550 °C

Temperature, °C	$\frac{\partial \mu}{\partial M}$	$\frac{\partial \mu}{\partial R_c}$	$\frac{\partial \mu}{\partial R_b}$	$\frac{\partial \mu}{\partial L}$	$\frac{\partial \mu}{\partial \omega}$
C	$s m^{-3}$	Pa s m ⁻¹	Pa s m ⁻¹	Pa s m ⁻¹	$Pa s^2$
60	7.33E2	1.83	-2.88	-1.42E-1	-1.13E-3
55	7.99E2	1.86	-2.93	-1.44E-1	-1.25E-3
80	5.50E2	1.83	-2.87	-1.41E-1	-8.43E-4
70	6.28E2	1.83	-2.88	-1.42E-1	-9.69E-4
50	8.79E2	1.90	-2.98	-1.47E-1	-1.40E-3
75	5.86E2	1.81	-2.85	-1.40E-1	-8.94E-4
65	6.76E2	1.83	-2.88	-1.42E-1	-1.04E-3
70	6.28E2	1.82	-2.86	-1.41E-1	-9.63E-4
60	7.33E2	1.85	-2.90	-1.43E-1	-1.14E-3
50	8.79E2	1.90	-2.98	-1.47E-1	-1.40E-3

Table D.17. Sensitivity coefficients used to calculate combined standard uncertainties in FLiNaK 1 viscosity measurements at 600 $^{\circ}$ C

Temperature, °C	$\frac{\partial \mu}{\partial M}$	$\frac{\partial \mu}{\partial R_c}$	$\frac{\partial \mu}{\partial R_b}$	$\frac{\partial \mu}{\partial L}$	$\frac{\partial \mu}{\partial \omega}$
	s m ⁻³	Pa s m ⁻¹	Pa s m ⁻¹	Pa s m ⁻¹	Pa s ²
60	7.33E2	1.41	-2.22	-1.10E-1	-8.71E-4
55	7.99E2	1.40	-2.21	-1.09E-1	-9.44E-4
80	5.50E2	1.37	-2.15	-1.06E-1	-6.31E-4
70	6.28E2	1.40	-2.20	-1.08E-1	-7.38E-4
50	8.79E2	1.45	-2.28	-1.12E-1	-1.07E-3
75	5.86E2	1.39	-2.18	-1.07E-1	-6.83E-4
65	6.76E2	1.39	-2.18	-1.07E-1	-7.89E-4
70	6.28E2	1.39	-2.18	-1.07E-1	-7.32E-4
60	7.33E2	1.40	-2.20	-1.09E-1	-8.63E-4
50	8.79E2	1.44	-2.26	-1.11E-1	-1.06E-3

Table D.18. Sensitivity coefficients used to calculate combined standard uncertainties in FLiNaK 1 viscosity measurements at 650 °C

Temperature,	<u> </u>	$\frac{\partial \mu}{\partial R_c}$	$\frac{\partial \mu}{\partial R_b}$	$\frac{\partial \mu}{\partial L}$	$\frac{\partial \mu}{\partial \omega}$
°C	$s m^{-3}$	Pa s m ⁻¹	Pa s m ⁻¹	Pa s m ⁻¹	Pa s ²
60	7.33E2	1.13	-1.78	-8.78E-2	-6.99E-4
55	7.99E2	1.14	-1.79	-8.83E-2	-7.66E-4
80	5.50E2	1.08	-1.70	-8.36E-2	-4.99E-4
70	6.28E2	1.11	-1.75	-8.63E-2	-5.88E-4
50	8.79E2	1.16	-1.83	-9.00E-2	-8.59E-4
75	5.86E2	1.11	-1.75	-8.60E-2	-5.48E-4
65	6.76E2	1.12	-1.76	-8.65E-2	-6.35E-4
70	6.28E2	1.12	-1.77	-8.71E-2	-5.94E-4
60	7.33E2	1.11	-1.74	-8.58E-2	-6.83E-4
50	8.79E2	1.15	-1.80	-8.88E-2	-8.48E-4

Table D.19. Sensitivity coefficients used to calculate combined standard uncertainties in FLiNaK 1 viscosity measurements at 700 $^{\circ}$ C

Temperature,	дμ	дμ	дμ	дμ	дμ
°C	∂М	∂R_c	∂R_b	$\overline{\partial L}$	$\overline{\partial \omega}$
C	$s m^{-3}$	Pa s m ⁻¹	Pa s m ⁻¹	Pa s m ⁻¹	Pa s ²
60	7.33E2	9.43E-1	-1.48	-7.30E-2	-5.81E-4
55	7.99E2	9.59E-1	-1.51	-7.43E-2	-6.45E-4
80	5.50E2	9.08E-1	-1.43	-7.03E-2	-4.19E-4
70	6.28E2	9.39E-1	-1.48	-7.27E-2	-4.96E-4
50	8.79E2	9.63E-1	-1.51	-7.46E-2	-7.12E-4
75	5.86E2	9.28E-1	-1.46	-7.18E-2	-4.57E-4
65	6.76E2	9.53E-1	-1.50	-7.38E-2	-5.42E-4
70	6.28E2	9.50E-1	-1.49	-7.36E-2	-5.02E-4
60	7.33E2	9.30E-1	-1.46	-7.20E-2	-5.73E-4
50	8.79E2	9.63E-1	-1.51	-7.46E-2	-7.12E-4

Table D.20. Sensitivity coefficients used to calculate combined standard uncertainties in FLiNaK 1 viscosity measurements at 800 $^{\circ}$ C

Temperature,	дμ	дμ	дμ	дμ	дμ
°C	$\overline{\partial M}$	$\overline{\partial R_c}$	$\overline{\partial R_b}$	$\overline{\partial L}$	$\overline{\partial \omega}$
C	$s m^{-3}$	Pa s m ⁻¹	Pa s m ⁻¹	Pa s m ⁻¹	Pa s ²
60	7.33E2	7.39E-1	-1.16	-5.72E-2	-4.55E-4
55	7.99E2	7.23E-1	-1.14	-5.60E-2	-4.86E-4
80	5.50E2	7.26E-1	-1.14	-5.62E-2	-3.36E-4
70	6.28E2	7.32E-1	-1.15	-5.67E-2	-3.86E-4
50	8.79E2	7.19E-1	-1.13	-5.56E-2	-5.31E-4
75	5.86E2	6.93E-1	-1.09	-5.37E-2	-3.42E-4
65	6.76E2	7.17E-1	-1.13	-5.56E-2	-4.08E-4
70	6.28E2	7.21E-1	-1.13	-5.58E-2	-3.81E-4
60	7.33E2	7.01E-1	-1.10	-5.43E-2	-4.32E-4
50	8.79E2	7.34E-1	-1.15	-5.68E-2	-5.43E-4

Table D.21. Sensitivity coefficients used to calculate combined standard uncertainties in FLiNaK 1 viscosity measurements at 900 $^{\circ}$ C

Temperature,	<u> </u>	$\frac{\partial \mu}{\partial R_c}$	$\frac{\partial \mu}{\partial R_h}$	$\frac{\partial \mu}{\partial L}$	$\frac{\partial \mu}{\partial \omega}$
°C	$s m^{-3}$	Pa s m ⁻¹	Pa s m ⁻¹	Pa s m ⁻¹	$Pa s^2$
60	7.33E2	6.24E-1	-9.81E-1	-4.83E-2	-3.85E-4
55	7.99E2	5.98E-1	-9.39E-1	-4.63E-2	-4.02E-4
80	5.50E2	6.21E-1	-9.76E-1	-4.81E-2	-2.87E-4
70	6.28E2	5.90E-1	-9.26E-1	-4.57E-2	-3.11E-4
50	8.79E2	6.12E-1	-9.61E-1	-4.74E-2	-4.52E-4
75	5.86E2	5.81E-1	-9.13E-1	-4.50E-2	-2.86E-4
65	6.76E2	6.00E-1	-9.42E-1	-4.64E-2	-3.41E-4
70	6.28E2	5.79E-1	-9.09E-1	-4.48E-2	-3.06E-4
60	7.33E2	5.99E-1	-9.41E-1	-4.64E-2	-3.69E-4
50	8.79E2	5.96E-1	-9.37E-1	-4.62E-2	-4.41E-4

Table D.22. Sensitivity coefficients used to calculate combined standard uncertainties in FLiNaK 2 viscosity measurements at 500 °C

Temperature,	<u> </u>	$\frac{\partial \mu}{\partial R_c}$	$\frac{\partial \mu}{\partial R_h}$	$\frac{\partial \mu}{\partial L}$	$\frac{\partial \mu}{\partial \omega}$
°C	s m ⁻³	Pa s m ⁻¹	Pa s m ⁻¹	Pa s m ⁻¹	Pa s ²
60	7.18E2	2.67	-4.17	-2.03E-1	-1.61E-3
55	7.83E2	2.63	-4.09	-1.99E-1	-1.73E-3
80	5.38E2	2.56	-3.99	-1.94E-1	-1.16E-3
70	6.15E2	2.56	-4.00	-1.94E-1	-1.33E-3
50	8.61E2	2.60	-4.05	-1.97E-1	-1.88E-3
75	5.74E2	2.58	-4.02	-1.95E-1	-1.24E-3
65	6.62E2	2.59	-4.03	-1.96E-1	-1.44E-3
70	6.15E2	2.54	-3.96	-1.93E-1	-1.32E-3
60	7.18E2	2.66	-4.15	-2.02E-1	-1.61E-3
50	8.61E2	2.58	-4.02	-1.96E-1	-1.87E-3

Table D.23. Sensitivity coefficients used to calculate combined standard uncertainties in FLiNaK 2 viscosity measurements at 550 $^{\circ}$ C

Temperature, °C	$\frac{\partial \mu}{\partial M}$	$\frac{\partial \mu}{\partial R_c}$	$\frac{\partial \mu}{\partial R_b}$	$\frac{\partial \mu}{\partial L}$	$\frac{\partial \mu}{\partial \omega}$
C	s m ⁻³	Pa s m ⁻¹	Pa s m ⁻¹	Pa s m ⁻¹	$Pa s^2$
60	7.18E2	1.91	-2.98	-1.45E-1	-1.15E-3
55	7.83E2	1.93	-3.01	-1.46E-1	-1.27E-3
80	5.38E2	1.95	-3.04	-1.48E-1	-8.82E-4
70	6.15E2	1.96	-3.06	-1.49E-1	-1.02E-3
50	8.61E2	1.93	-3.00	-1.46E-1	-1.39E-3
75	5.74E2	1.83	-2.86	-1.39E-1	-8.85E-4
65	6.62E2	1.89	-2.95	-1.43E-1	-1.05E-3
70	6.15E2	1.98	-3.08	-1.50E-1	-1.02E-3
60	7.18E2	1.90	-2.96	-1.44E-1	-1.15E-3
50	8.61E2	1.91	-2.98	-1.45E-1	-1.38E-3

Table D.24. Sensitivity coefficients used to calculate combined standard uncertainties in FLiNaK 2 viscosity measurements at 600 °C

Temperature,	дμ	дμ	дμ	дμ	дμ
°C	$\overline{\partial M}$	$\overline{\partial R_c}$	$\overline{\partial R_b}$	$\overline{\partial L}$	$\overline{\partial \omega}$
C	$s m^{-3}$	Pa s m ⁻¹	Pa s m ⁻¹	Pa s m ⁻¹	Pa s ²
60	7.18E2	1.44	-2.24	-1.09E-1	-8.69E-4
55	7.83E2	1.39	-2.16	-1.05E-1	-9.15E-4
80	5.38E2	1.38	-2.14	-1.04E-1	-6.23E-4
70	6.15E2	1.40	-2.18	-1.06E-1	-7.23E-4
50	8.61E2	1.44	-2.24	-1.09E-1	-1.04E-3
75	5.74E2	1.35	-2.11	-1.03E-1	-6.54E-4
65	6.62E2	1.40	-2.18	-1.06E-1	-7.79E-4
70	6.15E2	1.40	-2.18	-1.06E-1	-7.23E-4
60	7.18E2	1.41	-2.20	-1.07E-1	-8.53E-4
50	8.61E2	1.44	-2.24	-1.09E-1	-1.04E-3

Table D.25. Sensitivity coefficients used to calculate combined standard uncertainties in FLiNaK 2 viscosity measurements at 650 $^{\circ}$ C

Temperature,	$\frac{\partial \mu}{\partial \mathbf{r}}$	$\frac{\partial \mu}{\partial P}$	$\frac{\partial \mu}{\partial P}$	$\frac{\partial \mu}{\partial x}$	$\frac{\partial \mu}{\partial x}$
°C	∂ M	∂R_c	∂R_b	∂L	$\partial \omega$
	s m ⁻³	Pa s m ⁻¹	Pa s m ⁻¹	Pa s m ⁻¹	Pa s ²
60	7.18E2	1.11	-1.73	-8.40E-2	-6.69E-4
55	7.83E2	1.10	-1.71	-8.32E-2	-7.23E-4
80	5.38E2	1.08	-1.68	-8.18E-2	-4.89E-4
70	6.15E2	1.12	-1.75	-8.52E-2	-5.82E-4
50	8.61E2	1.19	-1.86	-9.04E-2	-8.63E-4
75	5.74E2	1.13	-1.76	-8.57E-2	-5.46E-4
65	6.62E2	1.12	-1.74	-8.47E-2	-6.22E-4
70	6.15E2	1.12	-1.75	-8.52E-2	-5.82E-4
60	7.18E2	1.11	-1.73	-8.40E-2	-6.69E-4
50	8.61E2	1.21	-1.88	-9.15E-2	-8.74E-4

Table D.26. Sensitivity coefficients used to calculate combined standard uncertainties in FLiNaK 2 viscosity measurements at 700 $^{\circ}$ C

Temperature,	$\frac{\partial \mu}{\partial M}$	$\frac{\partial \mu}{\partial R_c}$	$\frac{\partial \mu}{\partial R_h}$	$\frac{\partial \mu}{\partial L}$	$\frac{\partial \mu}{\partial \omega}$
°C	s m ⁻³	Pa s m ⁻¹	Pa s m ⁻¹	Pa s m ⁻¹	Pa s^2
60	7.18E2	8.91E-1	-1.39	-6.76E-2	-5.38E-4
55	7.83E2	9.45E-1	-1.47	-7.16E-2	-6.22E-4
80	5.38E2	8.79E-1	-1.37	-6.66E-2	-3.98E-4
70	6.15E2	9.28E-1	-1.45	-7.03E-2	-4.80E-4
50	8.61E2	9.63E-1	-1.50	-7.30E-2	-6.97E-4
75	5.74E2	8.96E-1	-1.40	-6.80E-2	-4.33E-4
65	6.62E2	9.40E-1	-1.47	-7.13E-2	-5.24E-4
70	6.15E2	9.28E-1	-1.45	-7.03E-2	-4.80E-4
60	7.18E2	8.91E-1	-1.39	-6.76E-2	-5.38E-4
50	8.61E2	9.63E-1	-1.50	-7.30E-2	-6.97E-4

Table D.27. Sensitivity coefficients used to calculate combined standard uncertainties in FLiNaK 2 viscosity measurements at 800 $^{\circ}$ C

Temperature,	дμ	<u> </u>	<u> </u>	<u></u>	дμ
°C	дМ	∂R_c	∂R_b	∂L	$\partial \omega$
C	$s m^{-3}$	Pa s m ⁻¹	Pa s m ⁻¹	Pa s m ⁻¹	$Pa s^2$
60	7.18E2	7.13E-1	-1.11	-5.41E-2	-4.30E-4
55	7.83E2	7.36E-1	-1.15	-5.58E-2	-4.85E-4
80	5.38E2	7.07E-1	-1.10	-5.36E-2	-3.20E-4
70	6.15E2	7.09E-1	-1.11	-5.38E-2	-3.67E-4
50	8.61E2	7.33E-1	-1.14	-5.56E-2	-5.31E-4
75	5.74E2	6.93E-1	-1.08	-5.25E-2	-3.35E-4
65	6.62E2	7.29E-1	-1.14	-5.53E-2	-4.06E-4
70	6.15E2	7.09E-1	-1.11	-5.38E-2	-3.67E-4
60	7.18E2	7.26E-1	-1.13	-5.50E-2	-4.38E-4
50	8.61E2	7.64E-1	-1.19	-5.79E-2	-5.53E-4

Table D.28. Sensitivity coefficients used to calculate combined standard uncertainties in FLiNaK 2 viscosity measurements at 900 °C

Tomporoturo	дμ	дμ	дμ	дμ	дμ
Temperature, °C	$\overline{\partial M}$	$\overline{\partial R_c}$	$\overline{\partial R_b}$	$\overline{\partial L}$	$\overline{\partial \omega}$
C	$s m^{-3}$	Pa s m ⁻¹	Pa s m ⁻¹	Pa s m ⁻¹	Pa s ²
60	7.18E2	6.37E-1	-9.92E-1	-4.83E-2	-3.84E-4
55	7.83E2	6.11E-1	-9.53E-1	-4.63E-2	-4.02E-4
80	5.38E2	6.02E-1	-9.38E-1	-4.56E-2	-2.72E-4
70	6.15E2	6.00E-1	-9.35E-1	-4.55E-2	-3.11E-4
50	8.61E2	6.57E-1	-1.02	-4.98E-2	-4.76E-4
75	5.74E2	6.11E-1	-9.53E-1	-4.63E-2	-2.95E-4
65	6.62E2	6.35E-1	-9.89E-1	-4.81E-2	-3.54E-4
70	6.15E2	6.00E-1	-9.35E-1	-4.55E-2	-3.11E-4
60	7.18E2	6.24E-1	-9.72E-1	-4.73E-2	-3.77E-4
50	8.61E2	6.72E-1	-1.05	-5.10E-2	-4.87E-4

Table D.29. Sensitivity coefficients used to calculate combined standard uncertainties in FLiNaK-L viscosity measurements at 500 °C

Temperature,	<u>θμ</u> <u>θΜ</u>	$\frac{\partial \mu}{\partial R_c}$	$\frac{\partial \mu}{\partial R_h}$	$\frac{\partial \mu}{\partial L}$	$\frac{\partial \mu}{\partial \omega}$
°C	s m ⁻³	Pa s m ⁻¹	Pa s m ⁻¹	Pa s m ⁻¹	Pa s^2
60	7.05E2	2.96	-4.57	-2.18E-1	-1.74E-3
55	7.69E2	3.06	-4.72	-2.26E-1	-1.96E-3
80	5.28E2	2.85	-4.39	-2.10E-1	-1.25E-3
70	6.04E2	2.91	-4.49	-2.15E-1	-1.46E-3
50	8.46E2	2.93	-4.53	-2.16E-1	-2.06E-3
75	5.64E2	2.92	-4.51	-2.15E-1	-1.37E-3
65	6.50E2	3.00	-4.64	-2.21E-1	-1.63E-3
70	6.04E2	2.95	-4.56	-2.18E-1	-1.49E-3
60	7.05E2	2.97	-4.59	-2.19E-1	-1.74E-3
50	8.46E2	2.93	-4.53	-2.16E-1	-2.06E-3

Table D.30. Sensitivity coefficients used to calculate combined standard uncertainties in FLiNaK-L viscosity measurements at 550 $^{\circ}$ C

Temperature,	дμ	дμ	<u> </u>	дμ	дμ
°C	$\overline{\partial M}$	∂R_c	∂R_b	$\overline{\partial L}$	$\overline{\partial \omega}$
C	$s m^{-3}$	Pa s m ⁻¹	Pa s m ⁻¹	Pa s m ⁻¹	Pa s ²
60	7.05E2	2.12	-3.28	-1.56E-1	-1.25E-3
55	7.69E2	2.10	-3.25	-1.55E-1	-1.35E-3
80	5.28E2	2.00	-3.08	-1.47E-1	-8.79E-4
70	6.04E2	2.09	-3.23	-1.54E-1	-1.05E-3
50	8.46E2	2.18	-3.36	-1.60E-1	-1.53E-3
75	5.64E2	2.05	-3.16	-1.51E-1	-9.61E-4
65	6.50E2	2.08	-3.21	-1.53E-1	-1.13E-3
70	6.04E2	2.07	-3.20	-1.53E-1	-1.04E-3
60	7.05E2	2.13	-3.30	-1.57E-1	-1.25E-3
50	8.46E2	2.18	-3.36	-1.60E-1	-1.53E-3

Table D.31. Sensitivity coefficients used to calculate combined standard uncertainties in FLiNaK-L viscosity measurements at 600 °C

Temperature,	дμ	<u></u> θμ	<u> </u>	<u> </u>	<u> </u>
°C	дМ	∂R_c	∂R_b	∂L	$\partial \omega$
C	s m ⁻³	Pa s m ⁻¹	Pa s m ⁻¹	Pa s m ⁻¹	Pa s ²
60	7.05E2	1.70	-2.62	-1.25E-1	-9.96E-4
55	7.69E2	1.67	-2.58	-1.23E-1	-1.07E-3
80	5.28E2	1.61	-2.49	-1.19E-1	-7.09E-4
70	6.04E2	1.57	-2.42	-1.15E-1	-7.87E-4
50	8.46E2	1.68	-2.60	-1.24E-1	-1.18E-3
75	5.64E2	1.64	-2.53	-1.21E-1	-7.68E-4
65	6.50E2	1.67	-2.58	-1.23E-1	-9.07E-4
70	6.04E2	1.57	-2.42	-1.15E-1	-7.87E-4
60	7.05E2	1.72	-2.66	-1.27E-1	-1.01E-3
50	8.46E2	1.73	-2.67	-1.27E-1	-1.22E-3

Table D.32. Sensitivity coefficients used to calculate combined standard uncertainties in FLiNaK-L viscosity measurements at 650 °C

Temperature,	$\frac{\partial \mu}{\partial M}$	$\frac{\partial \mu}{\partial R_c}$	$\frac{\partial \mu}{\partial R_b}$	$\frac{\partial \mu}{\partial L}$	$\frac{\partial \mu}{\partial \omega}$
°C	s m ⁻³	Pa s m ⁻¹	Pa s m ⁻¹	Pa s m ⁻¹	Pa s ²
60	7.05E2	1.35	-2.08	-9.96E-2	-7.92E-4
55	7.69E2	1.39	-2.14	-1.02E-1	-8.89E-4
80	5.28E2	1.24	-1.92	-9.18E-2	-5.48E-4
70	6.04E2	1.27	-1.96	-9.35E-2	-6.38E-4
50	8.46E2	1.28	-1.98	-9.45E-2	-9.02E-4
75	5.64E2	1.30	-2.00	-9.56E-2	-6.09E-4
65	6.50E2	1.34	-2.07	-9.89E-2	-7.27E-4
70	6.04E2	1.27	-1.96	-9.35E-2	-6.38E-4
60	7.05E2	1.38	-2.12	-1.01E-1	-8.08E-4
50	8.46E2	1.28	-1.98	-9.45E-2	-9.02E-4

Table D.33. Sensitivity coefficients used to calculate combined standard uncertainties in FLiNaK-L viscosity measurements at 700 °C

Temperature,	$\frac{\partial \mu}{\partial M}$	$\frac{\partial \mu}{\partial R_c}$	$\frac{\partial \mu}{\partial R_b}$	$\frac{\partial \mu}{\partial L}$	$\frac{\partial \mu}{\partial \omega}$
$^{\circ}\mathrm{C}$	s m ⁻³	Pa s m ⁻¹	Pa s m ⁻¹	Pa s m ⁻¹	$Pa s^2$
60	7.05E2	1.20	-1.85	-8.82E-2	-7.02E-4
55	7.69E2	1.22	-1.88	-9.00E-2	-7.81E-4
80	5.28E2	1.21	-1.86	-8.89E-2	-5.31E-4
70	6.04E2	1.17	-1.80	-8.62E-2	-5.88E-4
50	8.46E2	1.20	-1.86	-8.88E-2	-8.48E-4
75	5.64E2	1.15	-1.78	-8.50E-2	-5.41E-4
65	6.50E2	1.26	-1.94	-9.28E-2	-6.82E-4
70	6.04E2	1.11	-1.72	-8.21E-2	-5.60E-4
60	7.05E2	1.18	-1.83	-8.73E-2	-6.94E-4
50	8.46E2	1.20	-1.86	-8.88E-2	-8.48E-4

Table D.34. Sensitivity coefficients used to calculate combined standard uncertainties in FLiNaK-L viscosity measurements at 800 °C

Temperature,	<u> </u>	$\frac{\partial \mu}{\partial R_c}$	$\frac{\partial \mu}{\partial R_h}$	$\frac{\partial \mu}{\partial L}$	$\frac{\partial \mu}{\partial \omega}$
°C	s m ⁻³	Pa s m ⁻¹	Pa s m ⁻¹	Pa s m ⁻¹	$Pa s^2$
60	7.05E2	9.77E-1	-1.51	-7.21E-2	-5.74E-4
55	7.69E2	9.54E-1	-1.47	-7.04E-2	-6.11E-4
80	5.28E2	9.45E-1	-1.46	-6.97E-2	-4.16E-4
70	6.04E2	9.37E-1	-1.45	-6.91E-2	-4.71E-4
50	8.46E2	9.72E-1	-1.50	-7.17E-2	-6.85E-4
75	5.64E2	9.47E-1	-1.46	-6.98E-2	-4.44E-4
65	6.50E2	9.62E-1	-1.48	-7.09E-2	-5.21E-4
70	6.04E2	9.37E-1	-1.45	-6.91E-2	-4.71E-4
60	7.05E2	9.52E-1	-1.47	-7.02E-2	-5.58E-4
50	8.46E2	9.88E-1	-1.52	-7.28E-2	-6.96E-4

Table D.35. Sensitivity coefficients used to calculate combined standard uncertainties in FLiNaK-L viscosity measurements at 900 °C

Temperature,	дμ	дμ	дμ	дμ	дμ
°C	∂М	∂R_c	∂R_b	$\overline{\partial L}$	$\overline{\partial \omega}$
C	$s m^{-3}$	Pa s m ⁻¹	Pa s m ⁻¹	Pa s m ⁻¹	$Pa s^2$
60	7.05E2	8.75E-1	-1.35	-6.45E-2	-5.13E-4
55	7.69E2	8.00E-1	-1.23	-5.90E-2	-5.12E-4
80	5.28E2	8.39E-1	-1.30	-6.19E-2	-3.69E-4
70	6.04E2	8.05E-1	-1.24	-5.93E-2	-4.05E-4
50	8.46E2	8.33E-1	-1.29	-6.15E-2	-5.87E-4
75	5.64E2	8.33E-1	-1.29	-6.15E-2	-3.91E-4
65	6.50E2	8.67E-1	-1.34	-6.39E-2	-4.69E-4
70	6.04E2	7.72E-1	-1.19	-5.69E-2	-3.88E-4
60	7.05E2	8.75E-1	-1.35	-6.45E-2	-5.13E-4
50	8.46E2	8.95E-1	-1.38	-6.60E-2	-6.30E-4

Table D.36. Sensitivity coefficients used to calculate combined standard uncertainties in FLiNaK-H viscosity measurements at 500 $^{\circ}$ C

Temperature,	<u></u> θμ	<u> </u>	дμ	<u> </u>	<u> </u>
°C	∂M	∂R_c	∂R_b	∂L	$\partial \omega$
C	$s m^{-3}$	Pa s m ⁻¹	Pa s m ⁻¹	Pa s m ⁻¹	Pa s ²
60	6.81E2	3.16	-4.82	-2.25E-1	-1.79E-3
55	7.43E2	3.13	-4.76	-2.22E-1	-1.93E-3
80	5.11E2	3.07	-4.67	-2.18E-1	-1.30E-3
70	5.76E2	3.10	-4.70	-2.17E-1	-1.48E-3
50	8.17E2	3.18	-4.84	-2.25E-1	-2.15E-3
75	5.45E2	3.12	-4.75	-2.21E-1	-1.41E-3
65	6.29E2	3.10	-4.72	-2.20E-1	-1.62E-3
70	5.84E2	3.08	-4.68	-2.18E-1	-1.49E-3
60	6.81E2	3.06	-4.66	-2.17E-1	-1.73E-3
50	8.17E2	3.15	-4.79	-2.23E-1	-2.13E-3

Table D.37. Sensitivity coefficients used to calculate combined standard uncertainties in FLiNaK-H viscosity measurements at 550 °C

Temperature,	<u></u>	<u>θμ</u>	<u>θμ</u>	<u> </u>	<u></u>
°C	дМ	∂R_c	∂R_b	∂L	∂ω
C	$s m^{-3}$	Pa s m ⁻¹	Pa s m ⁻¹	Pa s m ⁻¹	Pa s ²
60	6.81E2	2.00	-3.05	-1.42E-1	-1.13E-3
55	7.43E2	2.07	-3.15	-1.47E-1	-1.28E-3
80	5.11E2	2.05	-3.13	-1.46E-1	-8.70E-4
70	5.76E2	2.08	-3.15	-1.46E-1	-9.95E-4
50	8.17E2	2.12	-3.23	-1.51E-1	-1.44E-3
75	5.45E2	2.09	-3.18	-1.48E-1	-9.43E-4
65	6.29E2	2.12	-3.23	-1.51E-1	-1.11E-3
70	5.84E2	2.10	-3.20	-1.49E-1	-1.02E-3
60	6.81E2	2.13	-3.24	-1.51E-1	-1.20E-3
50	8.17E2	2.14	-3.26	-1.52E-1	-1.45E-3

Table D.38. Sensitivity coefficients used to calculate combined standard uncertainties in FLiNaK-H viscosity measurements at 600 $^{\circ}$ C

Temperature, °C	$\frac{\partial \mu}{\partial M}$	$\frac{\partial \mu}{\partial R_c}$	$\frac{\partial \mu}{\partial R_b}$	$\frac{\partial \mu}{\partial L}$	$\frac{\partial \mu}{\partial \omega}$
	s m ⁻³	Pa s m ⁻¹	Pa s m ⁻¹	Pa s m ⁻¹	Pa s ²
60	6.81E2	1.59	-2.42	-1.13E-1	-8.97E-4
55	7.43E2	1.72	-2.62	-1.22E-1	-1.06E-3
80	5.11E2	1.57	-2.39	-1.11E-1	-6.65E-4
70	5.76E2	1.58	-2.40	-1.11E-1	-7.57E-4
50	8.17E2	1.60	-2.43	-1.13E-1	-1.08E-3
75	5.45E2	1.58	-2.41	-1.12E-1	-7.14E-4
65	6.29E2	1.59	-2.41	-1.13E-1	-8.27E-4
70	5.84E2	1.63	-2.48	-1.15E-1	-7.88E-4
60	6.81E2	1.59	-2.42	-1.13E-1	-8.97E-4
50	8.17E2	1.63	-2.48	-1.15E-1	-1.10E-3

Table D.39. Sensitivity coefficients used to calculate combined standard uncertainties in FLiNaK-H viscosity measurements at 650 °C

Temperature,	<u> </u>	$\frac{\partial \mu}{\partial R_c}$	$\frac{\partial \mu}{\partial R_b}$	$\frac{\partial \mu}{\partial L}$	$\frac{\partial \mu}{\partial \omega}$
$^{\circ}\mathrm{C}$	s m ⁻³	Pa s m ⁻¹	Pa s m ⁻¹	Pa s m ⁻¹	$Pa s^2$
60	6.81E2	1.27	-1.93	-8.98E-2	-7.15E-4
55	7.43E2	1.30	-1.97	-9.20E-2	-7.99E-4
80	5.11E2	1.28	-1.95	-9.07E-2	-5.42E-4
70	5.76E2	1.27	-1.93	-8.92E-2	-6.08E-4
50	8.17E2	1.35	-2.05	-9.57E-2	-9.14E-4
75	5.45E2	1.29	-1.97	-9.17E-2	-5.84E-4
65	6.29E2	1.29	-1.96	-9.14E-2	-6.71E-4
70	5.84E2	1.29	-1.97	-9.19E-2	-6.27E-4
60	6.81E2	1.32	-2.01	-9.35E-2	-7.44E-4
50	8.17E2	1.35	-2.05	-9.57E-2	-9.14E-4

Table D.40. Sensitivity coefficients used to calculate combined standard uncertainties in FLiNaK-H viscosity measurements at 700 $^{\circ}$ C

Tomporeture	дμ	дμ	дμ	дμ	дμ
Temperature, °C	$\overline{\partial M}$	$\overline{\partial R_c}$	$\overline{\partial R_b}$	$\overline{\partial L}$	$\overline{\partial \omega}$
C	$s m^{-3}$	Pa s m ⁻¹	Pa s m ⁻¹	Pa s m ⁻¹	Pa s ²
60	6.81E2	1.06	-1.61	-7.52E-2	-5.98E-4
55	7.43E2	1.08	-1.65	-7.70E-2	-6.69E-4
70	5.76E2	1.08	-1.64	-7.60E-2	-5.19E-4
50	8.17E2	1.13	-1.72	-8.03E-2	-7.67E-4
75	5.45E2	1.08	-1.65	-7.70E-2	-4.90E-4
65	6.29E2	1.10	-1.67	-7.78E-2	-5.72E-4
70	5.84E2	1.08	-1.65	-7.70E-2	-5.25E-4
60	6.81E2	1.07	-1.63	-7.61E-2	-6.06E-4
50	8.17E2	1.13	-1.72	-8.03E-2	-7.67E-4

Table D.41. Sensitivity coefficients used to calculate combined standard uncertainties in FLiNaK-H viscosity measurements at 800 °C

Temperature, °C	$\frac{\partial \mu}{\partial M}$	$\frac{\partial \mu}{\partial R_c}$	$\frac{\partial \mu}{\partial R_b}$	$\frac{\partial \mu}{\partial L}$	$\frac{\partial \mu}{\partial \omega}$
C	$s m^{-3}$	Pa s m ⁻¹	Pa s m ⁻¹	Pa s m ⁻¹	Pa s ²
60	6.81E2	8.00E-1	-1.22	-5.68E-2	-4.52E-4
55	7.43E2	8.17E-1	-1.24	-5.80E-2	-5.04E-4
80	5.11E2	8.23E-1	-1.25	-5.84E-2	-3.49E-4
70	5.76E2	7.97E-1	-1.21	-5.58E-2	-3.81E-4
50	8.17E2	8.06E-1	-1.23	-5.72E-2	-5.46E-4
75	5.45E2	8.06E-1	-1.23	-5.72E-2	-3.64E-4
65	6.29E2	7.98E-1	-1.22	-5.67E-2	-4.16E-4
70	5.84E2	7.75E-1	-1.18	-5.50E-2	-3.75E-4
60	6.81E2	7.75E-1	-1.18	-5.50E-2	-4.38E-4
50	8.17E2	7.75E-1	-1.18	-5.50E-2	-5.25E-4

Table D.42. Sensitivity coefficients used to calculate combined standard uncertainties in FLiNaK-H viscosity measurements at 900 °C

Temperature,	дμ	дμ	дμ	дμ	дμ
°C	$\overline{\partial M}$	$\overline{\partial R_c}$	$\overline{\partial R_b}$	$\overline{\partial L}$	$\overline{\partial \omega}$
C	$s m^{-3}$	Pa s m ⁻¹	Pa s m ⁻¹	Pa s m ⁻¹	Pa s ²
60	6.81E2	6.33E-1	-9.63E-1	-4.49E-2	-3.57E-4
55	7.43E2	6.20E-1	-9.44E-1	-4.40E-2	-3.82E-4
80	5.11E2	6.20E-1	-9.44E-1	-4.40E-2	-2.63E-4
70	5.76E2	5.87E-1	-8.89E-1	-4.11E-2	-2.80E-4
50	8.17E2	6.20E-1	-9.44E-1	-4.40E-2	-4.20E-4
75	5.45E2	5.99E-1	-9.12E-1	-4.25E-2	-2.71E-4
65	6.29E2	5.96E-1	-9.07E-1	-4.23E-2	-3.11E-4
70	5.84E2	5.75E-1	-8.76E-1	-4.09E-2	-2.79E-4
60	6.81E2	5.81E-1	-8.85E-1	-4.12E-2	-3.28E-4
50	8.17E2	6.20E-1	-9.44E-1	-4.40E-2	-4.20E-4

Table D.43. Fitted equations for average viscosity values of FLiNaK, FLiNaK 2, FLiNaK-L, and FLiNaK-H

Salt ID	Fitted Equation
FLiNaK 1	$\mu(T) = 1.317 + 537.412 \times EXP(-T(^{\circ}C)/118.253)$
FLiNaK 2	$\mu(T) = 1.437 + 596.041 \times EXP(-T(^{\circ}C)/115.306)$
FLiNaK-L	$\mu(T) = 2.337 + 928.829 \times EXP(-T(^{\circ}C)/104.569)$
FLiNaK H	$\mu(T) = 1.888 + 708.389 \times EXP(-T(^{\circ}C)/114.102)$

Table D.44. Sensitivity coefficients for temperature $\partial \mu / \partial T$ used to calculate combined standard uncertainties in viscosity measurements of FLiNaK 1, FLiNaK 2, FLiNaK-L, and FLiNaK-H, in Pa s °C⁻¹

Temperature, °C –	$\partial \mu / \partial T$, Pa s °C ⁻¹							
Temperature, C —	FLiNaK 1	FLiNaK 2	FLiNaK-L	FLiNaK-H				
500	-6.63E-05	-6.76E-05	-7.45E-05	-7.74E-05				
550	-4.34E-05	-4.38E-05	-4.62E-05	-4.99E-05				
600	-2.84E-05	-2.84E-05	-2.86E-05	-3.22E-05				
650	-1.86E-05	-1.84E-05	-1.77E-05	-2.08E-05				
700	-1.22E-05	-1.19E-05	-1.10E-05	-1.34E-05				
800	-5.24E-06	-5.01E-06	-4.23E-06	-5.57E-06				
900	-2.25E-06	-2.11E-06	-1.62E-06	-2.32E-06				

Table D.45. Calculated viscosities of FLiNaK 1 with expanded uncertainties, in cP

Rotational	Temperature, °C							
Velocity,	500	550	600	650	700	800	900	
rpm								
60	10.1 ± 0.4	7.1 ± 0.3	5.5 ± 0.3	4.4 ± 0.3	3.6 ± 0.3	2.9 ± 0.2	2.4 ± 0.2	
55	10.1 ± 0.4	7.2 ± 0.3	5.4 ± 0.3	4.4 ± 0.3	3.7 ± 0.3	2.8 ± 0.3	2.3 ± 0.3	
80	10.1 ± 0.4	7.1 ± 0.3	5.3 ± 0.3	4.2 ± 0.3	3.5 ± 0.2	2.8 ± 0.2	2.4 ± 0.2	
70	9.9 ± 0.4	7.1 ± 0.3	5.4 ± 0.3	4.3 ± 0.3	3.6 ± 0.3	2.8 ± 0.2	2.3 ± 0.2	
50	10.1 ± 0.4	7.3 ± 0.3	5.6 ± 0.3	4.5 ± 0.3	3.7 ± 0.3	2.8 ± 0.3	2.4 ± 0.2	
75	9.9 ± 0.4	7.0 ± 0.3	5.4 ± 0.3	4.3 ± 0.3	3.6 ± 0.3	2.7 ± 0.2	2.2 ± 0.2	
65	10.0 ± 0.4	7.1 ± 0.3	5.4 ± 0.3	4.3 ± 0.3	3.7 ± 0.3	2.8 ± 0.2	2.3 ± 0.2	
70	9.9 ± 0.4	7.1 ± 0.3	5.4 ± 0.3	4.4 ± 0.3	3.7 ± 0.3	2.8 ± 0.2	2.2 ± 0.2	
60	9.9 ± 0.4	7.2 ± 0.3	5.4 ± 0.3	4.3 ± 0.3	3.6 ± 0.3	2.7 ± 0.2	2.3 ± 0.2	
50	10.1 ± 0.4	7.3 ± 0.3	5.6 ± 0.3	4.4 ± 0.3	3.7 ± 0.3	2.8 ± 0.2	2.3 ± 0.3	
Average	10.0	7.2	5.4	4.4	3.6	2.8	2.3	

Table D.46. Calculated viscosities of FLiNaK 2 with expanded uncertainties, in cP

Rotational			T	emperature, °	С		
Velocity,	500	550	600	650	700	800	900
rpm							
60	10.1 ± 0.5	7.2 ± 0.4	5.5 ± 0.4	4.2 ± 0.4	3.4 ± 0.4	2.7 ± 0.4	2.4 ± 0.4
55	10.0 ± 0.5	7.3 ± 0.4	5.3 ± 0.4	4.2 ± 0.4	3.6 ± 0.4	2.8 ± 0.4	2.3 ± 0.4
80	9.7 ± 0.5	7.4 ± 0.4	5.2 ± 0.4	4.1 ± 0.4	3.3 ± 0.4	2.7 ± 0.4	2.3 ± 0.4
70	9.7 ± 0.5	7.5 ± 0.4	5.3 ± 0.4	4.3 ± 0.4	3.5 ± 0.4	2.7 ± 0.4	2.3 ± 0.4
50	9.9 ± 0.5	7.3 ± 0.4	5.4 ± 0.4	4.5 ± 0.4	3.7 ± 0.4	2.8 ± 0.4	2.5 ± 0.4
75	9.8 ± 0.5	7.0 ± 0.4	5.1 ± 0.4	4.3 ± 0.4	3.4 ± 0.4	2.6 ± 0.4	2.3 ± 0.4
65	9.8 ± 0.5	7.2 ± 0.4	5.3 ± 0.4	4.2 ± 0.4	3.6 ± 0.4	2.8 ± 0.4	2.4 ± 0.4
70	9.6 ± 0.5	7.5 ± 0.4	5.3 ± 0.4	4.3 ± 0.4	3.5 ± 0.4	2.7 ± 0.4	2.3 ± 0.4
60	10.1 ± 0.5	7.2 ± 0.4	5.4 ± 0.4	4.2 ± 0.4	3.4 ± 0.4	2.8 ± 0.4	2.4 ± 0.4
50	9.8 ± 0.5	7.2 ± 0.4	5.4 ± 0.4	4.6 ± 0.4	3.7 ± 0.4	2.9 ± 0.4	2.6 ± 0.4
Average	9.9	7.3	5.3	4.3	3.5	2.8	2.4

Table D.47. Calculated viscosities of FLiNaK-L with expanded uncertainties, in cP

Rotational	Temperature, °C								
Velocity,	500	550	600	650	700	800	900		
rpm									
60	10.9 ± 0.4	7.8 ± 0.3	6.3 ± 0.3	5.0 ± 0.3	4.4 ± 0.2	3.6 ± 0.3	3.2 ± 0.2		
55	11.3 ± 0.4	7.8 ± 0.3	6.2 ± 0.3	5.1 ± 0.3	4.5 ± 0.2	3.5 ± 0.2	2.9 ± 0.2		
80	10.5 ± 0.4	7.4 ± 0.3	5.9 ± 0.3	4.6 ± 0.3	4.4 ± 0.2	3.5 ± 0.2	3.1 ± 0.2		
70	10.7 ± 0.4	7.7 ± 0.3	5.8 ± 0.3	4.7 ± 0.3	4.3 ± 0.2	3.5 ± 0.2	3.0 ± 0.2		
50	10.8 ± 0.4	8.0 ± 0.3	6.2 ± 0.3	4.7 ± 0.3	4.4 ± 0.3	3.6 ± 0.3	3.1 ± 0.2		
75	10.8 ± 0.4	7.5 ± 0.3	6.0 ± 0.3	4.8 ± 0.3	4.2 ± 0.2	3.5 ± 0.2	3.1 ± 0.2		
65	11.1 ± 0.4	7.7 ± 0.3	6.2 ± 0.3	4.9 ± 0.3	4.6 ± 0.2	3.5 ± 0.2	3.2 ± 0.2		
70	10.9 ± 0.4	7.6 ± 0.3	5.8 ± 0.3	4.7 ± 0.3	4.1 ± 0.2	3.5 ± 0.2	2.8 ± 0.2		
60	11.0 ± 0.4	7.9 ± 0.3	6.4 ± 0.3	5.1 ± 0.3	4.4 ± 0.3	3.5 ± 0.2	3.2 ± 0.2		
50	10.8 ± 0.4	8.0 ± 0.3	6.4 ± 0.3	4.7 ± 0.3	4.4 ± 0.3	3.6 ± 0.2	3.3 ± 0.2		
Average	10.9	7.7	6.1	4.8	4.4	3.5	3.1		

Table D.48. Calculated viscosities of FLiNaK-H with expanded uncertainties, in cP

Rotational	Temperature, °C								
Velocity,	500	550	600	650	700	800	900		
rpm									
60	11.2 ± 0.6	7.1 ± 0.5	5.6 ± 0.5	4.5 ± 0.5	3.8 ± 0.5	2.8 ± 0.5	2.2 ± 0.5		
55	11.1 ± 0.6	7.4 ± 0.5	6.1 ± 0.5	4.6 ± 0.5	3.9 ± 0.5	2.9 ± 0.5	2.2 ± 0.5		
80	10.9 ± 0.6	7.3 ± 0.5	5.6 ± 0.5	4.5 ± 0.5	3.9 ± 0.5	2.9 ± 0.5	2.2 ± 0.5		
70	10.9 ± 0.6	7.3 ± 0.5	5.5 ± 0.5	4.5 ± 0.5	3.8 ± 0.5	2.8 ± 0.5	2.1 ± 0.5		
50	11.3 ± 0.6	7.5 ± 0.5	5.7 ± 0.5	4.8 ± 0.5	4.0 ± 0.5	2.9 ± 0.5	2.2 ± 0.5		
75	11.1 ± 0.6	7.4 ± 0.5	5.6 ± 0.5	4.6 ± 0.5	3.9 ± 0.5	2.9 ± 0.5	2.1 ± 0.5		
65	11.0 ± 0.6	7.5 ± 0.5	5.6 ± 0.5	4.6 ± 0.5	3.9 ± 0.5	2.8 ± 0.5	2.1 ± 0.5		
70	10.9 ± 0.6	7.5 ± 0.5	5.8 ± 0.5	4.6 ± 0.5	3.9 ± 0.5	2.8 ± 0.5	2.0 ± 0.5		
60	10.9 ± 0.6	7.6 ± 0.5	5.6 ± 0.5	4.7 ± 0.5	3.8 ± 0.5	2.8 ± 0.5	2.1 ± 0.5		
50	11.2 ± 0.6	7.6 ± 0.5	5.8 ± 0.5	4.8 ± 0.5	4.0 ± 0.5	2.8 ± 0.5	2.2 ± 0.5		
Average	11.1	7.4	5.7	4.6	3.9	2.8	2.1		

The effect of crucible and spindle diameter on rotational flow behavior at different rotational velocities was investigated by performing two series of viscosity measurements with silicone oil at room temperature in cylindrical crucibles with different inner diameters. The same spindle was used in both sets of measurements to create annular regions with different widths. Torque measurements are shown in Figure D.1. The use of high rotational velocities can induce turbulence in wide annular regions, which is observed as a sharp increase in measured torque at higher velocities. Equation 10 is only valid for measurements with laminar flow regimes. Measurements over a similar range of rotational velocities with a thinner annular region did not show a sharp increase in torque, indicating laminar flow was maintained over the entire range of velocities at which measurements were performed.

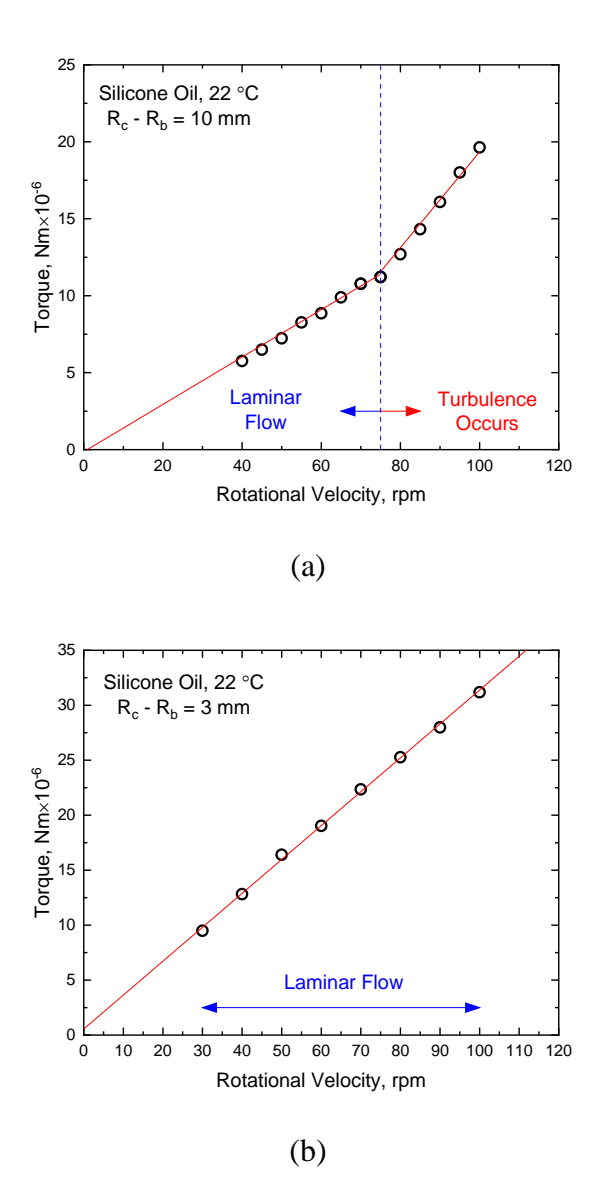


Figure D.1. Torque measurements of silicone oil performed in different sized crucibles [5].



Chemical and Fuel Cycle Technologies Division

Argonne National Laboratory 9700 South Cass Avenue, Bldg. 205 Lemont, IL 60439

www.anl.gov

